AD_____

Award Number: DAMD17-02-1-0134

TITLE: Biomarkers of Selenium Chemoprevention of Prostate Cancer

PRINCIPAL INVESTIGATOR: Yan Dong, Ph.D.

CONTRACTING ORGANIZATION: Health Research, Incorporated
Buffalo, New York 14263

REPORT DATE: January 2005

TYPE OF REPORT: Annual Summary

PREPARED FOR: U.S. Army Medical Research and Materiel Command
Fort Detrick, Maryland 21702-5012

REPORT DOCUMENTATION PAGE

Form Approved
OMB No. 074-0188

1. AGENCY USE ONLY (Leave blank)	2. REPORT DATE	3. REPORT TYPE AND DATES COVERED
	January 2005	Annual Summary (1 Jan 02 - 31 Dec 04)

4. TITLE AND SUBTITLE
Biomarkers of Selenium Chemoprevention of Prostate Cancer

5. FUNDING NUMBERS
DAMD17-02-1-0134

6. AUTHOR(S)
Yan Dong, Ph.D.

7. PERFORMING ORGANIZATION NAME(S) AND ADDRESS(ES)
Health Research, Incorporated
Buffalo, New York 14263

E-Mail: Yan.dong@roswellpark.org

8. PERFORMING ORGANIZATION REPORT NUMBER

9. SPONSORING / MONITORING AGENCY NAME(S) AND ADDRESS(ES)
U.S. Army Medical Research and Materiel Command
Fort Detrick, Maryland 21702-5012

10. SPONSORING / MONITORING AGENCY REPORT NUMBER

11. SUPPLEMENTARY NOTES

12a. DISTRIBUTION / AVAILABILITY STATEMENT
Approved for Public Release; Distribution Unlimited

12b. DISTRIBUTION CODE

13. ABSTRACT (Maximum 200 Words)

The present study examined the mechanism of selenium inhibition of prostate cell growth. We found that selenium blocks cell cycle progression and induces apoptosis. We applied microarray analysis to profile selenium-mediated gene expression changes. We found that the challenge of the microarray analysis is to extract critical information from the voluminous amount of data. We developed two bioinformatic approaches to analyze the array data in a systematic manner. Our data demonstrated that selenium significantly suppresses androgen receptor signaling, and counteracts the effect of androgen on the expression of a subset of androgen-regulated genes. Selenium also reverses the expression of genes implicated in prostate carcinogenesis. One example is the gut-enriched krüppel-like factor (GKLF) gene. GKLF expression is downregulated in colon and prostate cancers compared to normal tissues. Enforced overexpression of GKLF induces cell cycle arrest and apoptosis. GKLF-consensus element is present at very high frequency in the promoters of a cluster of early selenium-responsive genes. Selenium markedly induces GKLF DNA-binding activity and expression level. The changes could be detected as early as 1 hr after exposure to MSA. Thus, an immediate target like GKLF could serve as a key trigger of selenium action.

14. SUBJECT TERMS
Selenium-responsive biomarkers, microarray analysis, mechanism of selenium chemoprevention

15. NUMBER OF PAGES
42

16. PRICE CODE

17. SECURITY CLASSIFICATION OF REPORT	18. SECURITY CLASSIFICATION OF THIS PAGE	19. SECURITY CLASSIFICATION OF ABSTRACT	20. LIMITATION OF ABSTRACT
Unclassified	Unclassified	Unclassified	Unlimited

Table of Contents

A. INTRODUCTION:

A major goal of this project is to identify suitable biomarkers of selenium chemoprevention in human prostate cell models. These selenium-responsive biomarkers should be: (i) associated with the molecular mechanism of selenium chemoprevention, (ii) changed in a manner that is consistent with cancer risk reduction, and (iii) easily quantifiable in biopsied samples. We used the cDNA microarray technology to identify these biomarkers because it enables us to simultaneously monitor the expression pattern of a wide spectrum of genes in a single experiment.

B. BODY:

Cellular and molecular effects of selenium in PC-3 human prostate cancer cells: Please see the article (Dong *et al.*, Cancer Res., 63, 52-59, 2003) attached as an appendix for detailed description of the data. In summary, we found that the androgen-unresponsive PC-3 cells exhibited a dose- and time-dependent inhibition of growth following exposure to physiological concentrations of a selenium metabolite, methylseleninic acid (MSA). MSA retarded cell cycle progression at multiple transition points without changing the proportion of cells in different phases of the cell cycle. Flow cytometric analysis of annexin V- and propidium iodide-labeled cells showed a marked induction of apoptosis by MSA. Array analysis with the Affymetrix human genome U95A chip was then applied to profile the gene expression changes that might mediate the effects of selenium. Gene profiling was done in a time course experiment (at 12, 24, 36, and 48 hr) using synchronized cells. A large number of potential selenium-responsive genes with diverse biological functions were identified. These genes fell into 12 clusters of distinct kinetics pattern of modulation by MSA. The expression changes of 10 genes known to be critically involved in cell cycle regulation were selected for verification by Western analysis in order to determine the reliability of the array data. An agreement rate of 70% was obtained based on these confirmation experiments. From the array data, we were able to formulate a schematic diorama of signaling pathways that provide the supportive framework for understanding selenium-mediated cell cycle blockade. The data also provide valuable insights into novel biological effects of selenium, such as inhibition of cell invasion, DNA repair, and stimulation of TGF-β signaling.

Development of a Promoter-Based Microarray Data Mining Approach: In collaboration with Dr. Haitao Zhang, a bioinformatist at our Institute, we developed a novel bioinformatics-based approach to further analyze the Affymetrix GeneChip data generated in the PC-3 cells. The ultimate goal is to characterize key transcription factors that might mediate selenium-induced gene expression changes. The underlying premise of this approach is based on two fundamental principles: ♦ *Genes that are coordinately regulated should share common regulatory elements in their promoter regions.* ♦ *By identifying such common regulatory elements for a cluster of early selenium-responsive genes, we should be able to deduce the transcription factors associated with these elements. These transcription factors are potential proximal targets of selenium.*

To group genes based on their expression profiles across multiple time points, we used the Self Organizing Map (SOM) algorithm to do the analysis on all the genes that are

significantly modulated by MSA. This mode of analysis produced 16 distinct clusters (Fig. 1). We decided to select cluster 14 to pursue the bioinformatics interrogation as an exemplary case study. The characteristics of this cluster and the reasons for its selection are delineated below.

- ❖ There are 372 genes in the cluster; the sizable number should be sufficient to validate the feasibility and reliability of our bioinformatics approach.
- ❖ The genes in this cluster are all significantly downregulated (based on statistical computation) by MSA only at the 3-hr time point. The entire cluster returns to control level of expression at the subsequent time points of analysis (*i.e.*, 6, 12, 24, 36 and 48 hr). This pattern is consistent with a direct mechanism of selenium control of the activities of transcription factors.
- ❖ The fact that these 372 genes are downregulated upon exposure to selenium implies that they are expressed constitutively. In the array data, the change in the expression of a gene that is constitutively expressed in the control samples is inherently more reliable compared to the change observed with a gene that is not normally expressed in the control samples.

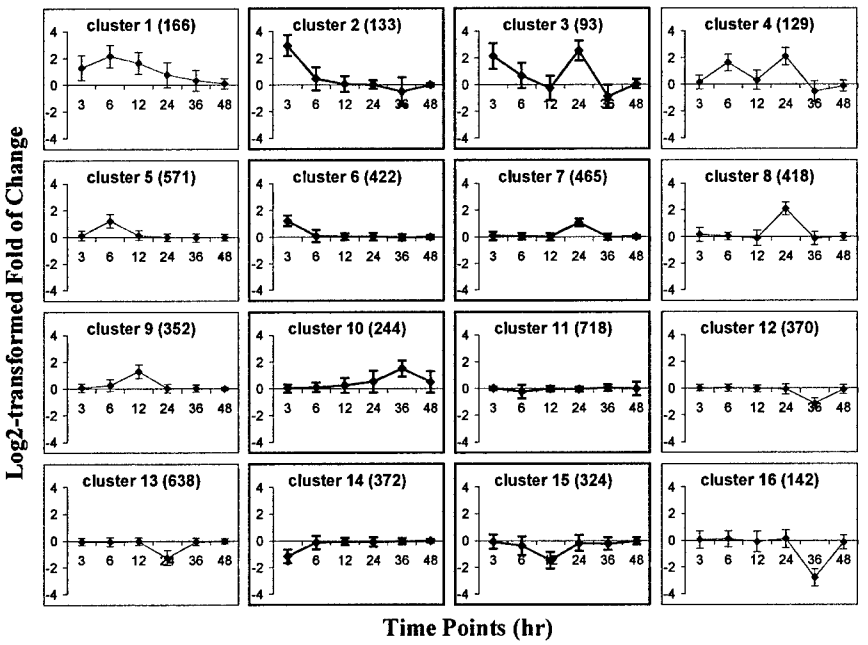

Fig. 1. Average gene expression profiles for each SOM cluster. The Log2-transformed fold of change for each gene in a cluster was averaged and plotted against duration of treatment. Data are presented as means ± SD. Numbers in parentheses represent the number of genes included in each cluster.

We were able to retrieve and analyze the promoter sequences of 287 genes (out of 372) with the custom Perl programs. The accession number of each transcript was used to map the transcript to a Unigene cluster and to obtain the Locus ID of the corresponding gene. The Locus ID was then used to query the NCBI LocusLink database in order to retrieve the unique reference sequence (RefSeq) of the gene. The latter was then matched against the human genome assembly at the University of California at Santa Cruz using the GoldenPath Genome Browser to

obtain its mapping information. Based on this information, 1 kb of promoter sequence was retrieved for each gene. The transcription factor-binding motifs presented in each promoter were then profiled using the Match program and the TRANSFAC 6.0 transcription factor database. To control for background noise, each of the promoter sequence was scrambled to generate a random sequence of the same base composition. The scrambled sequence was then profiled for transcription factor-binding motifs. The process was repeated 10 times, and the average occurrence frequency for each binding motif was calculated and assigned as background. The binding motifs with significantly higher frequencies (≥ 2 standard deviations) than the background noises were tabulated. The collective binding-motif profiles for all the promoters were then analyzed to search for common transcription factor-binding elements, and the corresponding transcription factors were classified as potential mediators of selenium action.

Table 1 shows a partial list of the common transcription factor-binding motifs identified in the promoters of the 287 genes analyzed. A substantial proportion of them (113/287 or 39%) contain the gut-enriched krüppel-like factor (GKLF)-consensus element in their promoter regions. The binding motifs for Sp1, Pax-4, Lyf-1, SRY, MZF1, C/EBP, and Elk-1 are also present at high frequencies. Since Sp1- and Lyf-1-consensus elements are highly present in TATA-less promoters, they might not be specifically involved in MSA-mediated transcriptional control but rather be important for regulating the constitutive expression of these genes. We are in the process of analyzing the promoters of two other clusters of early responsive genes, which were upregulated by MSA at the 3-hr time point. Clearly, our study demonstrates a novel approach of mining the large dataset generated by microarray analysis, and provides a paradigm of how to apply bioinformatics tools to investigate the molecular mechanism of not only cancer chemopreventive agents but also chemotherapeutic agents.

Table 1. Common Transcription Factor-Binding Motifs

	Matrix	Frequency	Gene list
GKLF	M00286	113	click
Sp1	M00196	90	click
Pax-4	M00380	90	click
Lyf-1	M00141	78	click
SRY	M00148	61	click
MZF1	M00084	47	click
C/EBP	M00159	40	click
Elk-1	M00007	40	click

Induction of GKLF DNA-binding activity by MSA: In order to confirm that GKLF is potentially a mediator of selenium action, we performed EMSA to assess the effect of MSA on the DNA-binding activity of GKLF. Nuclear extracts were prepared from PC-3 cells incubated in the absence or presence of 10 μM MSA for 3, 6, or 15 hr. A GKLF consensus element, 5'-ATGCAGGAGAAAG AAGGGCGTAGTATCTACTAG-3', was used as a probe in the EMSA. As shown in Fig. 2, MSA treatment resulted in an induction of GKLF DNA-binding activity. The specificity of the interaction and the presence of GKLF in the DNA-protein complex were confirmed by the competition experiment using an excess of unlabeled GKLF element as well as the supershift assay using an antibody against GKLF, respectively (Fig. 2).

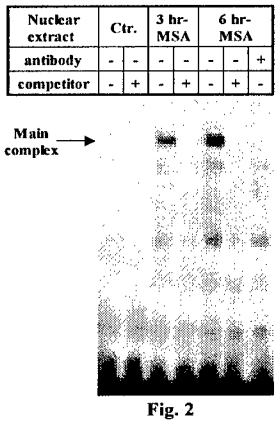

Fig. 2

Upregulation of GKLF by MSA: Our microarray data showed that MSA upregulates the level of GKLF transcript signal in PC-3 cells. We therefore conducted Northern blot analysis to corroborate this observation. As shown in Fig. 3A, the increase of GKLF mRNA level occurs

as early as 1 hr post-MSA treatment. GKLF expression was also examined in LNCaP cells. The changes were very similar to that seen in PC-3 cells (Fig. 3B).

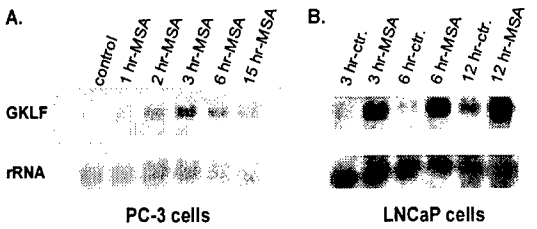

Fig. 3

Table 2. Effect of MSA on LNCaP cell growth

Treatment	Treatment Duration (hr)		
	24	48	72
MSA (μM)	% of untreated control[a]		
2.5	102.5±4.0	106.6±6.2	102.5±1.9
5	93.7±3.1	96.4±2.9	72.6±1.9[b]
10	77.1±8.4[b]	61.1±1.7[b]	55.4±3.7[b]

[a] Results are expressed as mean ± SEM (n=4).
[b] Significantly different from the control value ($P < 0.05$).

Cellular effects of selenium in LNCaP human prostate cancer cells: Table 2 shows the results of the effect of MSA treatment on the growth of the androgen-responsive LNCaP cells. A concentration of 2.5 μM MSA produced essentially no change, even after 3 days of treatment. Increasing the concentration of MSA to 5 μM inhibited cell growth by about 25%, but the effect was not observed until the 72-hr time point. The same magnitude of growth inhibition was observed at 24 h with 10 μM MSA, and by 72 hr, there were 50% fewer cells compared to the untreated culture.

We then performed cell cycle analysis of synchronized cells treated with 10 μM MSA for 24, 32 or 48 hr. The results in Fig. 4 show that a block at G_0/G_1 phase (accompanied by a decreased passage to S phase) was observed at 24 hr post-MSA treatment. The block persisted for at least eight more hours (significant difference at the 32 hr time point), but seemed to relax gradually when the culture was maintained for a longer period (the difference was no longer statistically significant at the 48 hr time point). At 48 hr post-MSA treatment, an increase in apoptotic cell death was evident (Fig. 5). The induction of apoptosis by MSA continued to escalate with time. The experiment described in Fig. 5 was carried out using the TUNEL assay. We had originally tried the annexin V staining method to assess apoptotic cell death by flow cytometric analysis (which we had successfully done with PC-3 cells). We found that this method produced an unusually high estimation of apoptosis, in the neighborhood of 20-25%, even for the untreated LNCaP cells. Visual inspection of these same cells under the microscope for chromatin condensation certainly did not support the results of the annexin V assay.

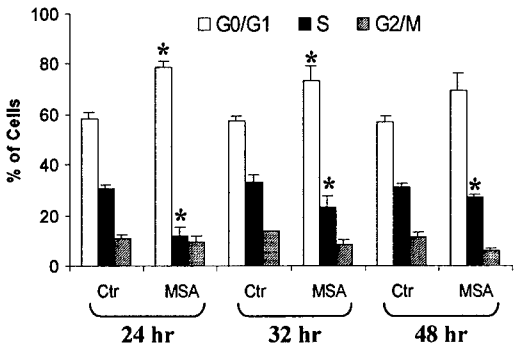

Fig. 4. Cell cycle distribution in LNCaP cells treated with MSA. Results are expressed as mean ± SE (n=3). *, statistically significant (P<0.05) compared to untreated control.

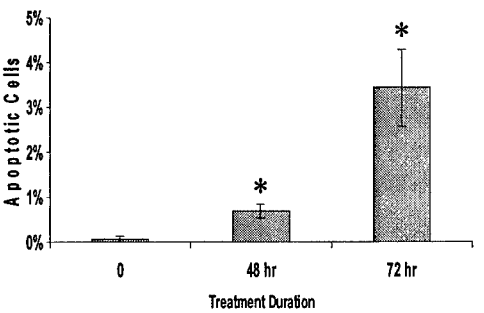

Fig. 5. Quantitation of apoptotic cell death by TUNEL assay in LNCaP cells treated with MSA. Results are expressed as mean ±SE (n=3). *, statistically significant increases (P<0.05).

Although annexin V staining is commonly used for the detection of apoptosis, we have since confirmed that it is not at all suitable for LNCaP cells for some unknown reasons (similar information was corroborated by Junxuan Lu at the University of Minnesota, personal communication).

Microarray analysis of LNCaP cells treated with MSA: In order to identify potential targets of MSA in LNCaP cells, we profiled the change in gene expression using a cDNA microarray. Please see a detailed description of the data in the manuscript (Zhang *et al.*, Cancer Genomics and Proteomics, *in press*) attached as an appendix.

MSA down-regulates AR and PSA expression, as well as AR *trans*-activating activity in LNCaP cells. Androgen receptor (AR) is a ligand-activated transcription factor (1). The availability of AR is likely to play a role in the transcriptional program activated by androgen. The microarray data of the effect of MSA on AR are highlighted in particular and shown in Table 3. The values are expressed as treatment to control signal ratio. Thus a value of ≤0.5 denotes a significant down-regulation by MSA. The decrease of AR expression was seen as early as 6 h. The level of AR transcript reached a nadir at 12 h, but gradually rebounded with time, although it was still slightly down by 48 h. Fig. 6A and 4B show the marked reduction of AR by Northern blot or real-time RT-PCR analysis, respectively, at 6, 12 or 24 h of MSA treatment. The decreases in AR message level were accompanied by parallel decreases in protein level, as shown by the Western blot in Fig. 6C.

Table 3. Repression of AR by MSA – microarray data*

Gene Name	Accession Number	Time Points (h)					
		3	6	12	24	36	48
AR	**AI659563**	0.8	0.4	0.2	0.3	0.7	0.8

*Expressed as treatment to control signal ratio. Values ≤0.5 denote significant down-regulation.

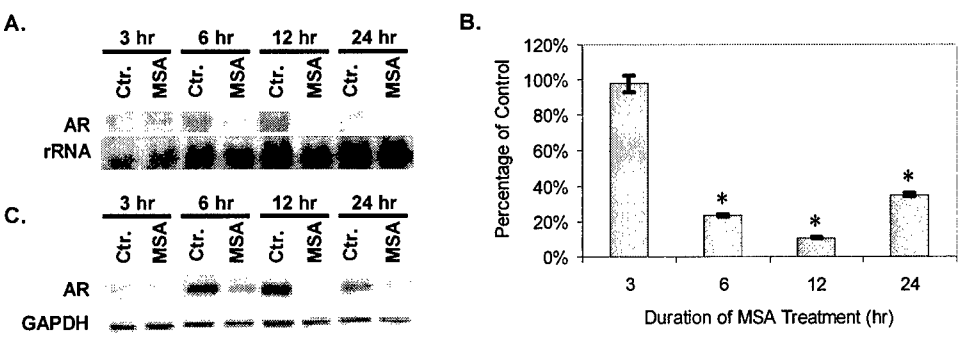

Fig. 6. Decreases of AR expression in MSA-treated cells. Panel A, Northern analysis. Panel B, Western analysis. Panel C, real time RT-PCR quantitation. *, statistically significant (P<0.001) compared to untreated control.

PSA is probably the most celebrated AR-regulated gene from a clinical standpoint because it is a well-accepted marker for the diagnosis and prognosis of prostate cancer. A down-regulation of AR by MSA would be expected to lead to decreases in PSA expression. Fig. 7A and 7B show the Northern blot and real-time RT-PCR data of PSA. Robust decreases in PSA transcript were observed at 6, 12 and 24 h after treatment with MSA. These changes were accompanied by a marked depression in PSA protein level, as shown by the Western blot in

Fig. 7C. It is noteworthy to point out that no perturbation of cell cycling was detected at 6 h post-MSA treatment, when there was already a strong suppression of both AR and PSA. Therefore, the down-regulation of PSA (and other androgen-responsive genes by extension) is unlikely to be related to some non-specific consequence of growth arrest.

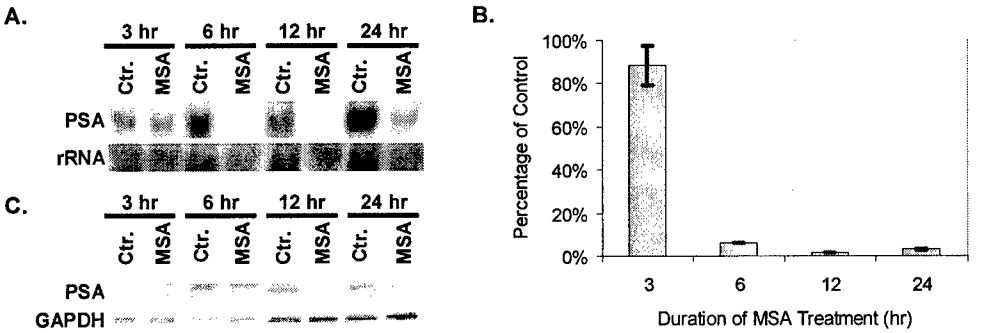

Fig. 7. Decreases of PSA expression in MSA-treated cells. Panel A, Northern analysis. Panel B, Western analysis. Panel C, real time RT-PCR quantitation. *, statistically significant ($P<0.001$) compared to untreated control.

With the use of a luciferase reporter construct linked to either the PSA promoter or the androgen-responsive element, we found that selenium inhibited the *trans*-activating activity of AR in LNCaP cells. Please see a detailed description of the data in the manuscript (Dong *et al.*, Cancer Res., 64, 19-22, 2004) attached as an appendix.

Selenium reverses the effect of androgen on the expression of androgen-regulated genes. AR signaling is known to play an important role in promoting prostate cancer progression (2). Consequently, disruption of AR signaling is an effective means of prostate cancer management. The fact that selenium is capable of decreasing the expression and *trans*-activating activity of AR underlies the justification of investigating whether the expression of AR-regulated genes might be counteracted by selenium. Recently, Zhao *et al.* also performed microarray analysis in MSA-treated LNCaP cells using a high-density cDNA array (3). In separate studies by DePrimo *et al.* (4) and Nelson *et al.* (5), LNCaP cells were treated with a synthetic androgen and microarray analyses were performed to identify genes responsive to androgen stimulation. In collaboration with Dr. Haitao Zhang, we developed a global data mining strategy to compare the two androgen datasets to the selenium-LNCaP datasets generated by Zhao *et al.* (3) and us. We identified a list of 38 genes of which the expression was reciprocally modulated by androgen and selenium. Please see a detailed description of the data in the manuscript (Zhang *et al.*, Cancer Genomics and Proteomics, *in press*) attached as an appendix.

Selenium reverses the expression of genes implicated in prostate carcinogenesis. The cellular responses of the androgen-responsive LNCaP cells and the androgen-refractory PC-3 cells to selenium are very similar. These two cell models represent different stages of prostate cancer progression. In order to identify relevant molecular targets underlying selenium chemopreventive action in incident prostate cancer or late stage relapse, we compared the selenium LNCaP and PC-3 microarray datasets to three recently published prostate cancer microarray datasets generated from human tumor specimen. We identified a subset of

dysregulated prostate cancer genes of which the expression was reversed or restored to normal by selenium intervention. Please see a detailed description of the three prostate cancer microarray datasets, our data analysis, as well as the list of the genes in the manuscript (Zhang *et al.*, Cancer Genomics and Proteomics, *in press*) attached as an appendix.

C. KEY RESEARCH ACCOMPLISHMENTS:

- Selenium-induced growth inhibition in PC-3 and LNCaP cells is achieved mainly by cell cycle blockade coupled to an induction of apoptosis.
- A large variety of potential selenium-responsive genes were identified by microarray analysis.
- From the PC-3 array data, we formulated a schematic diorama of signaling pathways that provide the supportive framework for understanding selenium-mediated cell cycle blockade. The data also provided valuable insights into novel biological effects of selenium, such as inhibition of cell invasion, initiation of DNA repair, and induction of TGF-β signaling.
- We developed a promoter-based bioinformatic microarray data mining approach, and identified GKLF as a potential proximal target of selenium.
- Selenium significantly downregulates the expression and *trans*-activating activity of AR in LNCaP cells. The decrease of an AR-regulated gene, PSA, follows a similar time response pattern upon exposure to selenium. The reduction of AR and PSA expression occurs well before any significant change in cell number.
- We performed a systematic microarray data mining analysis, and found that selenium could counteract the effect of androgen on the expression of a subset of androgen-regulated genes.
- Our microarray data mining analysis also showed that selenium reversed the expression of genes implicated in prostate carcinogenesis.

D. REPORTABLE OUTCOMES:

- ***Publications:***

Dong, Y., Zhang, H., Hawthorn, L., Ganther, H.E., and Ip, C. (2003) Delineation of the molecular basis for selenium-induced growth arrest in human prostate cancer cells by oligonucleotide array. *Cancer Res., 63, 52-59.*

Dong, Y., Lee, S.O., Zhang, H., Marshall, J., Gao, A., and Ip, C. (2004) Prostate specific antigen (PSA) expression is down-regulated by selenium through disruption of androgen receptor signaling. *Cancer Res., 64, 19-22.*

Zhang, H., Dong, Y., Marshall, J., Nowak, N., and Ip, C. (2005) Microarray data mining of potential selenium targets in chemoprevention of prostate cancer. *Cancer Genomics and Proteomics, in press.*

- ***Abstracts and Presentations:***

  Dong, Y., Zhang, H., Hawthorn, L., and Ip, C. (2002) Delineation of the Molecular Basis for Selenium-induced Growth Arrest in Human Prostate Cancer Cells by Oligonucleotide Array. *Proceedings of the American Association for Cancer Research, 43: 167.*

  Dong, Y., Zhang, H., Nowak, N.J., Hawthorn, L., and Ip, C. (2003) A Bioinformatics Approach to Delineate Selenium-mediated Transcription Control of Gene Expression Changes. *Proceedings of the American Association for Cancer Research, 44 (2nd Edition): 774.*

  Dong, Y., Zhang, H., Nowak, N.J., Hawthorn, L., and Ip, C. (2003) A Bioinformatics Approach to Identify the Molecular Mechanism of Selenium-mediated Gene Expression Changes. Poster presented at the Edward A. Smuckler Memorial Pathobiology of Cancer Workshop, Keystone, Colorado.

  Dong, Y., Zhang, H., and Ip, C. (2003) Selenium and genomics: a pas de deux to cancer control. Poster presented at the 2nd Annual International Conference on Frontiers in Cancer Prevention Research, Phoenix, AZ.

  Dong, Y., Zhang, H., Nowak, N.J., Marshall, J.R., and Ip, C. (2003) Selenium Affects an Array of Androgen-Regulated Genes and Other Targets Implicated in Prostate Carcinogenesis: Evidence from cDNA Microarray Analysis. Poster presented at the Prostate Cancer Foundation 10th Annual Scientific Retreat, New York, NY.

  Dong, Y., Lee, S.O., Zhang, H., Marshall, J.R., Nowak, N.J., Gao, A.C., and Ip, C. (2004) Selenium Countermands the Expression of Androgen-Regulated Genes and Other Targets Implicated in Prostate Carcinogenesis. *Proceedings of the American Association for Cancer Research, 45.*

- ***Personnel receiving pay from the research effort:***

  Yan Dong, Ph.D.

- ***Funding received:***

  DOD New Investigator Award (PI) 02/04 - 1/07

  - Title: GKLF as a Novel Target in Selenium Chemoprevention of Prostate Cancer
  - Award per year: $75,000

  NCI Howard Temin (K01) Career Development Award (PI) 04/05 – 03/10

  - Title: Androgen receptor signaling in selenium chemoprevention
  - Award per year: $120,000

- ***Employment received:***

  Assistant Member, Dept. of Cancer Chemoprevention, Roswell Park Cancer Institute, Buffalo, NY 14263

E. CONCLUSIONS:

The results from the current study indicate that selenium inhibits the growth of prostate cancer cells through cell cycle blockade and apoptosis induction. We applied microarray analysis to profile gene expression changes mediating selenium-induced growth inhibition. We found that the challenge of the microarray analysis is to extract critical information from the voluminous amount of array data. We therefore developed two bioinformatic approaches to analyze the array data in a systematic manner. Our data demonstrated that selenium significantly suppressed androgen receptor signaling, and counteracted the effect of androgen on the expression of a subset of androgen-regulated genes. Our microarray data mining analysis also showed that selenium reversed the expression of genes implicated in prostate carcinogenesis. One example is the gut-enriched krüppel-like factor (GKLF) gene. GKLF expression has been shown to be downregulated in colon and prostate cancers compared to normal tissues (6-8), thus suggesting a potential tumor suppressor function of GKLF. Enforced expression of GKLF was reported to inhibit DNA synthesis in fibroblasts, arrest the growth of vascular smooth muscle cells, and induce G_1/S block and apoptosis in colon cancer cells (9-12). We found that GKLF-consensus element is present at very high frequency in the promoters of a cluster of early selenium-responsive genes. Selenium markedly induced GKLF DNA-binding activity and expression level. The changes could be detected as early as 1 hr after exposure to MSA. Thus, an immediate target like GKLF could serve as a key trigger of selenium action. In summary, the present study has uncovered a number of potentially exciting clues regarding the action of selenium in prostate cancer prevention.

F. REFERENCES:

1. Evans, R. M. The steroid and thyroid hormone receptor superfamily. Science, *240*: 889-895, 1988.

2. Jenster, G. The role of the androgen receptor in the development and progression of prostate cancer. Semin.Oncol., *26*: 407-421, 1999.

3. Zhao, H., Whitfield, M. L., Xu, T., Botstein, D., and Brooks, J. D. Diverse effects of methylseleninic acid on the transcriptional program of human prostate cancer cells. Mol.Biol.Cell, *15*: 506-519, 2004.

4. DePrimo, S. E., Diehn, M., Nelson, J. B., Reiter, R. E., Matese, J., Fero, M., Tibshirani, R., Brown, P. O., and Brooks, J. D. Transcriptional programs activated by exposure of human prostate cancer cells to androgen. Genome Biol., *3*: RESEARCH0032, 2002.

5. Nelson, P. S., Clegg, N., Arnold, H., Ferguson, C., Bonham, M., White, J., Hood, L., and Lin, B. The program of androgen-responsive genes in neoplastic prostate epithelium. Proc.Natl.Acad.Sci.U.S.A, *99*: 11890-11895, 2002.

6. Shie, J. L., Chen, Z. Y., O'Brien, M. J., Pestell, R. G., Lee, M. E., and Tseng, C. C. Role of gut-enriched Kruppel-like factor in colonic cell growth and differentiation. Am.J.Physiol Gastrointest.Liver Physiol, *279*: G806-G814, 2000.

7. Dang, D. T., Bachman, K. E., Mahatan, C. S., Dang, L. H., Giardiello, F. M., and Yang, V. W. Decreased expression of the gut-enriched Kruppel-like factor gene in intestinal adenomas of multiple intestinal neoplasia mice and in colonic adenomas of familial adenomatous polyposis patients. FEBS Lett., *476*: 203-207, 2000.

8. Foster, K. W., Frost, A. R., McKie-Bell, P., Lin, C. Y., Engler, J. A., Grizzle, W. E., and Ruppert, J. M. Increase of GKLF messenger RNA and protein expression during progression of breast cancer. Cancer Res., *60*: 6488-6495, 2000.

9. Shields, J. M., Christy, R. J., and Yang, V. W. Identification and characterization of a gene encoding a gut-enriched Kruppel-like factor expressed during growth arrest. J.Biol.Chem., *271*: 20009-20017, 1996.

10. Nickenig, G., Baudler, S., Muller, C., Werner, C., Werner, N., Welzel, H., Strehlow, K., and Bohm, M. Redox-sensitive vascular smooth muscle cell proliferation is mediated by GKLF and Id3 in vitro and in vivo. FASEB J., *16*: 1077-1086, 2002.

11. Chen, X., Johns, D. C., Geiman, D. E., Marban, E., Dang, D. T., Hamlin, G., Sun, R., and Yang, V. W. Kruppel-like factor 4 (gut-enriched Kruppel-like factor) inhibits cell proliferation by blocking G1/S progression of the cell cycle. J.Biol.Chem., *276*: 30423-30428, 2001.

12. Chen, Z. Y., Shie, J., and Tseng, C. Up-regulation of gut-enriched kruppel-like factor by interferon-gamma in human colon carcinoma cells. FEBS Lett., *477*: 67-72, 2000.

[CANCER RESEARCH 63, 52–59, January 1, 2003]

Delineation of the Molecular Basis for Selenium-induced Growth Arrest in Human Prostate Cancer Cells by Oligonucleotide Array[1]

Yan Dong, Haitao Zhang, Lesleyann Hawthorn, Howard E. Ganther, and Clement Ip[2]

Departments of Cancer Prevention [Y. D., C. I.], and Cancer Genetics [H. Z., L. H.], Roswell Park Cancer Institute, Buffalo, New York 14263, and Department of Nutritional Sciences, University of Wisconsin, Madison, Wisconsin 53706 [H. E. G.]

ABSTRACT

Despite the growing interest in selenium intervention of prostate cancer in humans, scanty information is currently available on the molecular mechanism of selenium action. Our past research indicated that methylseleninic acid (MSA) is an excellent reagent for investigating the anticancer effect of selenium *in vitro*. The present study was designed to examine the cellular and molecular effects of MSA in PC-3 human prostate cancer cells. After exposure to physiological concentrations of MSA, these cells exhibited a dose- and time-dependent inhibition of growth. MSA retarded cell cycle progression at multiple transition points without changing the proportion of cells in different phases of the cell cycle. Flow cytometric analysis of annexin V- and propidium iodide-labeled cells showed a marked induction of apoptosis by MSA. Array analysis with the Affymetrix human genome U95A chip was then applied to profile the gene expression changes that might mediate the effects of selenium. Gene profiling was done in a time course experiment (at 12, 24, 36, and 48 h) using synchronized cells. A large number of potential selenium-responsive genes with diverse biological functions were identified. These genes fell into 12 clusters of distinct kinetics pattern of modulation by MSA. The expression changes of 10 genes known to be critically involved in cell cycle regulation were selected for verification by Western analysis to determine the reliability of the array data. An agreement rate of 70% was obtained based on these confirmation experiments. The array data enabled us to focus on the role of potential key genes (*e.g., GADD153, CHK2, p21^{WAF1}, cyclin A, CDK1,* and *DHFR*) that might be targets of MSA in impeding cell cycle progression. The data also provide valuable insights into novel biological effects of selenium, such as inhibition of cell invasion, DNA repair, and stimulation of transforming growth factor β signaling. The present study demonstrates the utility of a genome-wide analysis to elucidate the mechanism of selenium chemoprevention.

INTRODUCTION

Recruitment to the National Cancer Institute-sponsored SELECT[3] trial began in 2001. This is a Phase III, double-blind, placebo-controlled, 12-year trial designed to assess the effect of selenium and vitamin E, either individually or in combination, on the incidence of prostate cancer. The launching of this trial is largely driven by the milestone finding of Clark *et al.* (1) that selenized yeast supplementation was capable of significantly reducing the incidence of prostate (RR = 0.37), lung (RR = 0.54), and colon cancers (RR = 0.42). The SELECT protocol also provides for the establishment of a repository for prostate biopsy tissue, blood cells, and plasma. These materials will be put aside for research discoveries in the future. One of the secondary objectives of the trial is to study cellular and molecular biomarkers using the banked samples and to delineate their relevance with respect to prostate carcinogenesis and drug effects (2). Despite the considerable public interest in the potential benefit of selenium chemoprevention of prostate cancer, scanty information is currently available on the molecular targets or the signaling mechanism underlying the anticancer action of selenium. Our present study was aimed at addressing this gap of knowledge with the use of a human prostate cancer cell line.

Se-Met is the selenium compound used in the SELECT. It is, however, not particularly suitable for mechanism studies in cell culture. The reason is that Se-Met needs to be metabolized primarily in the liver to a monomethylated intermediate for the expression of its anticancer activity (3–6), and epithelial tissues generally have a low capacity to generate a monomethylated selenium metabolite from Se-Met. Consequently, concentrations of Se-Met that are 20–100 times above physiological levels are necessary to cause growth inhibition in cultured cells. Excessively high concentrations of Se-Met could produce a spectrum of nonspecific effects that may not be related to the anticancer effect of selenium. To obviate this problem, a stable monomethylated selenium metabolite, MSA (CH_3SeO_2H), was developed specifically for *in vitro* studies (7). We found that premalignant human breast cell lines were sensitive to growth inhibition and cell cycle block by MSA at a concentration as low as 2.5 μM (8). In addition, Jiang *et al.* (9) recently reported that MSA induced apoptosis in DU-145 human prostate cancer cells at a concentration of 5 μM. Sinha *et al.* (10) also showed that with mouse mammary tumor cells, a 10-min exposure to 5 μM MSA was sufficient to cause a change in the expression of a handful of genes as detected by the Atlas mouse cDNA expression array. The concentration of selenium used in the above studies is within the physiological range of selenium in the circulation. As expected, MSA also has excellent anticancer activity *in vivo* (7). We are, therefore, confident that the information obtained with MSA from cell culture studies would be relevant to the action of selenium.

In this study, we first examined the dose-dependent effect of MSA on the growth of the PC-3 human prostate cancer cell line. We then showed that growth inhibition by MSA was likely attributable to a combined effect on cell cycle block and apoptosis. Next we used the oligonucleotide array technology to gain further insight into the gene expression changes that might play a role in the regulation of these cellular events. Many potential selenium-responsive genes were identified by this method. These genes fell into 12 clusters of distinct kinetics pattern of modulation by MSA. The early response genes were grouped on the basis of their known functions in cell growth and tumorigenesis. From the array data, we were able to develop an integrated scheme of signaling pathways that might explain the action of selenium in blocking cell cycle progression.

MATERIALS AND METHODS

Selenium Reagents and Cell Line. MSA was synthesized as described previously (7). Se-Met was purchased from Sigma (St. Louis, MO). The PC-3 human prostate cancer cells were obtained from American Type Culture Collection (Manassas, VA). The cells were cultured in RPMI 1640 supple-

Received 7/5/02; accepted 10/30/02.

The costs of publication of this article were defrayed in part by the payment of page charges. This article must therefore be hereby marked *advertisement* in accordance with 18 U.S.C. Section 1734 solely to indicate this fact.

[1] This work was supported by Grant CA 91990 from the National Cancer Institute, AACR-Cancer Research Foundation of America Fellowship in Prevention Research, Department of Defense Postdoctoral Fellowship Award, and was partially supported by core resources of the Roswell Park Cancer Institute Cancer Center support Grant P30 CA 16056 from the National Cancer Institute.

[2] To whom requests for reprints should be addressed, at Department of Cancer Prevention, Roswell Park Cancer Institute, Elm and Carlton Streets, Buffalo, NY 14263. Phone: (716) 845-8875; Fax: (716) 845-8100; E-mail: clement.ip@roswellpark.org.

[3] The abbreviations used are: SELECT, Selenium and Vitamin E Chemoprevention Trial; MSA, methylseleninic acid; TUNEL, terminal deoxynucleotidyl transferase-mediated dUTP nick end labeling; PI, propidium iodide; GAPDH, glyceraldehyde-3-phosphate dehydrogenase; MTT, 3-(4,5-dimethylthiazol-2-yl)-2,5-diphenyltetrazolium bromide; TGF, transforming growth factor; RR, relative risk; BrdUrd, bromodeoxyuridine; Se-Met, selenomethionine; SOM, self-organizing map; MAPK, mitogen-activated protein kinase; PCNA, proliferating cell nuclear antigen.

mented with 10% fetal bovine serum, 100 units/ml penicillin, 100 μg/ml streptomycin, and 2 mM glutamine, and maintained in an atmosphere of 5% CO_2 in a 37°C humidified incubator.

MTT Cell Proliferation Assay. The assay, which is based on the conversion of the yellow tetrazolium salt MTT to purple formazan crystals by metabolically active cells (11), provides a quantitative determination of viable cells. Cells were seeded in 24-well plates at a density designed to reach 70–80% confluency at the time of assay. At 48 h after seeding, cells were treated with various concentrations of Se-Met or MSA in triplicate. After 24, 48, or 72 h of treatment, 200 μl of MTT was added to each well of cells, and the plate was incubated for 4 h at 37°C. The MTT crystals from both attached and floating cells were solubilized in isopropanol and subjected to centrifugation to pellet the cellular debris. Spectrophotometric absorbance of each sample was measured at 570 nm using a Spectra Microplate Reader (SLT-Labinstruments Ges.m.b.H., Salzburg, Austria).

Cell Cycle Analysis. PC-3 cells were plated at a density of 10^4 cells/cm^2 in T75 culture flasks and allowed to grow for 48 h to reach 70–80% confluency. Synchronization of cells was achieved by starving in serum-free medium for 48 h. Over 85% of cells were in G_0 phase at the end of this time period. On returning to regular growth medium for 6 h, cells were exposed to 10 μM MSA. The procedure of serum-starvation and refeeding has been described previously by Sinha and Medina (12) and Sinha *et al.* (13) to study the effect of selenium on cell cycling. After treatment for 24, 32, or 48 h, cells were trypsinized, washed in PBS, and fixed overnight in 70% ethanol at 4°C. The ethanol solution was subsequently removed after centrifugation, and cells were resuspended in a buffer containing 10 mM Tris (pH 7.5), 125 mM sucrose, 2.5 mM $MgCl_2$, 0.185% NP40, 0.02 mg/ml RNase A, 0.05% sodium citrate, and 25 μg/ml PI. After incubation on ice for 1 h, cells were analyzed for DNA content using a FACScan cytometer (Becton Dickinson).

BrdUrd Labeling Assay. PC-3 cells were plated at a density of 10^4 cells/cm^2 in T75 culture flasks and synchronized as described above. On returning to regular growth medium for 6 h, cells were exposed to 10 μM MSA for 24 or for 48 h. During the last 30 min of MSA treatment, cells were labeled with 10 μM BrdUrd (10 μl of 1 mM BrdUrd was added to each ml of culture media). BrdUrd-labeled cells were trypsinized, fixed, treated with DNase I, and stained with FITC-conjugated anti-BrdUrd antibody using the BrdUrd Flow Kit from BD Pharmigen (San Diego, CA). Stained cells were then quantified by flow cytometry, and the data were analyzed with the WinList software (Variety Software House, Topsham, ME).

Quantitation of Apoptosis by Flow Cytometry. PC-3 cells were plated at a density of 10^4 cells/cm^2 in T175 culture flasks. At 48 h after seeding, cells were exposed to either 5 or 10 μM MSA for 48 or 72 h. Adherent cells harvested by mild trypsinization were pooled together with detached cells. Cells were stained with biotin-conjugated Annexin V, FITC-conjugated streptavidin, and PI using the Annexin V-Biotin Apoptosis Detection kit (Oncogene Research Products, Boston, MA) as per the manufacturer's protocol. Apoptotic cells were subsequently counted by flow cytometry, and the data were analyzed with the WinList software (Variety Software House, Topsham, ME).

Oligonucleotide Array Analysis. PC-3 cells were plated at a density of 10^4 cells/cm^2 in 15-cm culture dishes. Synchronization was achieved as described above. After exposure to 10 μM MSA for 12, 24, 36, or 48 h, total RNA and protein were isolated using TRIzol (Life Technologies, Inc.). The experiment was repeated, and the total RNA collected from the replicate was pooled and submitted to microarray analysis using the U95A chip from Affymetrix (Santa Clara, CA). Biotinylated cRNA probe generation, as well as array hybridization, washing, and staining, was carried out according to the standard Affymetrix GeneChip protocol. Fluorescence intensity for each chip was captured with a Hewlett-Packard laser confocal scanner. Absolute analysis of each chip and comparative analysis of MSA-treated samples with the untreated control samples were performed by using the Affymetrix Microarray Suite software. The mean hybridization signal for each sample was set as 1000 arbitrary units to normalize the signal values of all of the genes on the chip (global normalization) between different samples. A treatment/control signal ratio of ≥ 2 or ≤ 0.5 was chosen as the criterion for induction or repression, respectively. These threshold values are commonly used in the literature for microarray expression analysis (14–16). GENECluster program (Massachusetts Institute of Technology, Boston, MA) and Affymetrix Data Mining Tool were used for clustering analysis.

Western Blot Analysis. Western blot analysis was performed as described previously (17) using the TRIzol isolated protein. Briefly, ~50 μg of protein was resolved over 10–15% SDS-PAGE and transferred to polyvinylidine difluoride membrane. The blot was blocked in blocking buffer [5% nonfat dry milk, 10 mM Tris (pH 7.5), 10 mM NaCl. and 0.1% Tween 20] overnight at 4°C, incubated with the primary antibody at 37°C for 1 h, followed by incubation with an antimouse antirabbit, or antisheep horseradish peroxidase-conjugated secondary antibody (Bio-Rad, Hercules, CA) at 37°C for 30 min. Individual protein bands were visualized by an enhanced chemiluminescence kit obtained from Amersham Pharmacia Biotech (Piscataway, NJ). Immunoreactive bands were quantitated by volume densitometry using the ImageQuant software (Molecular Dynamics, Sunnyvale, CA), and normalized to actin. The following monoclonal antibodies were used in this study (source): anti-actin (Sigma, St. Louis, MO); anti-DHFR, CDK1, and CDK2 (BD Transduction Laboratory, San Jose, CA); anti-PCNA (Santa Cruz Biotechnology, Santa Cruz, CA); and anti-cyclin A, cyclin E2, CDK4, $p21^{WAF1}$ (NeoMarkers, Fremont, CA). Polyclonal antibodies to CHK2 and GADD153 were obtained from Calbiochem (La Jolla, CA) and Santa Cruz Biotechnology (Santa Cruz, CA), respectively.

Statistical Analysis. The Student's two-tailed *t* test was used to determine significant differences between treatment and control values, and $P < 0.05$ was considered statistically significant.

RESULTS

Sensitivity of Human Prostate Cancer Cells to MSA. The inhibitory effects of MSA and Se-Met on the accumulation of PC-3 cells were assessed by the MTT assay. As shown in Table 1, MSA was able to significantly suppress the growth of PC-3 cells in a time- and dose-dependent manner. At 72 h of treatment, 5 μM MSA reduced cell number by ~25%. Increasing the concentration of MSA to 10 μM resulted in a more pronounced effect, leading to a greater magnitude of growth inhibition in a shorter period of exposure. In contrast, a concentration of 200 or 400 μM Se-Met was required to produce significant decreases in cell number at 72 h or 48 h, respectively. It is thus evident that MSA is much more potent than Se-Met in inhibiting growth of these prostate cells.

Cell Cycle Block by MSA. To determine whether the decrease in cell number accumulation by MSA was related to cell cycle arrest, we proceeded to assess the evidence of cell cycle perturbation by flow cytometry of ethanol-permeabilized cells stained with PI. Synchronized PC-3 cells were treated with 10 μM MSA for 24, 32, or 48 h. MSA did not cause any significant change in cell cycle distribution (Fig. 1). However, flow cytometry of BrdUrd-labeled cells showed that MSA treatment resulted in a drastic decrease in the number of cells synthesizing DNA (Fig. 2). Therefore, the data suggest that MSA probably blocked cell cycle progression at multiple stages. It should be noted that flow cytometry of PI-stained cells would not be able to detect a change in the proportion of cells in different phases of the cell

Table 1 *Effect of MSA or Se-Met on the accumulation of PC-3 cells at three treatment durations*

	% of untreated control[a]		
Treatment	24 h	48 h	72 h
MSA (μM)			
1	97.0 ± 3.5	98.9 ± 5.0	99.0 ± 4.9
2.5	107.2 ± 5.0	106.4 ± 3.8	101.8 ± 6.2
5	104.2 ± 5.0	103.7 ± 5.3	74.2 ± 6.5[b]
10	101.6 ± 6.3	46.3 ± 4.4[b]	38.4 ± 1.7[b]
Se-Met (μM)			
25	101.3 ± 4.0	112.7 ± 1.7	102.4 ± 3.5
50	101.5 ± 3.3	110.2 ± 2.5	94.6 ± 4.5
100	100.1 ± 2.1	110.7 ± 1.3	87.8 ± 5.6[b]
200	94.1 ± 1.2	97.2 ± 6.4	69.3 ± 6.4[b]
400	92.8 ± 5.5	75.3 ± 4.4[b]	50.1 ± 3.6[b]

[a] Results are expressed as mean ± SE ($n = 4$ independent experiments).
[b] Significantly different compared to the corresponding control value ($P < 0.05$).

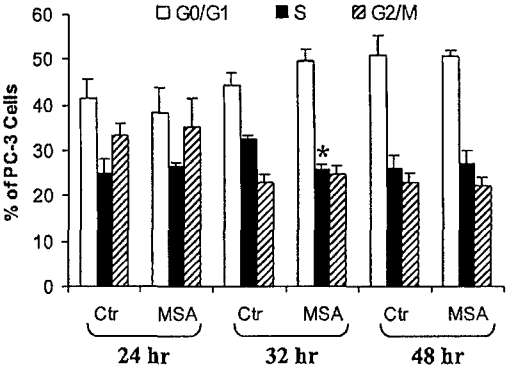

Fig. 1. Cell cycle distribution in PC-3 cells treated with MSA. Results are expressed as means ± SE (n = 3). *, statistically significant ($P < 0.05$) *versus* untreated control.

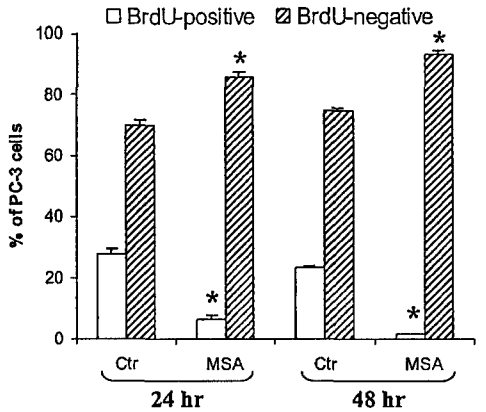

Fig. 2. BrdUrd (*BrdU*) labeling of PC-3 cells treated with MSA. Results are expressed as means ± SE (n = 3). *, statistically significant ($P < 0.05$) *versus* untreated control.

cycle (*i.e.*, the percentage of cells in G_0-G_1, S phase, or G_2-M) if there is a persistent slowdown in the transition in all phases of the cell cycle.

Induction of Apoptosis by MSA. In an attempt to determine whether MSA might also induce cell death, we incubated exponentially growing PC-3 cells for 48 or 72 h in the presence of 5 or 10 μM MSA, and quantified the extent of apoptosis by flow cytometric analysis of cells labeled with annexin V and PI. Phosphatidylserine externalization is a characteristic of cells undergoing apoptosis. Annexin V has a strong affinity for phosphatidylserine. Staining cells simultaneously with annexin V and PI allows the resolution of intact cells (double negative), early apoptotic cells (annexin V-positive and PI-negative), and late apoptotic or necrotic cells (double positive), which can be located in the lower left, lower right, and upper right quadrants of the cytograms of Fig. 3*A*, respectively. Because only cells that are annexin V-positive and PI-negative are truly representative of apoptotic cells, the percentage of this cell population was quantitated from four individual experiments and shown in a bar graph form in Fig. 3*B*. MSA caused an induction of apoptosis at the 48-h time point, and the effect was maintained with longer exposure to MSA for 72 h. The increase of apoptosis, which followed the occurrence of growth arrest, appeared to maximize with 5 μM MSA, and no further enhancement was detected with 10 μM MSA.

Profiling of MSA-responsive Genes by Oligonucleotide Array Analysis. We used the Affymetrix human genome U95A Chip to profile the changes in gene expression and to characterize selenium-responsive targets that might lead to cell growth inhibition by MSA. This GeneChip contains probes to 12,000 known genes. As it would be more informative to do the profiling at a series of time points than to do replicate analysis at a single time point, we decided to commit our available resources to the former design. For each time point at 12, 24, 36, and 48 h post-MSA, three separate preparations of RNA samples were pooled and submitted to array hybridization.

Pairwise comparative analysis between MSA-treated samples and the corresponding untreated control samples at each time point was performed by using the Affymetrix Microarray Suite software. This software determines whether a given gene is differently expressed based on a decision matrix including the net change in intensity values, fold of change, and other parameters. A no-change decision call was assigned a value of "1." Genes with expression changes of $\geq$2 or $\leq$0.5 were considered as MSA-responsive genes. The 2-fold difference limit was chosen based on our previous experience with microarray data analysis and was also in general agreement with other reported array experiments. Table 2 shows the number of genes induced or repressed by MSA at each time point. There were significantly fewer MSA-modulated genes at the 48-h time point than at the other three early time points. This could be because growth inhibition by MSA has reached ~50% at 48 h (Table 1) and because the underpinning molecular changes have already peaked and receded by this time.

To study in detail the kinetics of expression changes in response to

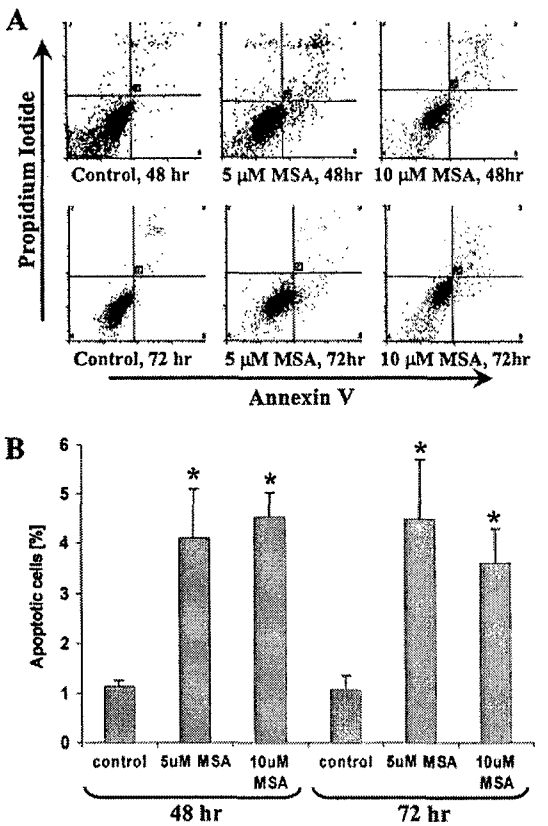

Fig. 3. Quantitation of apoptotic cells by flow cytometric analysis of MSA-treated PC-3 cells labeled with annexin V and PI. *A*, cytograms from flow cytometric analysis. Intact cells, early apoptotic cells, and late apoptotic and necrotic cells are located in the *lower left*, *lower right*, and *upper right quadrants* of the cytograms, respectively. *B*, percentages of early apoptotic cells. Data are presented as means ± SE (n = 4). *, statistically significant ($P < 0.05$) *versus* untreated control.

Table 2 *Number of genes modulated by MSA*

	Time point (h)			
Genes	12	24	36	48
Induced by MSA	502	926	255	133
Repressed by MSA	364	496	588	136

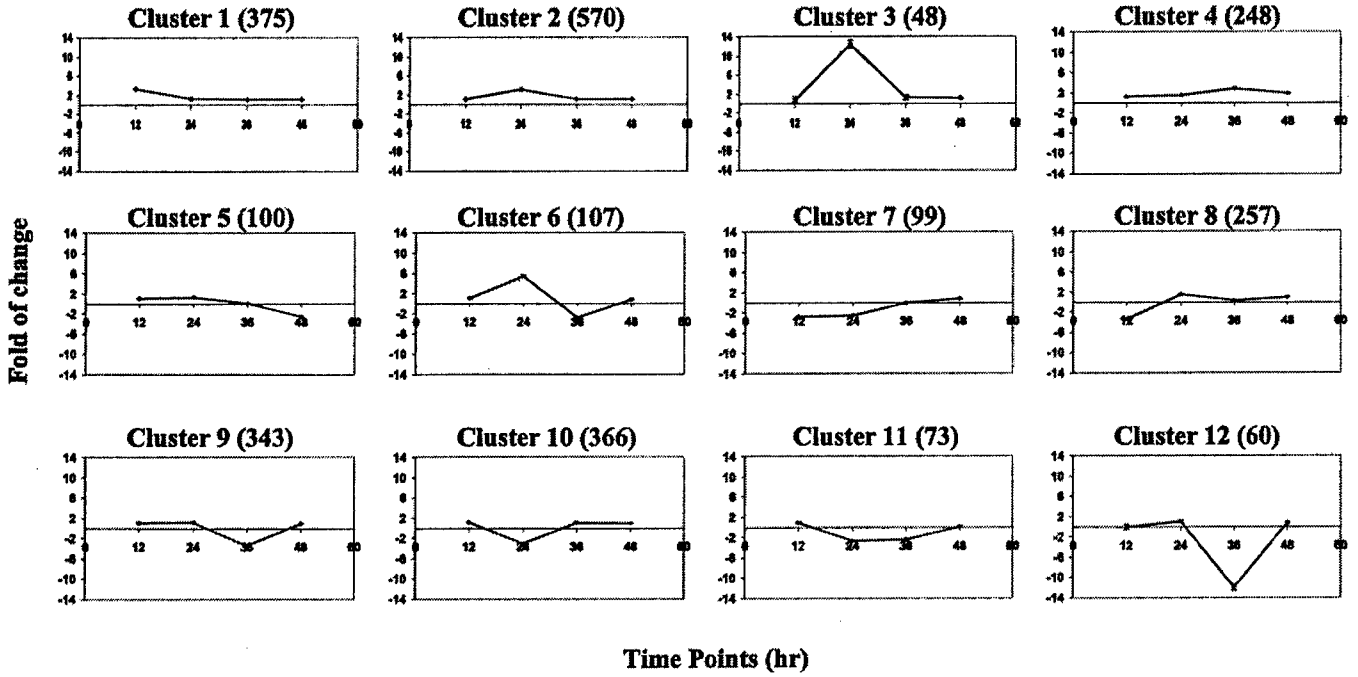

Fig. 4. Average gene expression profiles for each SOM cluster. The fold of change for each gene in a cluster was averaged and plotted against duration of treatment. Data are presented as means ± SE. *Numbers in parentheses*, the number of genes included in each cluster. Twelve clusters were derived from the clustering analysis, demonstrating different kinetics of modulation by MSA.

MSA treatment, the genes modulated by MSA at one or more time points were subjected to clustering analysis using the SOM algorithm. Clustering analysis avails to the grouping of genes according to similarities in their expression profiles across multiple time points. The SOM algorithm is ideal for pattern discovery and has been found to be useful in the elucidation of biological pathways, because genes that are regulated in a coordinated fashion are often related. A total of 2647 genes were included in this analysis. This represents 21% of the genes on the U95A GeneChip. These genes fell into 12 clusters of distinct kinetics pattern of modulation by MSA (Fig. 4), with the early response genes in clusters 1, 7, and 8; the intermediate response genes in clusters 2, 3, 6, 10, and 11; and the late response genes in clusters 4, 5, 9, and 12. Because cell growth inhibition by 10 μM MSA occurred between 24 to 48 h (Table 1), we consider the genes modulated by MSA at the 12-h time point as the early-response genes. We also believe that the change in expression of these early-response genes is important in initiating the cascade of events leading to the action of MSA. We, therefore, classify these early-response genes according to their known functions in cell growth/tumorigenesis (Table 3).

There is a prominent group of genes implicated in cell cycle regulation. Many negative cell cycle regulators were induced by MSA, including checkpoint proteins *RAD9* and *CHK2*, CDK inhibitors $p19^{INK4d}$ and $p21^{WAF1}$, *RB-binding protein 1*, *GADD45*, and *protein phosphatase 2C*. On the other hand, numerous cyclins, CDKs, and genes required for DNA replication or mitosis were repressed by MSA. Because these genes control the transition of different phases of the cell cycle, the change in their expression could mediate the inhibitory effect of MSA on cell cycle progression. There is a second group of genes involved in apoptosis. Both *toll-like receptor 2* and *caspase 9* were up-regulated by MSA. *Toll-like receptor 2* is a death receptor (18), and *caspase 9* is an upstream activator of the caspase cascade (19). In addition, MSA down-regulated the expression of *survivin*, a member of the IAP (inhibitor of apoptosis) family. The reason that so few apoptosis-regulatory genes were affected by MSA at the 12-h time point is probably because the induction of apoptosis by MSA did not become evident until after 48 h. An analysis of apoptosis gene expression changes at the 24- and 36-h time points will be the subject of a separate study.

In Table 3 is a group of genes encoding cytoskeleton components, cell membrane glycoproteins, as well as matrix metalloproteinases. The responses of cytoskeleton genes to MSA were varied. However, the up-regulation of invasion suppressors (*e.g., cadherins*) and the down-regulation of invasion activators (*e.g., integrins*, *endonexin*, hyaluronan receptors *CD44* and *RHAMM*, and *MMP21/22*) suggest a possible role of MSA in inhibiting tumor cell invasion. The table also shows a group of signal transduction genes that are responsive to MSA. In particular, there is a cluster of small GTPases and their associated factors, such as *Ras-like protein Tc10*, *GTPase activating factor-2*, *RAN-binding protein 8*, *G protein-coupled receptor 37*, *RAB31*, *RAB28*, *RAB7-like 1*, *regulator of G protein signaling 10*, *Rho E*, *Rho 2*, and *prenylated RAB acceptor 1*. These genes belong to the Ras and Rho family, the members of which are known to regulate diverse cellular functions, such as cell cycle progression, actin cytoskeleton organization, malignant transformation, and MAPK signaling cascades. In addition, MSA-mediated up-regulation of several MAPK cascade genes, including *MEK1*, *MEK3b*, *MEK5*, and *JNK1*, may amplify its effect on Ras/Rho signaling. Another noteworthy observation is the repression of a key player of the survival pathway, *PI3-kinase*. This suggests that selenium not only activates proapoptosis signals, but may also suppress survival signals to augment the stimulus to apoptosis.

MSA was found to modulate a large group of transcription factors, especially the zinc-finger family proteins (ZNFs), the myc proteins and associated factors, the ATF/CREB proteins and their binding proteins, as well as the inhibitor of DNA synthesis (Id) family proteins. Many of these transcription factors play critical roles in the regulation of cell cycle progression, apoptosis, and malignant transformation. The change in the expression of these *trans*-acting factors could lead to an altered transcription of a series of other genes. To wrap up the information summarized in Table 3, two growth factors

Table 3 *Functional classification of MSA early-response genes*

A value >1 represents induction; a value <1 represents repression.

Gene	Modulation
Cell cycle	
RAD9	3.0
RB-binding protein 1	2.0
$p19^{INK4d}$	2.0
GADD45	2.0
$p21^{WAF1}$	3.0
PP2C-β	4.0
PP2C-α2	2.0
CHK2	3.0
CDC8	0.6
CDC7-related kinase	0.5
M phase phosphoprotein 1	0.4
ribonucleotide reductase M1 subunit	0.4
STK15	0.5
Mitosin	0.5
thymidylate synthase	0.2
chromatin assembly factor-1 p150 subunit	0.5
CDK1	0.5
MCM7	0.3
replication factor C	0.4
replication protein A 32-kDa subunit	0.5
dihydrofolate reductase (DHFR)	0.2
PCTAIRE-1	0.3
DNA pol-ε subunit B	0.3
DNA pol-α	0.4
protein phosphatase 2A regulatory subunit α	0.2
Cyclin A	0.3
Cyclin E2	0.3
MCM6	0.5
Ki67a	0.2
DNA primase	0.4
Kinesin-like 1	0.2
MCM3	0.4
Lamin B2	0.4
CDK4	0.5
MCM5	0.2
PCNA	0.1
CDK2	0.5
Apoptosis	
toll-like receptor 2	2.6
Caspase 9	2.0
Survivin	0.3
Angiogenesis	
VEGF-C	0.4
Protein synthesis	
eIF-4γ	0.5
Growth factor	
bFGF	0.3
Wnt7a	0.3
Tumor suppressor/Growth inhibitor	
BRCA2	3.2
DLC-1	3.1
TGF-β	2.9
TGF-β type III receptor	3.6
BMP-4	4.8
PTEN	2.0
Transcription factor	
BACH1	2.2
Hox5.4	5.3
ZNF345	2.8
ZNF217	3.6
ZNF165	3.8
ZNF267	2.9
ZNF75	2.3
Ring ZNF	2.5
ZNF274	3.2
ZNF278	0.5
ZNF X-linked	0.3
Kruppel-like ZNF	3.5
CBP/p300-interacting transcativation	2.5
CREB1	3.0
ATF5	0.4
E74-like factor 3	2.4
SRC1	2.6
Id1	0.5
Id3	0.2
Forkhead box M1B	0.4
N-myc interactor	0.5
Myc-associated ZNF	0.2
b-myb	0.1
Jun-B	0.1
HNF-3α	0.5
TAFII70-α	0.5
NFκB p50	0.2
BAF57	0.5
HFH-11A	0.4
GADD153	8.0
DNA repair	
hPMS2	6.0
ERCC1	3.3
Signal transduction	
MEK1	2.3
MEK3b	2.1
MEK5	6.0
JNK1	3.0
Ras-like protein Tc10	3.8
GTPase activating factor-2	4.4
RAN-binding protein 8	3.1
G protein-coupled receptor 37	2.3
RAB31	2.5
RAB28	2.1
RAB7-like 1	2.4
Regulator of G protein signaling 10	2.0
Rho E	3.2
Rho 2	0.5
prenylated RAB acceptor 1	0.4
cAMP-regulated guanine nucleotide exchange factor II	2.2
CDP-DAG synthase	2.3
phospholipase C β4	2.1
receptor of retinoic acid	5.0
dual specificity phosphatase MKP-5	6.4
calmodulin-dependent protein kinase IV	2.0
PKC-α	3.4
PP1	2.3
PP5	0.2
PI 3-kinase	0.4
Cytoskeleton	
Adducin-γ	2.4
Calponin	5.3
Actin-binding protein 57	11.9
Cytokeratin 20	4.1
Tau	0.2
Filamin	0.2
Tubulin α 1 isoform 44	0.4
Non-muscle α-actinin	0.4
Adhesion/Invasion	
Cadherin-15	6.5
Cadherin-7	2.5
integrin β-5	0.2
integrin β-4	0.3
β 3-endonexin	0.5
CD44	0.5
RHAMM	0.2
MMP21/22	0.1

(*bFGF* and *Wnt7a*), an angiogenesis molecule (*VEGF-C*), and one translation-initiation factor gene (*eIF-4γ*) that is amplified in cancer cells (20), were down-regulated by MSA. In contrast, three tumor suppressor genes (*BRCA2*, *DLC-1*, and *PTEN*), three TGF-β family members or receptor (*TGF-β*, *TGF-β type III receptor*, and *BMP-4*), and two DNA repair genes (*hPMS2* and *ERCC1*) were up-regulated by MSA. The regulation of these genes may represent additional mechanisms by which MSA exerts its anticancer effect.

Confirmation of Array Data. We used Western blot analysis to confirm the changes in expression of a subset of 10 cell cycle genes: *CHK2*, *$p21^{WAF1}$*, *GADD153*, *cyclin A*, *DHFR*, *CDK1*, *CDK2*, *CDK4*, *PCNA*, and *cyclin E2*. As shown in Fig. 5 and Table 4, the Western expression changes of 7 genes (*CHK2*, *$p21^{WAF1}$*, *GADD153*, *cyclin A*, *DHFR*, *CDK1*, and *CDK2*) correlated well with the array data. This represents an agreement rate of 70%. The lack of complete concordance could be attributable to either false positive signals of the array data or the discrepancy between transcript and protein expression. One noteworthy finding is that although both array and Western analyses showed a down-regulation of CDK2 by MSA, the Western

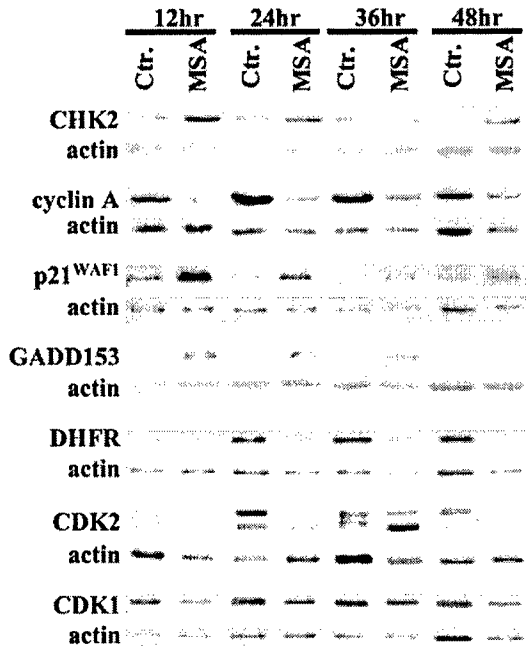

Fig. 5. Confirmation of array data by Western blot analysis. TRIzol-isolated proteins from PC-3 cells were subjected to immunoblotting using an antibody specific for CHK2, cyclin A, $p21^{WAF1}$, GADD153, DHFR, CDK2, or CDK1. Signals were normalized to the ones for actin to control for loading variation. The results shown here are representative of that from three similar independent experiments.

data additionally revealed a reduction of phosphorylated CDK2 (Fig. 5; Table 4). This dichotomy clearly reinforces a fundamental limitation of the array technology in that changes beyond the step of gene transcription are not detectable by this method.

DISCUSSION

Prostate cancer is the most common cancer diagnosed and the second leading cause of cancer-related deaths in men in the United States. However, little is known about the etiological factors for this disease. Consequently, it is not possible to institute primary intervention strategies to remove the causative agents from the environment. Secondary intervention strategies are, therefore, necessary to reduce the morbidity and mortality of prostate cancer, and selenium intervention has been championed as a viable option. The present study was undertaken to investigate the molecular targets and the signaling pathways underlying the anticancer activity of selenium in prostate.

Previous studies by Sinha and Medina and by Sinha *et al.* (12, 13) showed that selenium is able to block cell cycle progression at specific checkpoints, which might be explained by a decrease in CDK2 kinase activity. These experiments were done with mouse mammary tumor cells treated with 50 μM of methylselenocysteine; this concentration of selenium is at least 10 times higher than that found in the circulation under normal physiological condition. For this reason, MSA is a more appropriate agent for *in vitro* studies. Our results demonstrate that MSA inhibits the growth of prostate cancer cells by cell cycle blockade and apoptosis. We used the GeneChip technology to profile selenium-mediated gene expression changes in a time course experiment. Of a total of 12,000 genes screened, over 2,500 were identified to be responsive to selenium treatment. The shear magnitude of this number is somewhat unexpected. These genes were grouped into early-, intermediate-, and late-response clusters. Because the early-response genes are likely to be more important in initiating the effects of selenium, we focused our attention on them in our follow-up analysis.

Certain key cell cycle regulators are among the early-response genes. On the basis of their altered expression, we propose a number of tentative signaling pathways (in a cartoon format) that might mediate the outcome of cell cycle blockade by selenium. As shown in Fig. 6, selenium treatment increases the expression of $p21^{WAF1}$, which has dual functions in regulating the activity of CDK/cyclin complexes. Although $p21^{WAF1}$ is a potent inhibitor of cyclin E/A-dependent CDK1/2, it promotes the assembly and the nuclear translocation of cyclin D-CDK4/6 complexes, leading to an increase in cyclin D-associated kinase activity (21). However, the induction of $p19^{INK4d}$ by selenium counteracts the latter effect. The $p19^{INK4d}$ protein binds to and inhibits the cyclin D-CDK4/6 complexes, thus releasing $p21^{WAF1}$ from CDK4 and CDK6. The cooperative action of $p19^{INK4d}$ and $p21^{WAF1}$ leads ultimately to an inhibition of both cyclin D- and cyclin A/E-dependent kinases. The down-regulation of CDK1, CDK2 and cyclin A by selenium provides an amplified effect on this cascade of events. Complete phosphorylation/inactivation of pRB requires the sequential actions of cyclin D-CDK4/6 and cyclin E-CDK2 (22). Thus, $p19^{INK4d}$- and $p21^{WAF1}$-mediated inhibition of CDK2, CDK4, and CDK6 could result in decreased phosphorylation of pRB. Hypophosphorylated pRB interacts with, and negatively regulates, the activity of E2F transcription factors. Loss of E2F activity prevents the transcription of genes, *e.g., DHFR* and *cyclin A*, required for progression into S phase. In addition, although not depicted in Fig. 6, $p21^{WAF1}$ is able to bind to PCNA and directly inhibit its activity (23), and interact with E2F subunits and disrupt E2F-CDK-p107 DNA binding complex (24, 25). These changes, collectively, are expected to result in a blockade of DNA replication.

As shown in Fig. 7, the elevated expression of CHK2 by selenium treatment leads to increased phosphorylation of CDC25 proteins, which subsequently bind to 14-3-3 proteins and are exported to the cytoplasm. CDC25 proteins are responsible for removing the inhibitory phosphates from CDK1 and CDK2, allowing them to be activated

Table 4 *Comparison of expression changes detected by array and Western analyses*

The values represent treatment:control ratio.

	Array analysis					Western analysis[a]				
Gene	12 h	24 h	36 h	48 h	Diff Call[b]	12 h	24 h	36 h	48 h	Diff Call
CHK2	3	1	1	1	↑	3	4	1	10	↑
p21WAF1	3	1	1	1	↑	3	5	4	3	↑
GADD153	8	12	6	2	↑	14	6	8	1	↑
cyclin A	0.3	1	0.3	0.4	↓	0.3	0.3	0.4	1	↓
DHFR	0.25	1	0.5	1	↓	0.3	0.3	0.3	0.2	↓
CDK1	0.5	0.5	1	1	↓	0.3	0.7	1	1	↓
CDK2										
Phosphorylated	0.5	1	1	1	↓	0.4	0.06	0.6	0.09	↓
Unphosphorylated						0.3	0.3	10	0.8	↓

[a] The value represents the mean of three experiments. The SE is about 10%.
[b] Diff Call, difference call; ↑, increase; ↓, decrease.

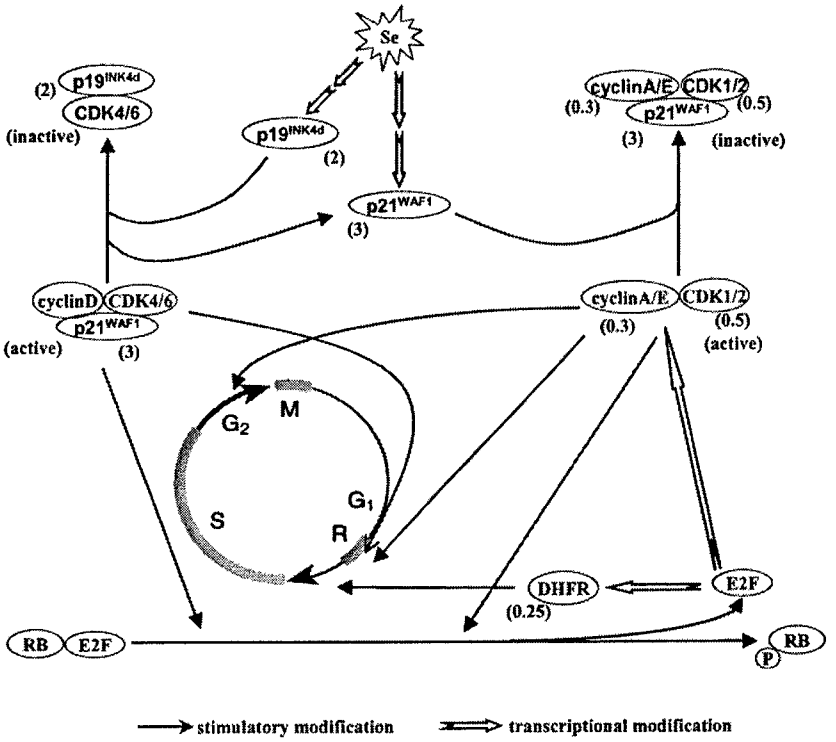

Fig. 6. Schematic representation of signaling pathways downstream of $p19^{INK4d}$ and $p21^{WAF1}$ mediating MSA-induced cell cycle blockade (see "Discussion"). The numbers in parentheses indicate the treatment:control-signal ratio detected by array analysis. Up-regulation is denoted by a ratio of ≥2, and down-regulation is denoted by a ratio of ≤0.5. All changes, except the one for $p19^{INK4d}$, were confirmed by Western blot analysis.

by CDK activating kinases (26, 27). A deficiency in nuclear CDC25 proteins prevents the activation of CDK1 and CDK2 to facilitate cell cycle progression. PP2Cs are phosphatases known to remove the activation phosphates from CDK1 and CDK2. An increased expression of PP2Cs by selenium will essentially lead to less active CDK1 and CDK2. CDK2 causes increased phosphorylation of MCMs either directly or indirectly through CDC7. MCMs are important for transition to S phase. By decreasing the expression of CDK2, CDC7, and MCMs, selenium is able to block DNA synthesis. Selenium can also induce a G_2-M block by increasing the expression of the checkpoint protein, RAD9. Furthermore, the expression of GADD153 is known to increase in response to a variety of growth arrest or DNA damage signals (28–35). GADD153 plays an essential role in cell cycle control and apoptosis (36). We recently found that in premalignant human breast cells, selenium induced an 8-fold increase in the expression of the *GADD153* gene (8). Similarly, a 6–14-fold induction (Table 4) was also observed in PC-3 cells. In summary, Figs. 6 and 7 show that different pathways modulated by selenium all converge to block cell cycle progression.

It is clear that selenium affects not just one key target, but a multitude of targets. In doing so, the impact of selenium is amplified. The diversity of the molecular responses also makes it difficult for transformed cells to escape the inhibitory effect of selenium. A reassuring aspect of our results is the considerable overlap of the selenium-modulated genes or signaling pathways identified in prostate cells with those previously identified in breast cells (8). The

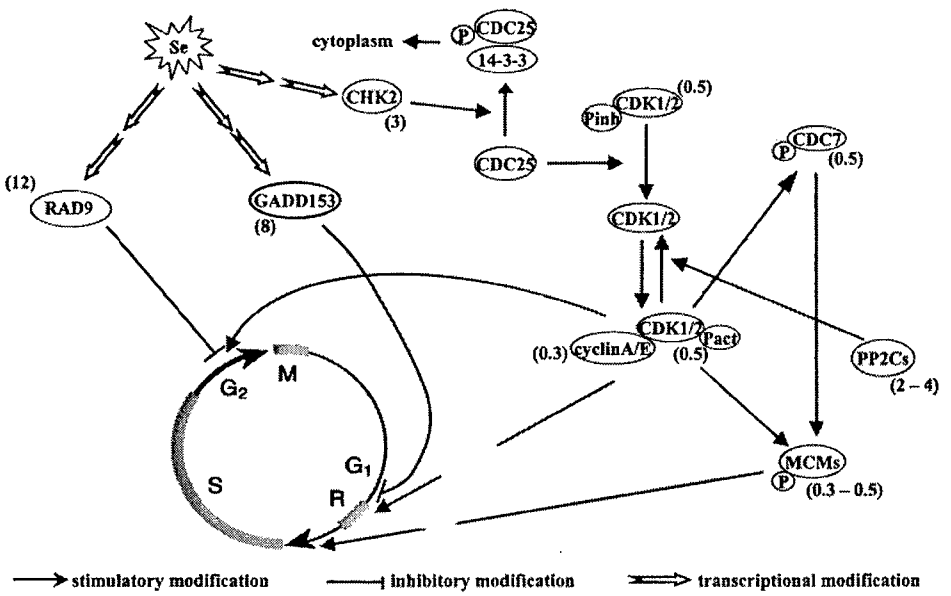

Fig. 7. Schematic representation of signaling pathways downstream of CHK2, GADD153, and RAD9 mediating MSA-induced cell cycle blockade (see "Discussion"). The numbers in parentheses indicate the treatment:control-signal ratio detected by array analysis. Up-regulation is denoted by a ratio of ≥2, and down-regulation is denoted by a ratio of ≤0.5.

congruency, however, is highlighted against a backdrop of certain differences in cell genotype and methodological issues. The PC-3 human prostate cancer cells are null for p53, whereas the premalignant MCF10AT human breast cells have a functional p53, suggesting that p53 is not required for the action of selenium The 12,000-gene oligonucleotide GeneChip was used in the prostate cell study, whereas the 200-gene membrane-based cDNA array was used in the breast cell study. Despite these differences, similar selenium targets were identified, including GADD153, cyclin A, CDK1, CDK2, CDK4, CDC25, E2Fs, as well as the MAPK/JNK and phosphoinositide-3 kinase pathways, thus lending confidence to the array data. Previous studies of gene expression changes in response to selenium have generally been limited to the analysis of a few or a subset of genes and, therefore, have provided only a very narrow view of the entire landscape. As far as we are aware of, this is the most comprehensive gene expression profiling study on the molecular mechanism of selenium in chemoprevention.

Venkateswaran *et al.* (37) recently reported that PC-3 cells are not growth inhibited by Se-Met unless they are transfected with a functional androgen receptor. Suffice it to point out that the sensitivity of PC-3 and another androgen-independent prostate cancer cell line, DU-145, to Se-Met has been documented by two other groups of investigators (38, 39). Furthermore, Jiang *et al.* (9) showed that DU-145 cells can be induced to undergo apoptosis by MSA at physiological concentrations. Together with our study, the weight of evidence seems to favor the notion that the responsiveness of prostate cancer cells to selenium is not dependent on the presence of a functional androgen receptor. Although androgen plays a critical role in prostate carcinogenesis, a significant proportion of prostate cancers eventually become androgen-unresponsive and refractory to hormonal therapy. The fact that androgen-unresponsive cells are sensitive to selenium-induced growth inhibition is encouraging because it suggests that selenium intervention may be a viable strategy for preventing prostate cancer recurrence after prostatectomy.

ACKNOWLEDGMENTS

We are grateful to Dorothy Donovan, Tamora Loftus, Todd Parsons, Rita Pawlak, Cathy Russin, and Janice Hoffmann for their excellent technical assistance.

REFERENCES

1. Clark, L. C., Combs, G. F., Jr., Turnbull, B. W., Slate, E. H., Chalker, D. K., Chow, J., Davis, L. S., Glover, R. A., Graham, G. F., Gross, E. G., Krongrad, A., Lesher, J. L., Jr., Park, H. K., Sanders, B. B., Jr., Smith, C. L., and Taylor, J. R. Effects of selenium supplementation for cancer prevention in patients with carcinoma of the skin. A randomized controlled trial. Nutritional Prevention of Cancer Study Group. J. Am. Med. Assoc., *276:* 1957–1963, 1996.
2. Hoque, A., Albanes, D., Lippman, S. M., Spitz, M. R., Taylor, P. R., Klein, E. A., Thompson, I. M., Goodman, P., Stanford, J. L., Crowley, J. J., Coltman, C. A., and Santella, R. M. Molecular epidemiologic studies within the selenium and vitamin E cancer prevention trial (SELECT). Cancer Causes Control, *12:* 627–633, 2001.
3. Ip, C. Differential effect of dietary methionine on the biopotency of selenomethionine and selenite in cancer chemoprevention. J. Natl. Cancer Inst. (Bethesda), *80:* 258–262, 1988.
4. Ip, C., and Hayes, C. Tissue selenium levels in selenium-supplemented rats and their relevance in mammary cancer protection. Carcinogenesis (Lond.), *10:* 921–925, 1989.
5. Ip, C., and Ganther, H. E. Activity of methylated forms of selenium in cancer prevention. Cancer Res., *50:* 1206–1211, 1990.
6. Ip, C., Hayes, C., Budnick, R. M., and Ganther, H. E. Chemical form of selenium, critical metabolites, and cancer prevention. Cancer Res., *51:* 595–600, 1991.
7. Ip, C., Thompson, H. J., Zhu, Z., and Ganther, H. E. *In vitro* and *in vivo* studies of methylseleninic acid: evidence that a monomethylated selenium metabolite is critical for cancer chemoprevention. Cancer Res., *60:* 2882–2886, 2000.
8. Dong, Y., Ganther, H. E., Stewart, C., and Ip, C. Identification of molecular targets associated with selenium-induced growth inhibition in human breast cells using cDNA microarrays. Cancer Res., *62:* 708–714, 2002.
9. Jiang, C., Wang, Z., Ganther, H., and Lu, J. Caspases as key executors of methyl selenium-induced apoptosis (anoikis) of DU-145 prostate cancer cells. Cancer Res., *61:* 3062–3070, 2001.
10. Sinha, R., Unni, E., Ganther, H. E., and Medina, D. Methylseleninic acid, a potent growth inhibitor of synchronized mouse mammary epithelial tumor cells *in vitro.* Biochem. Pharmacol., *61:* 311–317, 2001.
11. Vistica, D. T., Skehan, P., Scudiero, D., Monks, A., Pittman, A., and Boyd, M. R. Tetrazolium-based assays for cellular viability: a critical examination of selected parameters affecting formazan production. Cancer Res., *51:* 2515–2520, 1991.
12. Sinha, R., and Medina, D. Inhibition of cdk2 kinase activity by methylselenocysteine in synchronized mouse mammary epithelial tumor cells. Carcinogenesis (Lond.), *18:* 1541–1547, 1997.
13. Sinha, R., Kiley, S. C., Lu, J. X., Thompson, H. J., Moraes, R., Jaken, S., and Medina, D. Effects of methylselenocysteine on PKC activity, cdk2 phosphorylation and *gadd* gene expression in synchronized mouse mammary epithelial tumor cells. Cancer Lett., *146:* 135–145, 1999.
14. Wang, Y., Rea, T., Bian, J., Gray, S., and Sun, Y. Identification of the genes responsive to etoposide-induced apoptosis: application of DNA chip technology. FEBS Lett., *445:* 269–273, 1999.
15. Kaminski, N., Allard, J. D., Pittet, J. F., Zuo, F., Griffiths, M. J. D., Morris, D., Huang, X., Sheppard, D., and Heller, R. A. Global analysis of gene expression in pulmonary fibrosis reveals distinct programs regulating lung inflammation and fibrosis. Proc. Natl. Acad. Sci. USA, *97:* 1778–1783, 2000.
16. Chen, C-R., Kang, Y., and Massague, J. Defective repression of c-myc in breast cancer cells. Proc. Natl. Acad. Sci. USA, *98:* 992–999, 2001.
17. Dong, Y., Asch, H. L., Medina, D., Ip, C., Ip, M., Guzman, R., and Asch, B. B. Concurrent deregulation of gelsolin and cyclin D1 in the majority of human and rodent breast cancers. Int. J. Cancer, *81:* 930–938, 1999.
18. Aliprantis, A. O., Yang, R. B., Weiss, D. S., Godowski, P., and Zychlinsky, A. The apoptotic signaling pathway activated by Toll-like receptor-2. EMBO J., *19:* 3325–3336, 2000.
19. Kuida, K., Haydar, T. F., Kuan, C. Y., Gu, Y., Taya, C., Karasuyama, H., Su, M. S., Rakic, P., and Flavell, R. A. Reduced apoptosis and cytochrome c-mediated caspase activation in mice lacking caspase 9. Cell, *94:* 325–337, 1998.
20. Brass, N., Heckel, D., Sahin, U., Pfreundschuh, M., Sybrecht, G. W., and Meese, E. Translation initiation factor eIF-4γ is encoded by an amplified gene and induces an immune response in squamous cell lung carcinoma. Hum. Mol. Genet., *6:* 33–39, 1997.
21. Sherr, C. J., and Roberts, J. M. CDK inhibitors: positive and negative regulators of G_1-phase progression. Genes Dev., *13:* 1501–1512, 1999.
22. Lundberg, A. S., and Weinberg, R. A. Functional inactivation of the retinoblastoma protein requires sequential modification by at least two distinct cyclin-cdk complexes. Mol. Cell. Biol., *18:* 753–761, 1998.
23. Waga, S., Hannon, G. J., Beach, D., and Stillman, B. The p21 inhibitor of cyclin-dependent kinases controls DNA replication by interaction with PCNA. Nature (Lond.), *369:* 574–578, 1994.
24. Delavaine, L., and La Thangue, N. B. Control of E2F activity by p21Waf1/Cip1. Oncogene, *18:* 5381–5392, 1999.
25. Dimri, G. P., Nakanishi, M., Desprez, P. Y., Smith, J. R., and Campisi, J. Inhibition of E2F activity by the cyclin-dependent protein kinase inhibitor p21 in cells expressing or lacking a functional retinoblastoma protein. Mol. Cell. Biol., *16:* 2987–2997, 1996.
26. Falck, J., Mailand, N., Syljuasen, R. G., Bartek, J., and Lukas, J. The ATM-Chk2-Cdc25A checkpoint pathway guards against radioresistant DNA synthesis. Nature (Lond.), *410:* 842–847, 2001.
27. Matsuoka, S., Huang, M., and Elledge, S. J. Linkage of ATM to cell cycle regulation by the Chk2 protein kinase. Science (Wash. DC), *282:* 1893–1897, 1998.
28. Abcouwer, S. F., Schwarz, C., and Meguid, R. A. Glutamine deprivation induces the expression of GADD45 and GADD153 primarily by mRNA stabilization. J. Biol. Chem., *274:* 28645–28651, 1999.
29. Choi, A. M., Fargnoli, J., Carlson, S. G., and Holbrook, N. J. Cell growth inhibition by prostaglandin A2 results in elevated expression of gadd153 mRNA. Exp. Cell Res., *199:* 85–89, 1992.
30. Eymin, B., Dubrez, L., Allouche, M., and Solary, E. Increased gadd153 messenger RNA level is associated with apoptosis in human leukemic cells treated with etoposide. Cancer Res., *57:* 686–695, 1997.
31. Guyton, K. Z., Xu, Q., and Holbrook, N. J. Induction of the mammalian stress response gene *GADD153* by oxidative stress: role of AP-1 element. Biochem. J., *314(Pt 2):* 547–554, 1996.
32. Jeong, J. K., Huang, Q., Lau, S. S., and Monks, T. J. The response of renal tubular epithelial cells to physiologically and chemically induced growth arrest. J. Biol. Chem., *272:* 7511–7518, 1997.
33. Johnsson, A., Strand, C., and Los, G. Expression of GADD153 in tumor cells and stromal cells from xenografted tumors in nude mice treated with cisplatin: correlations with cisplatin- DNA adducts. Cancer Chemother. Pharmacol., *43:* 348–352, 1999.
34. Kim, R., Ohi, Y., Inoue, H., and Toge, T. Taxotere activates transcription factor AP-1 in association with apoptotic cell death in gastric cancer cell lines. Anticancer Res., *19:* 5399–5405, 1999.
35. Luethy, J. D., and Holbrook, N. J. Activation of the gadd153 promoter by genotoxic agents: a rapid and specific response to DNA damage. Cancer Res., *52:* 5–10, 1992.
36. Zinszner, H., Kuroda, M., Wang, X., Batchvarova, N., Lightfoot, R. T., Remotti, H., Stevens, J. L., and Ron, D. CHOP is implicated in programmed cell death in response to impaired function of the endoplasmic reticulum. Genes Dev., *12:* 982–995, 1998.
37. Venkateswaran, V., Klotz, L. H., and Fleshner, N. E. Selenium modulation of cell proliferation and cell cycle biomarkers in human prostate carcinoma cell lines. Cancer Res., *62:* 2540–2545, 2002.
38. Menter, D. G., Sabichi, A. L., and Lippman, S. M. Selenium effects on prostate cell growth. Cancer Epidemiol. Biomark. Prev., *9:* 1171–1182, 2000.
39. Redman, C., Scott, J. A., Baines, A. T., Basye, J. L., Clark, L. C., Calley, C., Roe, D., Payne, C. M., and Nelson, M. A. Inhibitory effect of selenomethionine on the growth of three selected human tumor cell lines. Cancer Lett., *125:* 103–110, 1998.

[CANCER RESEARCH 64, 19–22, January 1, 2004]

Advances in Brief

Prostate Specific Antigen Expression Is Down-Regulated by Selenium through Disruption of Androgen Receptor Signaling

Yan Dong,[1] Soo Ok Lee,[2,3] Haitao Zhang,[1] James Marshall,[1] Allen C. Gao,[2,3] and Clement Ip[1]

Departments of [1]Cancer Prevention and Population Sciences, [2]Medicine, and [3]Pharmacology and Therapeutics, Roswell Park Cancer Institute, Buffalo, New York

Abstract

A previous controlled intervention trial showed that selenium supplementation was effective in reducing the incidence of prostate cancer. Physiological concentrations of selenium have also been reported to inhibit the growth of human prostate cancer cells *in vitro*. The present study describes the observation that selenium was able to significantly down-regulate the expression of prostate-specific antigen (PSA) transcript and protein within hours in the androgen-responsive LNCaP cells. Decreases in androgen receptor (AR) transcript and protein followed a similar dose and time response pattern upon exposure to selenium. The reduction of AR and PSA expression by selenium occurred well before any significant change in cell number. With the use of a luciferase reporter construct linked to either the PSA promoter or the androgen responsive element, it was found that selenium inhibited the *trans*-activating activity of AR in cells transfected with the wild-type AR expression vector. Selenium also suppressed the binding of AR to the androgen responsive element site, as evidenced by electrophoretic mobility shift assay of the AR-androgen responsive element complex. In view of the fact that PSA is a well-accepted prognostic indicator of prostate cancer, an important implication of this study is that a selenium intervention strategy aimed at toning down the amplitude of androgen signaling could be helpful in controlling morbidity of this disease.

Introduction

Prostate cancer is the second most common cancer as well as the second most common cause of cancer death in men in the United States. Every year, there are ~190,000 new cases and 30,000 deaths from prostate cancer (1). Age is a major risk factor; the incidence is 1 in 53 for men in their 50s but 1 in 7 for men from 60 to 80 years of age. A chemopreventive modality that can suppress or delay the clinical symptoms of prostate cancer would be well suited for preserving the quality of life in high-risk elderly men. In a previous randomized, placebo-controlled cancer prevention trial in which prostate cancer was evaluated as a secondary end point (974 of the 1312 subjects in the cohort were men), supplementation with a nutritional dose of selenium was found to reduce prostate cancer incidence by 50% (2, 3). Recent studies by Dong *et al.* (4) showed that selenium inhibited human prostate cancer cell growth, blocked cell cycle progression at multiple transition points, and induced programmed cell death. Prostate specific antigen (PSA) is a gene known to be under the control of the androgen receptor (AR) and is a well-accepted marker for the diagnosis and prognosis of prostate cancer. In view of the clinical observation of the effectiveness of selenium in prostate cancer prevention, it is reasonable to believe that selenium might be able to reduce the expression of PSA. If confirmed, this attribute obviously has the advantage of forecasting the responsiveness to selenium intervention. In this report, we describe a series of experiments that were designed to test the hypothesis that selenium is capable of down-regulating PSA through a mechanism of attenuating the functional intensity of the AR signal transduction pathway.

As discussed previously (4), cultured prostate cells respond poorly to selenomethionine (a commonly used selenium reagent) and only when it is present at supraphysiological levels in the medium. A plausible explanation is that prostate cells have a low capacity in metabolizing selenomethionine to methylselenol (CH_3SeH), which is believed to be the active species for selenium chemoprevention (5). This process normally takes place in the liver and kidney. For this reason, methylseleninic acid (CH_3SeO_2H, abbreviated to MSA) was developed by Ip *et al.* (6) specifically for *in vitro* experiments. Once taken up by cells, MSA is readily reduced by glutathione and NADPH to methylselenol (which is rather unstable in itself) via a non-enzymatic reaction. The cellular and molecular responses of prostate cells to physiological concentrations of MSA have been documented in a number of publications (4, 7–10). Thus, we believe we have the right tool to study the effect of selenium on AR signaling.

Materials and Methods

Selenium Reagent, Prostate Cell Culture, and Cell Growth Analysis. MSA was synthesized as described previously (6). The LNCaP human prostate cancer cells were obtained from American Type Culture Collection (Manassas, VA). The cells were cultured in RPMI 1640 supplemented with 10% fetal bovine serum (FBS), 2 mM glutamine, 100 units/ml of penicillin, and 100 μg/ml of streptomycin (11). In some experiments, cells were cultured in an androgen-defined condition by using charcoal-stripped FBS in the presence of 10 nM R1881 (a potent synthetic androgen). The 3-(4,5-dimethylthiazol-2-yl)-2,5-diphenyltetrazolium bromide assay was performed 24, 48, or 72 h after MSA treatment as described previously (11). For the quantitative determination of AR and PSA transcripts and proteins, cells were exposed to MSA for much shorter periods of time, usually 24 h or less. Total RNA and protein were isolated using the TRIzol reagent (Invitrogen, Carlsbad, CA).

Real-Time Reverse Transcription-PCR. First-strand cDNA was synthesized from 100 ng of total RNA by SuperScript II reverse transcriptase (Invitrogen) following the manufacturer's protocol. The PCR primers and TaqMan probes for β-actin, AR, and PSA were Assays-on-Demand products from Applied Biosystems. Two μl of first-strand cDNA were mixed with 25 μl of 2× Taqman Universal PCR Master Mix (Applied Biosystems) and 2.5 μl of 20× primers/probe mixture in a 50-μl final volume. Temperature cycling and real-time fluorescence measurement were performed using an ABI prism 7700 Sequence Detection System (Applied Biosystems). The PCR conditions were as follows: an initial incubation at 50°C for 2 min, then a denaturation at 95°C for 10 min, followed by 40 cycles of 95°C for 15 s and 60°C for 1 min.

The relative quantitation of gene expression was performed using the comparative C_T ($\Delta\Delta C_T$) method (12). Briefly, the threshold cycle number (C_T) was obtained as the first cycle at which a statistically significant increase in fluorescence signal was detected. Data normalization was carried out by subtracting the C_T value of β-actin from that of the target gene. The $\Delta\Delta C_T$ was calculated as the difference of the normalized C_T values (ΔC_T) of the treatment

Received 9/4/03; revised 10/17/03; accepted 11/03/03.

Grant support: Department of Defense Postdoctoral Fellowship Award and an AACR-Cancer Research Foundation of America Fellowship in Prevention Research Award (to Y. D.), Grant CA90271 (to A. C. G.) and Grant CA91990 (to C. I.) from the National Cancer Institute, and also in part by Cancer Center Support Grant P30 CA16056 (to R. P. C. I.) from the National Cancer Institute.

The costs of publication of this article were defrayed in part by the payment of page charges. This article must therefore be hereby marked *advertisement* in accordance with 18 U.S.C. Section 1734 solely to indicate this fact.

Notes: Y. Dong and S. O. Lee contributed equally to this work.

Requests for reprints: Allen C. Gao or Clement Ip, Department of Surgical Oncology, Roswell Park Cancer Institute, Elm and Carlton Streets, Buffalo, NY 14263.

and control samples: $\Delta\Delta C_T = \Delta C_{T\ \text{treatment}} - \Delta C_{T\ \text{control}}$. Finally, $\Delta\Delta C_T$ was converted to fold of change by the following formula: Fold of change = $2^{-\Delta\Delta C_T}$.

Western Blot Analysis. Details of the procedure were described previously (4). Immunoreactive bands were quantitated by volume densitometry and normalized against either glyceraldehyde-3-phosphate dehydrogenase or α-actin. The following monoclonal antibodies were used (source): anti-glyceraldehyde-3-phosphate dehydrogenase (Chemicon, Temecula, CA), anti-α-actin (Sigma Chemical Co., St. Louis, MO), anti-AR (BD Transduction Laboratory, San Jose, CA), and anti-PSA (Santa Cruz Biotechnology, Santa Cruz, CA).

Transfection and Luciferase Assay. An aliquot of 3×10^5 cells was placed in a 6-well plate and then transfected with a total amount of 5 μg of DNA using Superfect (Qiagen, Valencia, CA) according to the manufacturer's instructions. Two different constructs were evaluated: the PSA promoter-luciferase reporter plasmid (13) and the androgen responsive element (ARE)-luciferase reporter plasmid (14). The total amount of plasmid DNA was normalized to 5 μg/well by the addition of empty plasmid. The DNA/liposome mixture was removed 3 h later, and cells were treated with different concentrations of MSA in the presence of 10 nM R1881. Cell extracts were obtained after 24 h, and luciferase activity was assayed using the Luciferase Assay System (Promega, Madison, WI). Protein concentration in cell extracts was determined by the Coomassie Plus protein assay kit (Pierce, Rockford, IL). Luciferase activities were normalized by the protein concentration of the sample. All transfection experiments were performed in triplicate wells and repeated at least four times.

Nuclear Lysate Preparation. Nuclear protein extract was prepared as described previously (15). Cells were harvested, washed with PBS twice, and resuspended in a hypotonic buffer [10 mM HEPES-KOH (pH 7.9), 1.5 mM $MgCl_2$, 10 mM KCl, and 0.1% NP40] and incubated on ice for 10 min. Nuclei were precipitated with 3000 × *g* centrifugation at 4°C for 10 min. After washing once with the hypotonic buffer, the nuclei were lysed in a lysis buffer [50 mM Tris-HCl (pH 8.0), 150 mM NaCl, and 1% Triton X-100] and incubated on ice for 30 min. The nuclear lysate was precleared by 20,000 × *g* centrifugation at 4°C for 15 min. Protein concentration was determined by the Coomassie Plus protein assay kit.

Electrophoretic Mobility Shift Assay (EMSA). A quantity of 20 μg of nuclear protein extract was incubated in a 20-μl solution containing 10 mM HEPES (pH 7.9), 80 mM NaCl, 10% glycerol, 1 mM DTT, 1 mM EDTA, 100 μg/ml poly(deoxyinosinic-deoxycytidylic acid), and the radiolabeled double-stranded AR consensus binding motif 5′-CTAGAAGTCTGGTACAGGGT-GTTCTTTTTGCA-3′ (Santa Cruz Biotechnology). The protein-DNA complexes were resolved on a 4.5% nondenaturing polyacrylamide gel containing 2.5% glycerol in 0.25× Tris-borate EDTA at room temperature, and the results were autoradiographed. Quantitation of AR DNA-binding activity in the "protein-DNA" bandshift was measured using the Molecular Imager FX System (Bio-Rad, Hercules, CA). For the supershift experiment, 20 μg of cell extract protein were incubated with the monoclonal AR antibody (Santa Cruz Biotechnology) for 1 h at 4°C before incubation with the radiolabeled probe.

Results

MSA Inhibits LNCaP Cell Growth in a Dose- and Time-dependent Manner. Table 1 shows the results of the effect of MSA treatment on cell growth. The data are expressed as percentages of the untreated control. A concentration of 2.5 μM MSA produced essentially no change, even after 3 days of treatment. Increasing the concentration of MSA to 5 μM inhibited cell growth by about 25%, but the effect was not observed until the 72-h time point. The same magnitude of growth inhibition was observed at 24 h with 10 μM MSA, and by 72 h, there were 50% fewer cells compared with the untreated culture. The experiment therefore established the dose and time response to MSA with respect to growth inhibition. This information is important because the down-regulation of PSA and AR by selenium occurs well before the onset of growth inhibition (see below).

Table 1 *Effect of MSA on the accumulation of LNCaP cells*[a]

Treatment	Treatment duration (h)[b]		
	24	48	72
MSA (μM)			
2.5	102.5 ± 4.0	106.6 ± 6.2	102.5 ± 1.9
5	93.7 ± 3.1	96.4 ± 2.9	72.6 ± 1.9[c]
10	77.1 ± 8.4[c]	61.1 ± 1.7[c]	55.4 ± 3.7[c]

[a] As a percentage of untreated control.
[b] Results are expressed as mean ± SE (n = 4 independent experiments).
[c] Significantly different compared with the corresponding control value ($P < 0.05$).

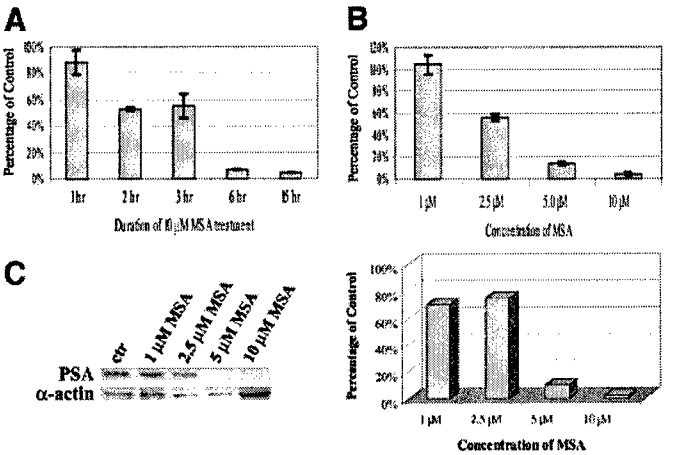

Fig. 1. Effect of MSA on PSA expression. *A* and *B*, changes in PSA mRNA, as determined by quantitative RT-PCR, as a function of time of treatment with MSA or as a function of MSA concentration. With the exception of the 1-h and the 1 μM MSA data points, the remaining data points are significantly different ($P < 0.01$) from the control, which is set as 100%. *Bars*, SE. *C*, Western blot data of changes in PSA protein level as a function of different concentrations of MSA (*left side*) and normalized quantitative changes compared with the control value of 100% (*right side*).

MSA Suppresses PSA mRNA and Protein Expression in LNCaP Cells. The modulation of PSA mRNA by MSA was assessed quantitatively by real-time RT-PCR. Cells were treated with 10 μM MSA for various lengths of time; the PSA results are shown in Fig. 1*A*. A marked decrease in PSA mRNA was detected as early as 2 h after exposure to MSA; the mRNA level dropped to <10% of the control value by 6 and 15 h. As shown in Fig. 1*B*, the depression of PSA mRNA was dependent on the concentration of MSA in the range between 2.5 and 10 μM; the assay was performed after exposure to MSA for 15 h. As little as 2.5 μM MSA reduced PSA mRNA level by 40%. This level of MSA had no effect on cell growth. Even with 10 μM MSA, the near complete elimination of PSA mRNA expression occurred before there was any detectable change in growth. The decrease in PSA protein level by MSA at 15 h, as determined by Western blot analysis, is shown in Fig. 1*C, left panel*. The right panel shows the normalized quantitative changes compared with the control value of 100%. Small decreases in PSA protein were evident with 1 or 2.5 μM MSA. At 5 or 10 μM MSA, the level of PSA protein became very low or hardly detectable. The experiments described in Fig. 1 were done with cells cultured in 10% FBS. In addition, we carried out another set of experiments with cells cultured in charcoal-stripped FBS containing 10 nM R1881 (a potent synthetic androgen). The down-regulation of PSA mRNA by MSA, as a function of dose and time, was qualitatively similar to that observed with the FBS culture (data not shown).

MSA Suppresses AR mRNA and Protein Expression in LNCaP Cells. The expression of PSA is known to be regulated by AR, which is a ligand-activated transcription factor. Our next step was to investigate the expression of AR mRNA in response to MSA by real-time RT-PCR. Fig. 2*A* shows the time course of response to 10 μM MSA. Within the first hour, there was a 50% decrease in AR mRNA. The transcript level continued to drop down to 20% or below with longer

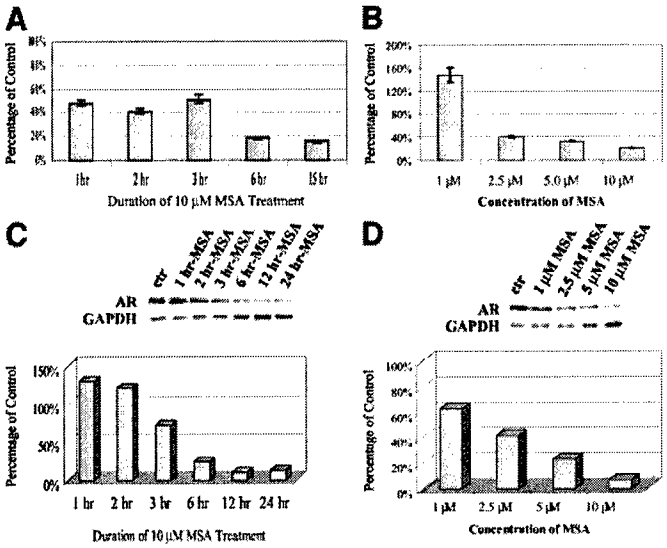

Fig. 2. Effect of MSA on AR expression. *A* and *B*, change in AR mRNA, as determined by quantitative RT-PCR, as a function of time of treatment with MSA or as a function of MSA concentration. All of the data are significantly different ($P < 0.01$) from the control, which is set as 100%. *Bars*, SE. *C*, Western blot data of changes in AR protein level as a function of time of treatment with 10 μM MSA. *D*, Western blot data of changes in AR protein level as a function of different concentrations of MSA. *GAPDH*, glyceraldehyde-3-phosphate dehydrogenase.

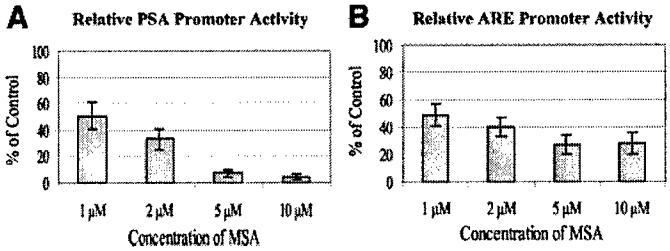

Fig. 3. Effect of MSA on PSA promoter activity (*A*) and ARE promoter activity (*B*). The cells were cultured in charcoal-stripped FBS containing 10 nM R1881. The results are expressed as percentages of untreated control. All of the data points are significantly different ($P < 0.01$) from the control value. *Bars*, SE.

treatment with MSA. The dose response to MSA is shown in Fig. 2*B*; these assays were done at the 15-h time point. Interestingly, 1 μM MSA actually increased slightly the level of AR mRNA. However, raising the concentration of MSA to 2.5 μM or above caused a very significant depression of the AR transcript to 40% or less of the control value. We next examined AR protein expression in response to 10 μM MSA. As shown in Fig. 2*C*, MSA down-regulated AR protein level progressively as a function of time over a period of 24 h. Initially, the reduction in protein appeared to lag behind the reduction in transcript by at least 2–3 h. The delay in response might be reflective of the time needed for protein turnover. Fig. 2*D* shows the effect of different concentrations of MSA on expression of the AR protein. MSA produced a graded suppression of the AR protein in a dose-dependent manner. In general, the changes in protein level were consistent with the real-time RT-PCR results with the exception of the 1 μM MSA data point.

MSA Inhibits AR *trans*-Activating Activity. LNCaP cells have a mutant but functional AR. In an attempt to determine the ability of MSA to interfere with AR *trans*-activating activity, we transiently transfected LNCaP cells with an expression vector for the wild-type AR and the PSA promoter-luciferase reporter plasmid. This region of the PSA regulatory element contains the promoter and enhancer and has been demonstrated to be responsive to androgen stimulation (13). As shown in Fig. 3*A*, MSA inhibited the luciferase reporter in a dose-dependent manner. Thus, the PSA promoter activity was decreased by 50, 67, 93, or 96% in the presence of 1, 2, 5, or 10 μM MSA, respectively.

Activated AR exerts its function by binding to the ARE site. Because the PSA promoter contains many regulatory elements in addition to the ARE, one could argue that the decrease in PSA promoter activity might not necessarily be attributable to a change in AR *trans*-activating activity. To address this issue, we transiently transfected LNCaP cells with an expression vector for the wild-type AR and the ARE-luciferase reporter plasmid. This construct contains three repeats of the ARE region ligated in tandem to the luciferase reporter (14). As shown in Fig. 3*B*, the ARE-luciferase activity was inhibited by 50, 60, or 75% in the presence of 1, 2, or 5 μM MSA, respectively. The result obtained with 10 μM MSA was similar to that with 5 μM MSA.

MSA Decreases Binding of AR to ARE. To determine whether MSA might reduce the DNA binding activity of the AR protein to the ARE, we performed EMSA using radiolabeled oligonucleotides of the ARE with nuclear extract from LNCaP cells treated for 30 min with various concentrations of MSA. As shown in Fig. 4, *A* and *B*, a decrease in AR-ARE complex formation was evident with MSA treatment compared with the untreated control. We can rule out the reduced availability of the AR protein as a contributing factor, because there was no change in AR protein after only 30 min of

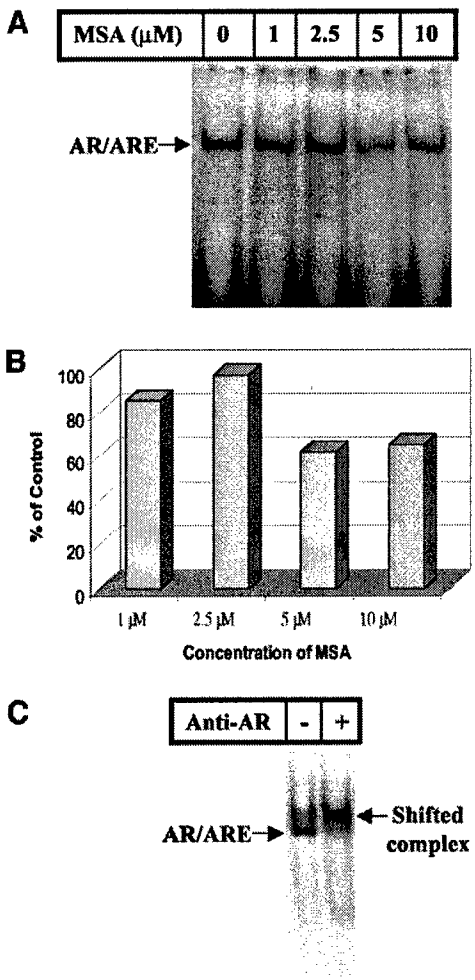

Fig. 4. *A*, EMSA results of AR binding to ARE as a function of different concentrations of MSA. *B*, quantitative determination of the EMSA results. *C*, supershift of the AR/ARE complex with antibody against AR.

treatment with MSA (see Fig. 2*C*). The specificity of the AR-ARE complex was demonstrated by the supershift assay using an antibody against AR (Fig. 4*C*).

Discussion

This report is the first to show that a selenium metabolite is able to down-regulate the expression of PSA in human prostate cancer cells via a mechanism involving disruption of the androgen signal transduction pathway. On the basis of the information from this study, selenium decreases AR transcript and protein and inhibits AR *trans*-activating activity. Selenium can also diminish the binding of AR to the ARE site. However, we cannot at this time distinguish whether this is attributable to a block in nuclear translocation of the activated AR or a physical interference of AR association with the ARE through modulation of other co-regulators. These various possibilities will be investigated systematically in the future. It is noteworthy that the reduction in AR and PSA expression occurs at least 20 h before any significant decrease in cell number. This kind of bellwether change at the molecular level might be one of the causes underlying the sensitivity of prostate cells to selenium treatment.

In a recent paper, Bhamre *et al.* (16) reported that although supraphysiological levels of selenomethionine inhibited LNCaP cell growth, selenomethionine did not specifically affect the production of PSA when the results were normalized to the decreased number of viable cells. As explained in the "Introduction," selenomethionine is not a suitable selenium reagent for cell biology studies *in vitro*, because it is poorly metabolized by cultured epithelial cells to the active monomethylated intermediate. Not surprisingly, many cellular and molecular events that are normally sensitive to modulation by physiological levels of MSA (4, 7–11) respond very sluggishly to selenomethionine, and only when it is present at excessively high levels in the medium. Thus, the discrepancy between our study and that of Bhamre *et al.* (16) can be reconciled by the differences in biochemical reactivity between MSA and selenomethionine.

The clonal expansion of prostate cancer at the early stage is mostly dependent on androgen stimulation. A selenium intervention strategy aimed at dampening the amplitude of androgen signaling could be helpful for controlling prostate cancer in high-risk men. PSA is a well-accepted diagnostic and prognostic biomarker of prostate cancer progression. The down-regulation of PSA by selenium therefore has significant clinical implication. In patients treated with selenium, the monitoring of PSA in the circulation could potentially be evaluated as a barometer to gauge the efficacy of intervention. The benefit might also be extended to the prevention of relapses after endocrine therapy. Recurrent prostate cancer is generally hormone refractory, although the expression of AR is maintained regardless of the clinical stage of the disease (17, 18). The fact that PSA continues to be produced by the pathologically advanced cancer suggests that the AR signal transduction pathway is still intact. Several hypotheses have been proposed to explain this phenomenon. Mutations of the AR may enable cells to be sensitized by very low levels of androgens, or perhaps even by non-androgen steroids (19). Alternatively, the receptor may become promiscuous and can be activated by non-steroidal growth factors and cytokines (20). Prostate cancer may also adapt to androgen deprivation by increasing the expression of AR through gene amplification (21, 22). We have developed a LNCaP subline that is not responsive to androgen but is capable of producing a copious amount of PSA. We are planning to use this cell model to further investigate the role of selenium in AR function when the presence of androgen is no longer required.

References

1. Greenlee, R. T., Murray, T., Bolden, S., and Wingo, P. A. Cancer Statistics, 2000. CA Cancer J. Clin., *50:* 7–33, 2001.
2. Clark, L. C., Combs, G. F., Turnbull, B. W., Slate, E. H., Chalker, D. K., Chow, J., Davis, L. S., Glover, R. A., Graham, G. F., Gross, E. G., Krongrad, A., Lesher, J. L., Park, K., Sanders, B. B., Smith, C. L., and Taylor, R. Effects of selenium supplementation for cancer prevention in patients with carcinoma of the skin: a randomized controlled trial. J. Am. Med. Assoc., *276:* 1957–1985, 1996.
3. Duffield-Lillico, A. J., Dalkin, B. L., Reid, M. E., Turnbull, B. W., Slate, E. H., Jacobs, E. T., Marshall, J. R., and Clark, L. C. Selenium supplementation, baseline plasma selenium and incidence of prostate cancer: an analysis of the complete treatment period of the Nutritional Prevention of Cancer Trial. Br. J. Urol. Int., *91:* 608–612, 2003.
4. Dong, Y., Zhang, H., Hawthorn, L., Ganther, H. E., and Ip, C. Delineation of the molecular basis for selenium-induced growth arrest in human prostate cancer cells by oligonucleotide array. Cancer Res., *63:* 52–59, 2003.
5. Ip, C., Dong, Y., and Ganther, H. E. New concepts in selenium chemoprevention. Cancer Metastasis Rev., *21:* 281–289, 2002.
6. Ip, C., Thompson, H. J., Zhu, Z., and Ganther, H. E. *In vitro* and *in vivo* studies of methylseleninic acid: evidence that a monomethylated selenium metabolite is critical for cancer chemoprevention. Cancer Res., *60:* 2882–2886, 2000.
7. Jiang, C., Wang, Z., Ganther, H., and Lu, J. Caspases as key executors of methyl selenium-induced apoptosis (anoikis) of DU-145 prostate cancer cells. Cancer Res., *61:* 3062–3070, 2001.
8. Wang, Z., Jiang, C., and Lu, J. Induction of caspase-mediated apoptosis and cell-cycle G_1 arrest by selenium metabolite methylselenol. Mol. Carcinogen., *34:* 113–120, 2002.
9. Jiang, C., Wang, Z., Ganther, H., and Lu, J. Distinct effects of methylseleninic acid *versus* selenite on apoptosis, cell cycle, and protein kinase pathways in DU145 human prostate cancer cells. Mol. Cancer Ther., *1:* 1059–1066, 2002.
10. Zu, K., and Ip, C. Synergy between selenium and vitamin E in apoptosis induction is associated with activation of distinctive initiator caspases in human prostate cancer cells. Cancer Res., *63:*, 6988–6995, 2003.
11. Dong, Y., Ganther, H. E., Stewart, C., and Ip, C. Identification of molecular targets associated with selenium-induced growth inhibition in human breast cells using cDNA microarrays. Cancer Res., *62:* 708–714, 2002.
12. Livak, L. J., and Schmittgen, T. D. Analysis of relative gene expression data using real-time quantitative PCR and the $2^{-\Delta\Delta CT}$ method. Methods, *25:* 402–408, 2001.
13. Pang, S., Dannul, J., Kaboo, R., Xie, Y., Tso, C. L., Michel, K., de Kernion, J. B., and Belldegrun, A. S. Identification of a positive regulatory element responsible for tissue-specific expression of prostate-specific antigen. Cancer Res., *57:* 495–499, 1997.
14. Onate, S. A., Boonyaratanakornkit, V., Spencer, T. E., Tsai, S. Y., Tsai, M. J., Edwards, D. P., and O'Malley, B. W. The steroid receptor coactivator-1 contains multiple receptor interacting and activation domains that cooperatively enhance the activation function 1 (AF1) and AF2 domains of steroid receptors. J. Biol. Chem., *273:* 12101–12108, 1998.
15. Lin, D. L., Whitney, M. C., Yao, Z., and Keller, E. T. Interleukin-6 induces androgen responsiveness in prostate cancer cells through up-regulation of androgen receptor expression. Clin. Cancer Res., *7:* 1773–1781, 2001.
16. Bhamre, S., Whitin, J. C., and Cohen, H. J. Selenomethionine does not affect PSA secretion independent of its effect on LNCaP cell growth. Prostate, *54:* 315–321, 2003.
17. Sadi, M. V., Walsh, P. C., and Barrack, E. R. Immunohistochemical study of androgen receptors in metastatic prostate cancer—comparison of receptor content and response to hormonal therapy. Cancer (Phila.), *67:* 3057–3064, 1991.
18. Hobisch, A., Culig, Z., Radmayr, C., Bartsch, G., Klocker, H., and Hittmair, A. Androgen receptor status of lymph node metastases from prostate cancer. Prostate, *28:* 129–135, 1996.
19. Zhao, X. Y., Malloy, P. J., Krishnan, A. V., Swami, S., Navone, N. M., Peehl, D. M., and Feldman, D. Glucocorticoids can promote androgen-independent growth of prostate cancer cells through a mutated androgen receptor. Nat. Med., *6:* 703–706, 2000.
20. Culig, Z., Hobisch, A., Hittmair, A., Peterziel, H., Cato, A. C. B., Bartsch, G., and Klocker, H. Expression, structure, and function of androgen receptor in advanced prostatic carcinoma. Prostate, *35:* 63–70, 1998.
21. Visakorpi, T., Hyytinen, E., Koivisto, P., Tanner, M., Keinanen, R., Palmberg, C., Palotie, A., Tammela, T., Isola, J., and Kallioniemi, O. P. *In vivo* amplification of the androgen receptor gene and progression of human prostate cancer. Nat. Genet., *9:* 401–406, 1995.
22. Koivisto, P., Kononen, J., Palmberg, C., Tammela, T., Hyytinen, E., Isola, J., Trapman, J., Cleutjens, K., Noordzij, A., Visakorpi, T., and Kallioniemi, O. P. Androgen receptor gene amplification: a possible molecular mechanism for androgen deprivation therapy failure in prostate cancer. Cancer Res., *57:* 314–319, 1997.

CANCER GENOMICS & PROTEOMICS 2: xxx-xxx (2005)

No: 111-Z
Please mark the appropriate section for this paper
☐ Experimental
☐ Clinical
☐ Epidemiological

Microarray Data Mining for Potential Selenium Targets in Chemoprevention of Prostate Cancer

HAITAO ZHANG[1], YAN DONG[1], HONGJUAN ZHAO[2], JAMES D. BROOKS[2], LESLEYANN HAWTHORN[3], NORMA NOWAK[3], JAMES R. MARSHALL[1], ALLEN C. GAO[4] and CLEMENT IP[1]

[1]Division of Cancer Prevention and Population Sciences, [3]Department of Cancer Genetics, [4]Departments of Medicine, Pharmacology and Therapeutics, Roswell Park Cancer Institute, Buffalo, NY 14263, [2]Department of Urology, Stanford University School of Medicine, Stanford, CA 94305, U.S.A.

Abstract. *Background: A previous clinical trial showed that selenium supplementation significantly reduced the incidence of prostate cancer. We report here a bioinformatics approach to gain new insights into selenium molecular targets that might be relevant to prostate cancer chemoprevention. Materials and Methods: We first performed data mining analysis to identify genes which are consistently dysregulated in prostate cancer using published datasets from gene expression profiling of clinical prostate specimens. We then devised a method to systematically analyze three selenium microarray datasets from the LNCaP human prostate cancer cells, and to match the analysis to the cohort of genes implicated in prostate carcinogenesis. Moreover, we compared the selenium datasets with two datasets obtained from expression profiling of androgen-stimulated LNCaP cells. Results: We found that selenium reverses the expression of genes implicated in prostate carcinogenesis. In addition, we found that selenium could counteract the effect of androgen on the expression of a subset obtained from androgen regulated genes. Conclusion: The above information provides us with a treasure of new clues to investigate the mechanism of selenium chemoprevention of prostate cancer. Furthermore, these selenium target genes could also serve as biomarkers in future clinical trials to gauge the efficacy of selenium intervention.*

Abbreviations: AR, androgen receptor; ARE, androgen responsive element; MSA, methylseleninic acid; PCa, prostate cancer; PSA, prostate specific antigen; TGFβ, transforming growth factor β.

Correspondence to: Clement Ip, Roswell Park Cancer Institute, Elm & Carlton Streets, Buffalo, NY 14263, U.S.A. e-mail: Clement.Ip@roswellpark.org

Key Words: Selenium, chemoprevention, prostate carcinogenesis, androgen receptor.

Supplementation with a nutritional dose of selenium was found to reduce prostate cancer incidence by 50% in a randomized, placebo-controlled cancer prevention trial (1-3). Prostate cancer was actually a secondary endpoint in this study, which was designed originally to evaluate the effect of selenium on non-melanoma skin cancer. We reported previously that a selenium metabolite, in the form of methylseleninic acid or MSA, suppressed the growth of both the androgen-responsive LNCaP and the androgen-refractory PC-3 human prostate cancer cells (4,5). Growth inhibition by MSA was time- and dose-dependent, with an IC_{50} of ~10 μM at 48 hours of treatment. In order to identify the molecular alterations that might be responsible for the growth inhibitory effect of selenium, we profiled gene expression changes in PC-3 cells using the Affymetrix 12K-gene oligonucleotide chip (4,5). Several working hypotheses have been generated from this dataset regarding the mechanisms of selenium action (4,5). In the present study, we completed a similar selenium array analysis in the androgen-responsive LNCaP cells using a 3K custom cDNA array. The smaller array is expected to improve the sensitivity of the assay, although the advantage is compromised by the reduced size of the dataset. Recently, Zhao *et al.* also performed microarray analysis in MSA treated-LNCaP cells using a high-density cDNA array (6). Our goal was to make use of these three selenium datasets and develop a global data mining strategy to earmark putative prostate cancer genes which are sensitive to selenium intervention.

Our approach was to compare the selenium datasets to three recently published prostate cancer microarray datasets generated from human tumor specimen. The first was an Affymetrix oligonucletide array study in 50 normal and 52 prostate cancers reported by Singh *et al.* (7). The second, described by Welsh *et al.* (8), was similar to the first with the exception that fewer number of samples were examined (9

normal and 25 prostate cancers). The third was an analysis of 41 normal and 62 prostate cancers by Lapointe *et al.* (9) using a 26K-gene cDNA microarray. These three prostate cancer datasets offer a rich source of information of dysregulated genes implicated in prostate carcinogenesis.

Androgen receptor (AR) signaling is known to play an important role in promoting prostate cancer progression (10). Consequently disruption of AR signaling is an effective means of prostate cancer management. We newly reported that selenium is capable of decreasing the expression and transactivating activity of AR (4). This novel finding underlies the justification of applying microarray analysis to investigate whether the expression of AR-regulated genes might be counteracted by selenium. Recent events have made this query possible. In separate studies by DePrimo *et al.* (11) and Nelson *et al.* (12), LNCaP cells were treated with a synthetic androgen and microarray analyses were then performed to identify genes responsive to androgen stimulation. These two androgen datasets are well suited to serve as a tool to mine the selenium datasets for additional clues. Collectively, the timely publication of a number of prostate cancer and androgen microarrays in the past two years provides an opportunity and sets the stage for the present effort to advance our understanding of selenium chemoprevention of prostate cancer.

Materials and Methods

Our own cDNA microarray analysis of LNCaP cells treated with selenium. The culture conditions of LNCaP cells have been described in detail previously (4). After exposure to 10 mM MSA for 3, 6, 12, 24, 36, or 48 h, total RNA and protein were isolated using TRIzol (Invitrogen, Carlsbad, CA). The RNA collected from three independent experiments was pooled and subjected to microarray analysis using a 3K human cDNA microarray printed at the Microarray and Genomics Core Facility at Roswell Park Cancer Institute. This custom cDNA array was constructed based on the genes which were found to be modulated by selenium in PC-3 cells from our previous study (5). Each gene on this array was spotted in triplicate. Probe generation and array hybridization were conducted according to a protocol developed by the Core Facility (http://microarrays.roswellpark.org/Protocols). The hybridization signals were captured using an Affymetrix 428 array scanner (Affymetrix, Santa Clara, CA), and analyzed using the ImaGene software (BioDiscovery, Inc., Marina Del Ray, CA). Poor quality spots, along with spots with signal levels indistinguishable from background, were disgarded. The extracted image data were then processed by a series of steps including background subtraction, data normalization, ratio calculation, and statistical analysis of replicate spots. Data processing was done with the use of the ImaGene (BioDiscovery, Inc., Marina Del Ray, CA) and the GeneTraffic software (Iobion Informatics LLC, La Jolla, CA), the statistical package R, and in-house PERL programs. In order to control for the noise introduced by the fluorescent dyes, Cy3 and Cy5, each array experiment was performed twice with the labeling dyes reversed to eliminate dye biases, and the signal ratios from these two experiments were averaged. A $\log_2$-transformed treatment to control signal ratio of ≥ 1 or ≤ -1 was chosen as the criteria for induction or repression, respectively. These threshold values are commonly used in the literature for microarray expression analysis (13,14). Hierarchical clustering analysis was performed using the Hierarchical Clustering Explorer software from the University of Maryland.

Processing of publicly available microarray datasets. The datasets from the six published gene expression profiling studies (cited as references 7-9 in the Introduction) were downloaded from the authors' respective websites. Our own selenium PC-3 dataset (cited as reference 5 in the Introduction) and selenium LNCaP dataset are available at the Roswell Park website (http://falcon.roswellpark.org/publication/CIp/dataMining). In view of the fact that the eight microarrays were originated from different sources, one must appreciate that different identifiers, including cDNA clone IDs, probe set IDs, and GenBank accession numbers, were used to label the genes. In order to facilitate data comparison, these identifiers were mapped to the UniGene database (Build 136) at the National Center for Biotechnology Information (NCBI). The UniGene Cluster IDs were used to cross-reference genes in different datasets.

Permutation t-test analysis of prostate cancer datasets. For the three prostate cancer datasets (7-9), only samples classified as primary prostate cancer or normal prostate were included in the analysis; all other sample types were excluded from the original datasets. In order to identify genes that are differentially expressed between normal and cancer tissues, permutation *t*-test analysis was performed individually with each dataset. The *t*-statistics of a gene was calculated by the following formula:

$$t = \frac{\mu_1 - \mu_2}{\sqrt{\frac{\sigma_1^2}{n_1} + \frac{\sigma_2^2}{n_2}}}$$

where μ_i is the mean expression value of a given gene in the i^{th} group, σ_i^2 is the variance of that gene, and n_i is the sample size of the i^{th} group. The procedure of permutation was carried out on a gene-by-gene basis by randomly assigning each data point to either the normal or cancer group, while maintaining the total sample size of each group. This process was repeated 10,000 times and the *p*-value was defined as the fraction of *t*-statistics generated from randomization that was greater than or equal to the *t*-statistics generated from the actual data points. This method of analysis makes allowance for missing data points; however anything with less than 5 data points is generally not expected to have sufficient statistical power and is therefore excluded from the analysis. A list of dysregulated genes was compiled based on the following criteria: p-values less than 0.001, and consistent changes in at least two out of the three datasets. The false discovery rate (q) was calculated as follows: $q = \frac{p \times n}{i}$, where p is the p-value, n is the total number of genes, and i is the number of genes with a p-value less than p. The above analyses were performed with in-house PERL programs.

Merging of datasets. Our selenium LNCaP dataset and Zhao's selenium LNCaP dataset (6) were generated by an essentially identical protocol. The merging of these two datasets, or for that matter, other compatible datasets, would greatly increase the power and precision of the analysis provided that certain key parameters are properly safeguarded. Since the above two array

experiments were conducted at multiple time points, it is necessary to devise a method in categorizing the pattern of expression changes across all time points. The data were filtered first to admit only those changes (induction or repression) that were over the 2-fold threshold (*i.e.* $\log_2$-transformed ratio ≥ 1 or ≤ -1). A decision call of induction or repression was made for each gene only if $\geq 70\%$ of the filtered data points showed the same direction of change. A consolidated LNCaP dataset was generated by merging the two LNCaP datasets and discarding genes with conflicting decision calls. The two androgen datasets of DePrimo *et al.* (11) and Nelson *et al.* (12) were merged in a similar manner. The above analyses were performed with in-house PERL programs.

Functional annotation of transcripts. Once a gene has been identified to be a target of selenium intervention, we assign it to a functional category for informational purposes. Functional annotation of transcripts was performed by using the Gene Ontology (GO) database and literature review. The UniGene cluster IDs of these genes were used to query the LocusLink database at NCBI (http://www.ncbi.nlm.nih.gov/ LocusLink/) in order to extract the GO terms associated with these genes.

Results

Microarray data mining of genes implicated in prostate carcinogenesis. The three prostate cancer datasets (7-9) were chosen for our investigation because they represent the largest gene expression profiling studies comparing normal and cancerous prostate tissues. No statistical analysis, however, was performed in these three studies to identify putative prostate cancer genes. Since each of these datasets has independent measurements of gene expression in the normal and tumor groups, we undertook a systematic statistical evaluation of their results. Permutation *t*-test was carried out on each dataset, and genes with p values < 0.001 were selected as differentially expressed between the normal and cancer groups. Based on this criterion, 5,306 genes were pulled out from the Lapointe study (7-9), 672 from the Singh study (7-9), and 1,527 from the Welsh study (7-9). Our selection method has a false discovery rate of 0.005, 0.019, and 0.008, respectively. For cross-validation, we reduced the number of genes to those with the same expression pattern in at least 2 out of 3 datasets. This procedure narrowed the list down to 1,067 genes with aberrant expression in prostate cancer. Among these, 497 or 46.6% are up-regulated, and 570 or 53.4% are down-regulated. The top 50 up- or down-regulated genes that appear in all three datasets, ranked by the average ratio, are listed in Tables IA and IB. The complete list can be accessed at our website.

Microarray analysis of LNCaP cells treated with selenium. A hierarchical clustering algorithm was applied to group genes according to their expression pattern across six time points following treatment with MSA. The clustering analysis of 762 selenium-responsive genes is shown in Figure 1. The branch points in the dendrogram correspond to each gene, and the length of the branches reflects the degree of relatedness. Red and green squares represent up-regulation and down-regulation, respectively, relative to the control values. Black squares indicate no change, and gray squares signify data of insufficient quality. The gene identified and the raw array data are available at our website. Four distinct clusters emerge from this analysis. Clusters A and C are composed of genes with a gradual or a rapid increase in expression level, respectively. Clusters B and D represent the group of genes with a rapid or gradual reduction in expression level, respectively.

Selenium reverses the expression of genes implicated in prostate carcinogenesis. The cellular responses of the androgen-responsive LNCaP cells and the androgen-nonresponsive PC-3 cells to selenium are very similar. These two cell models represent different stages of prostate cancer progression. In order to identify relevant molecular targets underlying selenium chemopreventive action in incident prostate cancer or late stage relapse, we matched the prostate cancer datasets to the selenium LNCaP and PC-3 datasets. The goal was to identify dysregulated prostate cancer genes which could be reversed or restored to normal by selenium in both LNCaP and PC-3 cells. In this analysis, we compared 1,067 genes that are consistently dysregulated in prostate cancer and 427 genes that are sensitive to selenium modulation in both LNCaP and PC3 cells. We found that there are a total of 71 genes common to both datasets. Among these, 25 are regulated in the same direction, 42 are regulated reciprocally, and four are regulated spuriously. Theoretically, when comparing a random list of 1,067 genes with another random list of 427 genes from the human genome (estimated to contain a total of ~30,000 genes), the number of overlap one would expect to obtain is: $\frac{1067}{30000} \times \frac{427}{30000} \times 30000 \approx 15$ genes. Assuming there is a 50% chance of these 15 genes to be modulated reciprocally (*i.e.* a random distribution), the number of genes in this category would be reduced by half to 7.5. This number is far less than the 42 reciprocally regulated genes we have identified. Therefore, it is very unlikely that the outcome of our data mining method is due to chance. These 42 genes are listed in Table II. A negative value denotes down-regulation, while a positive value indicates up-regulation. The flip-flop between the PCa (prostate cancer) column and the two Se columns is self-evident. Three genes, UMPK, SERPINB5, and FOXA1, are also present in Tables IA or IB. It should be noted that the genes in these two tables are only subsets of the cohort of prostate cancer genes used in this analysis.

The genes in Table II are further classified into a number of functional categories. Because of space

Table IA. *Top 50 up-regulated genes in prostate cancers.*

Unigene ID	Symbol	Gene description	log_2 transformed ratio#			
			Lapointe	Welsh	Singh	Average
Hs.49598*	AMACR	alpha-methylacyl-CoA racemase	3.31	3.53	3.29	3.38
Hs.118483	MYO6	myosin VI	1.81	2.21	4.36	3.26
Hs.27311	SIM2	single-minded homolog 2 (Drosophila)	1.58	4.00	3.21	3.23
Hs.820	HOXC6	homeo box C6	0.60	3.12	4.08	3.18
Hs.432750*	HPN	hepsin (transmembrane protease, serine 1)	2.51	2.82	3.38	2.95
Hs.458360	UMPK	uridine monophosphate kinase	0.88	2.58	3.93	2.94
Hs.93304	PLA2G7	phospholipase A2, group VII	1.50	2.33	3.69	2.79
Hs.306812	BUCS1	butyryl Coenzyme A synthetase 1	2.70	2.35	3.17	2.78
Hs.412020	BICD1	Bicaudal D homolog 1 (Drosophila)	1.21	2.09	2.87	2.21
Hs.155419	BIK	BCL2-interacting killer (apoptosis-inducing)	0.56	1.60	3.06	2.1
Hs.296638*	PLAB	prostate differentiation factor	0.83	2.83	1.81	2.05
Hs.154103*	LIM	LIM protein (similar to rat protein kinase C-binding enigma)	1.57	1.91	2.22	1.93
Hs.405961	OASIS	old astrocyte specifically induced substance	0.70	1.38	2.67	1.82
Hs.76901	PDIR	for protein disulfide isomerase-related	0.69	2.05	1.99	1.7
Hs.334707	ACY1	aminoacylase 1	0.77	2.00	1.67	1.57
Hs.380460	ICA1	islet cell autoantigen 1, 69kDa	0.70	0.84	2.45	1.57
Hs.360509	FBP1	fructose-1,6-bisphosphatase 1	1.15	1.51	1.82	1.52
Hs.38972	TSPAN-1	tetraspan 1	0.62	1.76	1.83	1.5
Hs.356894	HSD17B4	hydroxysteroid (17-beta) dehydrogenase 4	0.78	1.76	1.71	1.48
Hs.278611	GALNT3	UDP-N-acetyl-alpha-D-galactosamine:polypeptide N-acetylgalactosaminyltransferase 3 (GalNAc-T3)	0.80	1.44	1.76	1.39
Hs.440478	ANK3	ankyrin 3, node of Ranvier (ankyrin G)	1.08	1.79	1.17	1.38
Hs.306251	ERBB3	v-erb-b2 erythroblastic leukemia viral oncogene homolog 3 (avian)	0.28	1.24	2.05	1.36
Hs.247817	HIST1H2BK	histone 1, H2bk	0.86	1.73	1.34	1.35
Hs.444439*	PAICS	phosphoribosylaminoimidazole carboxylase, phosphoribosylaminoimidazole succinocarboxamide synthetase	0.79	1.23	1.82	1.34
Hs.83919	GCS1	glucosidase I	0.57	1.32	1.85	1.34
Hs.156682	IGSF4	immunoglobulin superfamily, member 4	0.63	1.76	1.32	1.31
Hs.75139	ARFIP2	ADP-ribosylation factor interacting protein 2 (arfaptin 2)	0.42	1.47	1.71	1.30
Hs.512670	BCAT2	branched chain aminotransferase 2, mitochondrial	0.53	1.31	1.79	1.30
Hs.434243	KIBRA	KIBRA protein	0.71	1.44	1.59	1.29
Hs.297343	CAMKK2	calcium/calmodulin-dependent protein kinase kinase 2, beta	0.87	1.78	0.97	1.26
Hs.387140	FLJ20323	hypothetical protein FLJ20323	0.37	1.18	1.85	1.25
Hs.405410	OGT	O-linked N-acetylglucosamine (GlcNAc) transferase	0.61	1.15	1.75	1.24
Hs.21293*	UAP1	UDP-N-acteylglucosamine pyrophosphorylase 1	1.05	1.27	1.39	1.24
Hs.155040	ZNF217	zinc finger protein 217	0.73	1.43	1.45	1.24
Hs.82280	RGS10	regulator of G-protein signalling 10	1.00	0.85	1.62	1.20
Hs.76285*	DKFZP564B167	DKFZP564B167 protein	0.79	1.29	1.38	1.17
Hs.449815		similar to My016 protein	0.28	0.92	1.85	1.16
Hs.234521	MAPKAPK3	mitogen-activated protein kinase-activated protein kinase 3	0.47	1.12	1.61	1.14
Hs.2551	ADRB2	adrenergic, beta-2-, receptor, surface	0.52	1.45	1.28	1.13
Hs.357901*	SOX4	SRY (sex determining region Y)-box 4	0.94	1.36	1.05	1.13
Hs.406534	HMG20B	high-mobility group 20B	0.55	1.17	1.50	1.12
Hs.166697	LRIG1	leucine-rich repeats and immunoglobulin-like domains 1	0.77	1.37	1.15	1.12
Hs.118638*	NME1	non-metastatic cells 1, protein (NM23A) expressed in	0.74	1.14	1.39	1.11
Hs.79064	DHPS	deoxyhypusine synthase	0.42	0.48	1.89	1.10
Hs.21894	ARHCL1	ras homolog gene family, member C like 1	0.60	1.59	0.82	1.07
Hs.424551	P24B	integral type I protein	0.54	1.26	1.29	1.07
Hs.75432	IMPDH2	IMP (inosine monophosphate) dehydrogenase 2	0.77	1.01	1.35	1.06
Hs.163484	FOXA1	forkhead box A1	0.33	1.16	1.46	1.05
Hs.291385	ATP8A1	ATPase, aminophospholipid transporter, Class I, type 8A, member 1	0.85	1.19	1.10	1.05
Hs.423095	NUCB2	nucleobindin 2	0.51	1.40	1.10	1.05

Table IB. *Top 50 down-regulated genes in prostate cancers.*

Unigene ID	Symbol	Gene description	$\log_2$ transformed ratio			
			Lapointe	Welsh	Singh	Average
Hs.75652	GSTM5	glutathione S-transferase M5	-1.80	-1.47	-∞	-2.21
Hs.77854	RGN	regucalcin (senescence marker protein-30)	-1.05	-2.44	-5.06	-2.10
Hs.339831	PENK	proenkephalin	-1.24	-1.71	-4.21	-1.94
Hs.34114	ATP1A2	ATPase, Na+/K+ transporting, alpha 2 (+) polypeptide	-1.37	-2.39	-2.22	-1.92
Hs.80552	DPT	dermatopontin	-1.50	-1.89	-2.35	-1.87
Hs.7357	CLIPR-59	CLIP-170-related protein	-0.70	-2.81	-3.76	-1.85
Hs.301914	DAT1	Neuronal specific transcription factor DAT1	-1.09	-1.83	-3.45	-1.83
Hs.440324	NRLN1	Neuralin 1	-1.41	-2.28	-1.88	-1.81
Hs.78748	RIMS3	regulating synaptic membrane exocytosis 3	-1.17	-1.42	-3.96	-1.76
Hs.448805	GPRC5B	G protein-coupled receptor, family C, group 5, member B	-1.14	-1.55	-3.41	-1.76
Hs.55279	SERPINB5	serine (or cysteine) proteinase inhibitor, clade B (ovalbumin), member 5	-1.38	-2.02	-1.92	-1.75
Hs.78792	NCAM1	neural cell adhesion molecule 1	-1.40	-1.29	-3.20	-1.75
Hs.60177	DZIP1	zinc finger DAZ interacting protein 1	-0.77	-1.82	-4.84	-1.73
Hs.5378	SPON1	spondin 1, (f-spondin) extracellular matrix protein	-1.09	-1.19	-6.12	-1.70
Hs.408	COL4A6	Collagen, type IV, alpha 6	-1.26	-1.97	-1.98	-1.70
Hs.406238	AOX1	Aldehyde oxidase 1	-1.31	-1.96	-1.77	-1.65
Hs.234863	TSPAN-2	tetraspan 2	-0.95	-1.32	-3.90	-1.60
Hs.348387	GSTM4	glutathione S-transferase M4	-1.46	-1.73	-1.62	-1.60
Hs.408767	CRYAB	crystallin, alpha B	-1.62	-1.74	-1.31	-1.55
Hs.411509	GSTP1	glutathione S-transferase pi	-1.24	-1.38	-2.19	-1.55
Hs.101850	RBP1	retinol binding protein 1, cellular	-0.98	-1.41	-2.41	-1.48
Hs.211933	COL13A1	Collagen, type XIII, alpha 1	-0.65	-1.54	-3.28	-1.47
Hs.80395	MAL	mal, T-cell differentiation protein	-0.93	-0.81	-∞	-1.45
Hs.93841	KCNMB1	potassium large conductance calcium-activated channel, subfamily M, beta member 1	-1.37	-1.90	-1.14	-1.44
Hs.74034	CAV1	Caveolin 1, caveolae protein, 22kDa	-1.71	-1.65	-1.05	-1.44
Hs.139851*	CAV2	Caveolin 2	-1.35	-1.34	-1.62	-1.43
Hs.302085	PTGIS	prostaglandin I2 (prostacyclin) synthase	-1.09	-1.52	-1.76	-1.43
Hs.103839	EPB41L3	erythrocyte membrane protein band 4.1-like 3	-0.77	-1.81	-1.92	-1.40
Hs.436657	CLU	Clusterin	-1.35	-1.55	-1.30	-1.40
Hs.421621	COX7A1	cytochrome c oxidase subunit VIIa polypeptide 1 (muscle)	-1.23	-1.73	-1.17	-1.36
Hs.79015	MOX2	antigen identified by monoclonal antibody MRC OX-2	-1.08	-1.65	-1.39	-1.36
Hs.131380	SGCD	sarcoglycan, delta (35kDa dystrophin-associated glycoprotein)	-0.76	-1.96	-1.59	-1.35
Hs.5422*	GPM6B	glycoprotein M6B	-0.80	-1.17	-2.47	-1.33
Hs.2006	GSTM3	glutathione S-transferase M3 (brain)	-0.27	-2.01	-2.87	-1.31
Hs.156007*	DSCR1L1	Down syndrome critical region gene 1-like 1	-1.10	-1.73	-1.15	-1.30
Hs.430166	PLS3	plastin 3 (T isoform)	-0.63	-1.09	-3.16	-1.29
Hs.24587	EFS	embryonal Fyn-associated substrate	-1.56	-0.54	-2.25	-1.28
Hs.8022	TU3A	TU3A protein	-1.42	-1.15	-1.27	-1.28
Hs.439040	RPESP	RPE-spondin	-0.99	-1.27	-1.64	-1.28
Hs.2463	ANGPT1	angiopoietin 1	-1.40	-1.41	-0.98	-1.25
Hs.362805*	MEIS2	Meis1, myeloid ecotropic viral integration site 1 homolog 2 (mouse)	-1.12	-1.47	-1.13	-1.23
Hs.300772	TPM2	tropomyosin 2 (beta)	-1.16	-1.80	-0.80	-1.20
Hs.372031*	PMP22	peripheral myelin protein 22	-1.00	-1.79	-0.90	-1.18
Hs.79386	LMOD1	leiomodin 1 (smooth muscle)	-0.76	-2.17	-0.96	-1.18
Hs.414407	HEC	highly expressed in cancer, rich in leucine heptad repeats	-0.80	-1.10	-1.76	-1.17
Hs.137569	TP73L	tumor protein p73-like	-1.36	-1.19	-0.94	-1.16
Hs.75350*	VCL	Vinculin	-1.18	-1.31	-0.99	-1.15
Hs.150358	DPYSL3	dihydropyrimidinase-like 3	-0.94	-1.49	-1.04	-1.14
Hs.79226	FEZ1	fasciculation and elongation protein zeta 1 (zygin I)	-0.33	-1.30	-2.55	-1.13
Hs.81412	LPIN1	lipin 1	-0.69	-1.33	-1.47	-1.12

#log2-tranformed cancer to normal signal ratio. The average is obtained by calculating the mean of the three linear ratios and transforming the mean to log2 value.

*these genes are also present in Rhodes *et al.* (35).

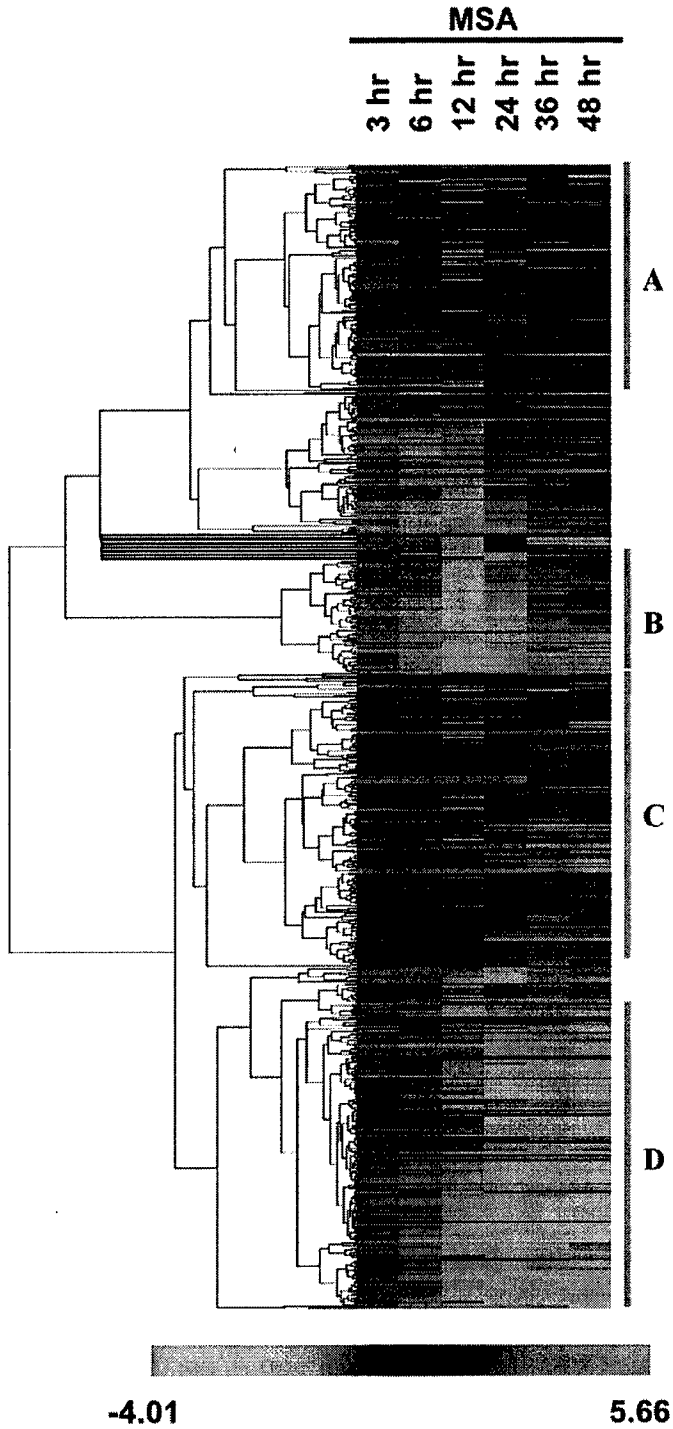

Figure 1. *One-dimensional hierarchical clustering of selenium-responsive genes in LNCaP cells. Rows represent individual genes, and columns represent different time points. Each cell represents the expression level of a gene at a given time point, with red and green indicating up- and down-regulation, respectively, black indicates no change, and gray indicates missing values.*

limitation, it is not possible to elaborate the function of each of these genes. Suffice it to note that a significant number of them is involved in controlling cell cycle progression and/or cell death, including AHR (15), CHC1 (16), CDKN1C (17), ATF5 (18), and FOXO1A (19-21). Selenium modulates their expression in a way that is consistent with cell growth inhibition, cell cycle block, and apoptosis stimulation. Table 2 also shows that selenium is able to up-regulate the expression of four genes with tumor suppressing activities. SERPINB5, also known as maspin, is a serine proteinase inhibitor capable of suppressing tumor invasion, apoptosis, and angiogenesis (22-24). It has

Table II. *Selenium reverses the expression of genes implicated in prostate carcinogenesis: common to LNCaP and PC-3 cells.*

UniGene ID	Symbol	Gene description	Fold Change (log_2)*		
			PCa	Se/LNCaP	Se/PC3
Cell proliferation/Apoptosis					
Hs.170087	AHR	aryl hydrocarbon receptor	-0.81	3.96	2.46
Hs.9754	ATF5	activating transcription factor 5	0.62	-1.31	-3.14
Hs.106070	CDKN1C	cyclin-dependent kinase inhibitor 1C (p57, Kip2)	-0.87	1.16	2.14
Hs.196769	CHC1	chromosome condensation 1	1.06	-1.05	-1.68
Hs.184161	EXT1	exostoses (multiple) 1	-0.53	1.20	1.00
Hs.170133#	FOXO1A	forkhead box O1A (rhabdomyosarcoma)	-0.86	1.17	1.26
Hs.82028	TGFBR2	transforming growth factor, beta receptor II (70/80kDa)	-0.76	1.31	1.2
Signal transduction					
Hs.337774	ARHGEF2	rho/rac guanine nucleotide exchange factor (GEF) 2	-0.86	1.26	1.85
Hs.116796	DIXDC1	DIX domain containing 1	-1.23	2.31	1.00
Hs.381928	DVL3	dishevelled, dsh homolog 3 (Drosophila)	-0.61	1.88	3.29
Hs.211569	GRK5	G protein-coupled receptor kinase 5	-1.49	2.32	2.10
Hs.436004	JAK1	Janus kinase 1 (a protein tyrosine kinase)	-0.53	1.89	2.46
Hs.79219	RGL1	ral guanine nucleotide dissociation stimulator-like 1	-2.15	1.04	3.81
Transcriptional regulation					
Hs.163484	FOXA1	forkhead box A1	1.46	-1.36	-1.00
Hs.166017	MITF	microphthalmia-associated transcription factor	-0.55	1.13	1.68
Tumor Suppressor Genes					
Hs.386952	CYLD	cylindromatosis (turban tumor syndrome)	-1.20	1.19	1.20
Hs.446537	GSN	gelsolin (amyloidosis, Finnish type)	-1.38	1.78	1.43
Hs.55279#	SERPINB5	serine (or cysteine) proteinase inhibitor, clade B, member 5	-2.02	1.04	1.81
Hs.152207	SSBP2	single-stranded DNA binding protein 2	-0.68	1.72	1.63
Oncogenes					
Hs.390567	FYN	FYN oncogene related to SRC, FGR, YES	-0.52	2.00	2.04
Hs.223025	RAB31	RAB31, member RAS oncogene family	-1.05	1.94	1.43
Cytoskeleton					
Hs.26208	COL16A1	collagen, type XVI, alpha 1	-1.34	1.35	2.68
Hs.440387	EPB41L2	erythrocyte membrane protein band 4.1-like 2	-0.78	1.25	1.07
Metabolism					
Hs.264330	ASAHL	N-acylsphingosine amidohydrolase (acid ceramidase)-like	1.62	-1.63	-2.74
Hs.303154	IDS	iduronate 2-sulfatase (Hunter syndrome)	-0.43	1.60	1.49
Hs.167531	MCCC2	methylcrotonoyl-Coenzyme A carboxylase 2 (beta)	2.26	-1.27	-1.43
Hs.458360#	UMPK	uridine monophosphate kinase	3.93	-1.03	-1.00
Other functions					
Hs.408767	CRYAB	crystallin, alpha B	-1.74	1.84	2.17
Hs.8302	FHL2	four and a half LIM domains 2	-1.25	1.13	1.26
Hs.848	FKBP4	FK506 binding protein 4, 59kDa	0.93	-1.22	-1.14
Hs.81361	HNRPAB	heterogeneous nuclear ribonucleoprotein A/B	0.51	-1.26	-1.00
Hs.372571	MBNL2	muscleblind-like 2 (Drosophila)	-1.09	2.93	1.63
Hs.390162	OPTN	Optineurin	-1.94	3.71	1.72
Hs.1501	SDC2	syndecan 2	-0.96	1.01	1.68
Hs.439643	SLC16A7	solute carrier family 16, member 7	-1.20	1.41	1.32
Unknown					
Hs.27621		CDNA FLJ12815 fis, clone NT2RP2002546	-1.49	1.10	1.26
Hs.440808	FNBP1	formin binding protein 1	-1.42	1.16	1.32
Hs.336429	GABARAPL1	GABA(A) receptor-associated protein like 1	-0.68	1.03	1.43
Hs.42322	PALM2	paralemmin 2	-1.00	1.24	1.81
Hs.224262	PJA2	praja 2, RING-H2 motif containing	-0.50	1.36	1.68
Hs.439776	STOM	Stomatin	-0.91	1.50	1.32
Hs.433838	STX12	syntaxin 12	-0.56	1.35	1.00

* For LNCaP and PC-3, the ratio is the maximum value of the data points from all the time- and concentration-series of selenium treatment. For PCa, it is the largest value from three prostate cancer datasets.

also present in Table 1A or 1B

Table III. *Selenium reverses the expression of genes implicated in prostate carcinogenesis: unique to LNCaP cells.*

UniGene ID	Symbol	Gene description	Fold Change (log_2)*	
			PCa	Se
Cell proliferation/Apoptosis				
Hs.77311	BTG3	BTG family, member 3	-0.66	1.42
Hs.95577	CDK4	cyclin-dependent kinase 4	0.42	-1.08
Hs.348153	CUL1	cullin 1	-0.34	1.45
Hs.118638	NME1	non-metastatic cells 1, protein (NM23A) expressed in	1.39	-1.21
Hs.169840	TTK	TTK protein kinase	1.24	-1.13
Signal transduction				
Hs.197081	AKAP12	A kinase (PRKA) anchor protein (gravin) 12	-0.93	1.16
Hs.271809	GPR161	G protein-coupled receptor 161	-0.89	1.01
Hs.433488	GUCY1A3	guanylate cyclase 1, soluble, alpha 3	3.10	-1.53
Hs.149900	ITPR1	inositol 1,4,5-triphosphate receptor, type 1	-1.44	1.53
Transcriptional regulation				
Hs.76884	ID3	inhibitor of DNA binding 3, dominant negative helix-loop-helix protein	-0.99	4.55
Hs.408222	PBX1	pre-B-cell leukemia transcription factor 1	-1.00	1.29
Hs.360174	SNAI2	snail homolog 2 (Drosophila)	-1.29	1.22
Transporter				
Hs.307915	ABCC4	ATP-binding cassette, sub-family C (CFTR/MRP), member 4	2.56	-1.08
Hs.99865	EPIM	Epimorphin	-1.63	1.05
Hs.14732	ME1	malic enzyme 1, NADP(+)-dependent, cytosolic	-1.04	1.55
Hs.221974	SNAP25	synaptosomal-associated protein, 25kDa	-1.39	1.88
Cytoskeleton				
Hs.403989	ACTG2	actin, gamma 2, smooth muscle, enteric	-1.51	1.02
Hs.440478	ANK3	ankyrin 3, node of Ranvier (ankyrin G)	1.79	-1.51
Hs.446375	MAPRE2	microtubule-associated protein, RP/EB family, member 2	-0.78	1.24
Hs.108924	SORBS1	sorbin and SH3 domain containing 1	-1.28	1.91
Metabolism				
Hs.440117	ALG8	asparagine-linked glycosylation 8 homolog	1.12	-1.25
Hs.75616	DHCR24	24-dehydrocholesterol reductase	1.43	-1.07
Hs.268012	FACL3	fatty-acid-Coenzyme A ligase, long-chain 3	0.83	-1.14
Hs.75485	OAT	ornithine aminotransferase (gyrate atrophy)	-0.77	2.16
Hs.79886	RPIA	ribose 5-phosphate isomerase A (ribose 5-phosphate epimerase)	0.44	-1.46
Protease/Protease inhibitor				
Hs.181350	KLK2	kallikrein 2, prostatic	0.97	-2.27
Hs.171995	KLK3	kallikrein 3, (prostate specific antigen)	0.69	-2.45
Hs.21858	SERPINE2	serine (or cysteine) proteinase inhibitor, clade E, member 2	-0.92	1.23
Other functions				
Hs.237506	DNAJB5	DnaJ (Hsp40) homolog, subfamily B, member 5	-3.65	1.06
Hs.173381	DPYSL2	dihydropyrimidinase-like 2	-1.05	1.14
Hs.315177	IFRD2	interferon-related developmental regulator 2	0.44	-1.23
Hs.5025	NEBL	Nebulette	-0.78	1.57
Hs.131727	PFAAP5	phosphonoformate immuno-associated protein 5	-0.81	1.13
Hs.438582	PRNP	prion protein (p27-30)	-0.94	1.19
Hs.250607	UTRN	utrophin (homologous to dystrophin)	0.88	-1.01
Hs.435800	VIM	Vimentin	-0.61	1.61
Unknown				
Hs.48450		Human mRNA, trinucleotide repeat sequence.	-1.02	1.21
Hs.428112	DEAF1	deformed epidermal autoregulatory factor 1 (Drosophila)	0.82	-1.15
Hs.4747	DKC1	dyskeratosis congenita 1, dyskerin	0.86	-1.11
Hs.112605	DKFZP564O043	hypothetical protein DKFZp564O043	-0.72	1.58
Hs.301839	HABP4	hyaluronan binding protein 4	-0.86	1.33
Hs.278483	HIST1H4J	histone 1, H4j	3.31	-1.98
Hs.157818	KCNAB1	potassium voltage-gated channel, shaker-related subfamily, beta member 1	-1.48	1.38
Hs.408142	KIAA1109	hypothetical protein KIAA1109	-0.56	1.58
Hs.309244	KIAA1579	hypothetical protein FLJ10770	-0.48	2.29
Hs.90797	LOC129642	hypothetical protein BC016005	2.39	-1.40
Hs.270411	PLEKHC1	pleckstrin homology domain containing, family C, member 1	-1.48	1.46
Hs.5957	PTPLB	protein tyrosine phosphatase-like, member b	1.00	-1.06
Hs.356342	RPL27A	ribosomal protein L27a	0.52	-1.21

* For LNCaP, the ratio is the maximum value of the data points from all the time- and concentration-series of selenium treatment. For PCa, it is the average tumor to normal ratio.

been reported that the expression of SERPINB5 decreases with increasing prostate cancer malignancy (25). Gelsolin is under-expressed in several cancer types, including prostate (26-29). CYLD is a deubiquitinating enzyme which negatively regulates the activation of NFκB, an anti-apoptotic factor (30). Restoring the lost expression of CYLD in prostate cancer cells could conceivably sensitize them to apoptosis induction. SSBP2 is a translocation target in a leukemia cell line and is classified as a tumor suppressor candidate gene (31). It is intriguing that the expression of two oncogenes, FYN and RAB31, is down-regulated in prostate cancer. FYN is a member of the protein-tyrosine kinase oncogene family (32), and RAB31 belongs to the RAS oncogene family (33). The role of these genes in prostate carcinogenesis is not clear; nonetheless selenium is found to elevate the expression of both genes.

As a reminder, Table II is produced to highlight the putative prostate cancer genes sensitive to reversal of expression by selenium in both LNCaP and PC-3 cells. For the sake of thoroughness, we also present the analyses of two additional sets of prostate cancer genes which are uniquely modulated by selenium in either LNCaP (Table III) or PC-3 cells (Table IV). Due to the size of these tables, it would be tiresome to go through the data in any comprehensive fashion. Depending on future interests and evolving knowledge, this kind of information has value in seeking out clues and generating hypotheses.

Selenium reverses the effect of androgen on the expression of androgen-regulated genes. In an attempt to identify the androgen-regulated genes of which the expression is opposed by selenium, we compared the list of androgen-regulated genes (422 genes) to the list of selenium-responsive genes in LNCaP (1,031 genes). A partial summary of our analysis is shown in Table V. The AR (androgen-regulated) column shows the genes which are sensitive to androgen. A positive sign means up-regulation, while a minus means down-regulation. A total of 92 genes were found to be present in both datasets. As a control, a list of 1,031 genes were selected randomly from the selenium LNCaP dataset, and compared with the list of androgen-regulated genes to identify genes in common. This process was repeated 10 times, and the number of overlap is 30.4±1.6 (mean±SEM), which is significantly less than the actual number of 92 genes common to the androgen and selenium datasets ($p<0.0005$). Out of these 92 genes, only 38 genes (~41%) are reciprocally modulated by androgen and selenium (Table V). These 38 genes are the ones presented in Table V. In the Discussion, we will offer additional explanation of why only a fraction of AR-targets are oppositely modulated by androgen and selenium, even though selenium is a potent inhibitor of androgen signaling.

Discussion

Using prostate cancer chemoprevention as a research problem, Williams and Brooks (34) recently made a poignant commentary that microarray analysis holds great promise in unraveling the mechanisms of anticancer agents. Here we report for the first time a data mining approach to gain insight into the mechanisms of selenium utilizing published microarray datasets. The paradigm combines laboratory- and bioinformatics-based research to identify molecular targets or biomarkers of prostate cancer intervention by selenium. We recognize that this approach is only a first step in the discovery process. Nonetheless, the information extracted from this kind of analysis has significant potential in generating new leads to guide future research endeavors.

Rhodes *et al.* recently reported a meta-analysis of 4 datasets from prostate cancer gene expression profiling studies (35). Our study differs from the Rhodes study in a number of ways. First, two of the largest available datasets by Lapointe *et al.* (9) and Singh *et al.* (7) were not included in their analysis. Second, the Rhodes study compared localized prostate cancer to benign prostate tissue. The latter was inclusive of both normal prostate and benign prostatic hyperplasia (BPH). It has been reported that normal prostate and BPH have distinct gene expression patterns (36,37). Therefore, combining normal prostate and BPH into one single group could obscure some of the differences between normal and cancerous prostate. Third, instead of using a meta-analysis, we performed permutation t-test on each of the three datasets because they are large enough to generate independent and statistically verifiable information on their own. As a validation of our approach, the majority (~80%) of the top 40 over- and underexpressed genes of the Rhodes study are also present in our analysis (See our website). Additionally, our analysis picked up a few more genes (not found in the Rhodes paper) that are well known to be deregulated in prostate cancer, such as KLK2, KLK3 (PSA) (see our website), GSTP1, and SERPINB5 (Table IB).

We have identified 42 genes which are dysregulated in prostate cancer and are counter-regulated by selenium in both LNCaP and PC3 cells (Table II). In order to assess the significance of this analysis, we compared the functions of these genes with those of the 25 genes which are similarly regulated in prostate cancer and by selenium and found two major differences. First, there is no tumor suppressor gene modulated in the same direction in prostate cancer and by selenium. In contrast, there are four tumor suppressor genes which are downregulated in prostate cancer but are found to be upregulated by selenium (Table II). Second, there is only one cell cycle regulatory gene modulated in the same direction in prostate cancer and by selenium. In contrast,

Table IV. *Selenium reverses the expression of genes implicated in prostate carcinogenesis: unique to PC-3 cells.*

UniGene ID	Symbol	Gene description	Fold Change (log_2)	
			PCa	Se
Cell Proliferation/Apoptosis				
Hs.109752	C6orf108	chromosome 6 open reading frame 108	0.67	-1.14
Hs.282410	CALM1	calmodulin 1 (phosphorylase kinase, delta)	-0.93	3.07
Hs.2132	EPS8	epidermal growth factor receptor pathway substrate 8	-1.29	2.10
Hs.65029	GAS1	growth arrest-specific 1	-1.67	1.14
Hs.370873	IFI16	interferon, gamma-inducible protein 16	-0.68	1.20
Hs.253067	MAEA	macrophage erythroblast attacher	0.34	-1.14
Hs.118630	MXI1	MAX interacting protein 1	-0.98	1.81
Hs.72660	PTDSR	phosphatidylserine receptor	-0.74	1.26
Hs.23582	TACSTD2	tumor-associated calcium signal transducer 2	0.99	-1.07
Cell Adhesion				
Hs.415997	COL6A1	collagen, type VI, alpha 1	-1.36	2.81
Hs.79226	FEZ1	fasciculation and elongation protein zeta 1 (zygin I)	-2.55	1.49
Hs.277324	GALNT1	UDP-N-acetyl-alpha-D-galactosamine:polypeptide N-acetylgalactosaminyltransferase 1	1.43	-1.07
Hs.437536	LAMA4	laminin, alpha 4	-1.24	1.00
Hs.436983	LAMB3	laminin, beta 3	-1.73	1.49
Hs.194431	KIAA0992	palladin	-1.35	1.38
Hs.46531	PGM5	phosphoglucomutase 5	-1.46	1.38
Cytoskeleton				
Hs.208641	ACTA2	actin, alpha 2, smooth muscle, aorta	-1.11	1.38
Hs.309415	CAPZA1	capping protein (actin filament) muscle Z-line, alpha 1	0.58	-1.00
Hs.65248	DNCI1	dynein, cytoplasmic, intermediate polypeptide 1	-1.46	1.07
Hs.58414	FLNC	filamin C, gamma (actin binding protein 280)	-2.17	1.68
Hs.80342	KRT15	keratin 15	-1.68	1.32
Hs.103042	MAP1B	microtubule-associated protein 1B	-1.37	1.00
Hs.433814	MYL9	myosin, light polypeptide 9, regulatory	-1.56	2.46
Hs.162953	MYRIP	myosin VIIA and Rab interacting protein	1.36	-1.96
Hs.387905	SPTAN1	spectrin, alpha, non-erythrocytic 1 (alpha-fodrin)	-0.71	1.26
Hs.163111	SVIL	supervillin	-1.34	1.49
Hs.133892	TPM1	tropomyosin 1 (alpha)	-1.35	1.38
Lipid Metabolism				
Hs.403436	DCI	dodecenoyl-Coenzyme A delta isomerase	1.13	-1.20
Hs.446676	LYPLA1	lysophospholipase I	1.18	-1.14
Hs.211587	PLA2G4A	phospholipase A2, group IVA (cytosolic, calcium-dependent)	-0.71	1.68
Protease/Protease Inhibitor				
Hs.440961	CAST	calpastatin	-0.45	1.14
Hs.83942	CTSK	cathepsin K (pycnodysostosis)	-1.10	1.43
Hs.117874	PACE4	paired basic amino acid cleaving system 4	1.20	-1.43
Hs.41072	SERPINB6	serine (or cysteine) proteinase inhibitor, clade B (ovalbumin), member 6	0.82	-1.07
Hs.173594	SERPINF1	serine (or cysteine) proteinase inhibitor, clade F, member 1	-1.24	1.32
Signal Transduction				
Hs.256398	ADAM22	a disintegrin and metalloproteinase domain 22	-1.23	1.00
Hs.409783	ANK2	ankyrin 2, neuronal	-1.08	1.00
Hs.6838	ARHE	ras homolog gene family, member E	-1.35	1.68
Hs.245540	ARL4	ADP-ribosylation factor-like 4	-0.76	1.20
Hs.444947	C8FW	phosphoprotein regulated by mitogenic pathways	1.38	-3.31
Hs.12436	CAMK2G	calcium/calmodulin-dependent protein kinase (CaM kinase) II gamma	-1.57	3.92
Hs.458426	CCK	cholecystokinin	-1.37	1.89
Hs.163867	CD14	CD14 antigen	0.88	-1.43
Hs.352554	CDC42EP3	CDC42 effector protein (Rho GTPase binding) 3	-1.11	2.10
Hs.255526	DTNA	dystrobrevin, alpha	-0.69	1.07
Hs.117060	ECM2	extracellular matrix protein 2, female organ and adipocyte specific	-0.93	1.00
Hs.211202	EDNRA	endothelin receptor type A	-1.59	1.20
Hs.82002	EDNRB	endothelin receptor type B	-1.57	1.14
Hs.381870	EFEMP2	EGF-containing fibulin-like extracellular matrix protein 2	-1.25	1.89
Hs.133968	FRAG1	FGF receptor activating protein 1	0.78	-2.51

UniGene ID	Symbol	Gene description	Fold Change (log_2)	
			PCa	Se
Hs.74471	GJA1	gap junction protein, alpha 1, 43kDa (connexin 43)	-1.51	1.14
Hs.265829	ITGA3	integrin, alpha 3 (antigen CD49C, alpha 3 subunit of VLA-3 receptor)	-1.23	2.54
Hs.188021	KCNH2	potassium voltage-gated channel, subfamily H (eag-related), member 2	-0.82	2.54
Hs.446645	KDELR2	KDEL (Lys-Asp-Glu-Leu) endoplasmic reticulum protein retention receptor 2	0.53	-1.00
Hs.357004	LOC169611	hypothetical protein LOC169611	-2.11	1.00
Hs.21917	LPHN3	latrophilin 3	-2.35	1.43
Hs.155048	LU	Lutheran blood group (Auberger b antigen included)	1.57	-1.63
Hs.370849	MADH7	MAD, mothers against decapentaplegic homolog 7 (Drosophila)	-0.60	1.32
Hs.61638	MYO10	myosin X	1.35	-1.20
Hs.445402	PCTK3	PCTAIRE protein kinase 3	-2.77	1.58
Hs.77439	PRKAR2B	protein kinase, cAMP-dependent, regulatory, type II, beta	-0.75	1.14
Hs.349845	PRKCB1	protein kinase C, beta 1	-1.36	1.58
Hs.47438	SH3BGR	SH3 domain binding glutamic acid-rich protein	-1.76	1.26
Hs.169300	TGFB2	transforming growth factor, beta 2	-1.53	1.96
Hs.342874	TGFBR3	transforming growth factor, beta receptor III (betaglycan, 300kDa)	-1.47	1.85
Hs.332173	TLE2	transducin-like enhancer of split 2 (E(sp1) homolog, Drosophila)	-0.55	1.38
Hs.274329	TP53AP1	TP53 activated protein 1	0.91	-1.00
Hs.459470	WSB2	WD repeat and SOCS box-containing 2	0.88	-1.14
Hs.79474	YWHAE	tyrosine 3-monooxygenase/tryptophan 5-monooxygenase activation protein, epsilon polypeptide	1.10	-1.26
Transcription/Transcriptional Regulation				
Hs.356416	CBX7	chromobox homolog 7	-1.12	1.43
Hs.405961	CREB3L1	cAMP responsive element binding protein 3-like 1	2.67	-2.20
Hs.43697	ETV5	ets variant gene 5 (ets-related molecule)	-3.64	1.54
Hs.171262	ETV6	ets variant gene 6 (TEL oncogene)	-0.63	2.00
Hs.331	GTF3C1	general transcription factor IIIC, polypeptide 1, alpha 220kDa	0.90	-1.14
Hs.127428	HOXA9	homeo box A9	1.14	-1.00
Hs.134859	MAF	v-maf musculoaponeurotic fibrosarcoma oncogene homolog (avian)	-0.87	2.23
Hs.368950	MEF2C	MADS box transcription enhancer factor 2, polypeptide C	-0.88	2.14
Hs.443881	PAXIP1L	PAX transcription activation domain interacting protein 1 like	0.31	-1.26
Hs.3192	PCBD	6-pyruvoyl-tetrahydropterin synthase/dimerization cofactor of hepatocyte nuclear factor 1 alpha (TCF1)	0.79	-1.14
Hs.432574	POLR2H	polymerase (RNA) II (DNA directed) polypeptide H	0.87	-1.00
Hs.78202	SMARCA4	SWI/SNF related, matrix associated, actin dependent regulator of chromatin, subfamily a, member 4	0.67	-1.07
Hs.444445	SMARCD3	SWI/SNF related, matrix associated, actin dependent regulator of chromatin, subfamily d, member 3	-1.91	2.56
Hs.173911	ZNF24	zinc finger protein 24 (KOX 17)	0.46	-1.58
Hs.419763	ZNF43	zinc finger protein 43 (HTF6)	0.39	-1.07
Transporter				
Hs.374535	ATP2A2	ATPase, Ca++ transporting, cardiac muscle, slow twitch 2	-0.65	1.85
Hs.343522	ATP2B4	ATPase, Ca++ transporting, plasma membrane 4	-2.23	2.41
Hs.1602	DPYD	dihydropyrimidine dehydrogenase	-0.79	1.58
Hs.31720	HEPH	hephaestin	-1.34	1.38
Hs.188021	KCNH2	potassium voltage-gated channel, subfamily H (eag-related), member 2	-0.82	2.54
Hs.102308	KCNJ8	potassium inwardly-rectifying channel, subfamily J, member 8	-0.92	1.07
Hs.446645	KDELR2	KDEL (Lys-Asp-Glu-Leu) endoplasmic reticulum protein retention receptor 2	0.53	-1.00
Hs.101307	SLC14A1	solute carrier family 14 (urea transporter), member 1 (Kidd blood group)	-4.07	1.07
Hs.84190	SLC19A1	solute carrier family 19 (folate transporter), member 1	2.54	-1.14
Hs.417948	TCN2	transcobalamin II; macrocytic anemia	-0.60	1.00
Tumor Suppressor Gene/Oncogene				
Hs.171262	ETV6	ets variant gene 6 (TEL oncogene)	-0.63	1.07
Hs.65029	GAS1	growth arrest-specific 1	-1.67	1.14
Hs.349470	SNCG	synuclein, gamma (breast cancer-specific protein 1)	-3.68	1.89
Hs.203557	ST7	suppression of tumorigenicity 7	0.35	-2.61
Hs.8022	TU3A	TU3A protein	-1.42	1.14

UniGene ID	Symbol	Gene description	Fold Change (log_2)	
			PCa	Se
Other functions				
Hs.75313	AKR1B1	aldo-keto reductase family 1, member B1 (aldose reductase)	-0.67	1.49
Hs.1227	ALAD	aminolevulinate, delta-, dehydratase	-1.32	2.63
Hs.153591	ALG3	asparagine-linked glycosylation 3 homolog (yeast, alpha-1,3-mannosyltransferase)	0.44	-1.00
Hs.102	AMT	aminomethyltransferase (glycine cleavage system protein T)	-0.80	1.43
Hs.135554	APG-1	heat shock protein (hsp110 family)	-0.90	1.20
Hs.78614	C1QBP	complement component 1, q subcomponent binding protein	0.75	-1.00
Hs.413482	C21orf33	chromosome 21 open reading frame 33	0.67	-1.43
Hs.323053	DKFZp547K1113	hypothetical protein DKFZp547K1113	-0.76	1.20
Hs.444619	DXS9879E	DNA segment on chromosome X (unique) 9879 expressed sequence	0.48	-2.29
Hs.511915	ENO2	enolase 2 (gamma, neuronal)	-1.85	1.49
Hs.412103	FLJ34588	Smhs2 homolog (rat)	0.66	-1.20
Hs.28264	FLJ90798	hypothetical protein FLJ90798	-1.20	1.49
Hs.386567	GBP2	guanylate binding protein 2, interferon-inducible	-0.92	1.32
Hs.121017	HIST1H2AE	histone 1, H2ae	3.67	-2.63
Hs.417332	HIST2H2AA	histone 2, H2aa	1.47	-1.14
Hs.44024	MRPL19	mitochondrial ribosomal protein L19	0.83	-1.26
Hs.9235	NME4	non-metastatic cells 4, protein expressed in	0.87	-1.20
Hs.447045	PPIL2	peptidylprolyl isomerase (cyclophilin)-like 2	0.61	-1.00
Hs.153355	QKI	quaking homolog, KH domain RNA binding (mouse)	-0.49	1.14
Hs.81256	S100A4	S100 calcium binding protein A4	-2.59	2.17
Hs.288215	SIAT7B	sialyltransferase 7 B	-0.95	1.26
Hs.511400	SND1	staphylococcal nuclease domain containing 1	0.97	-1.00
Hs.498154	SNX1	sorting nexin 1	-0.93	1.43
Hs.2943	SRP19	signal recognition particle 19kDa	0.97	-1.63
Hs.326	TARBP2	TAR (HIV) RNA binding protein 2	0.57	-1.07
Hs.8752	TMEM4	transmembrane protein 4	1.00	-1.26
Hs.112986	TMEM5	transmembrane protein 5	0.72	-1.07
Hs.370530	TRIM14	tripartite motif-containing 14	0.65	-1.07
Hs.66708	VAMP3	vesicle-associated membrane protein 3 (cellubrevin)	-0.49	1.68
Unknown				
Hs.148258	BC008967	hypothetical gene BC008967	-1.59	1.32
Hs.277888	CG018	hypothetical gene CG018	-0.9	1.68
Hs.425144	CRA	cisplatin resistance associated	-4.91	3.09
Hs.183650	CRABP2	cellular retinoic acid binding protein 2	-1.93	1.49
Hs.108080	CSRP1	cysteine and glycine-rich protein 1	-1.53	1.32
Hs.200692	DKFZP564G2022	DKFZP564G2022 protein	1.15	-1.32
Hs.75486	FBXL8	F-box and leucine-rich repeat protein 8	-0.81	1.43
Hs.7358	FLJ13110	hypothetical protein FLJ13110	-0.80	2.07
Hs.242271	HHL	expressed in hematopoietic cells, heart, liver	-1.67	1.00
Hs.236774	HMGN4	high mobility group nucleosomal binding domain 4	-0.55	1.07
Hs.18705	KIAA1233	KIAA1233 protein	-1.44	1.00
Hs.234265	LAP1B	lamina-associated polypeptide 1B	-0.51	1.00
Hs.443881	PAXIP1L	PAX transcription activation domain interacting protein 1 like	0.31	-1.26
Hs.78748	RIMS3	regulating synaptic membrane exocytosis 3	-3.96	1.00
Hs.98259	SAMD4	sterile alpha motif domain containing 4	-2.01	1.49
Hs.76536	TBL1X	transducin (beta)-like 1X-linked	-1.07	1.32
Hs.27860		MRNA; cDNA DKFZp586M0723 (from clone DKFZp586M0723)	-2.88	1.38
Hs.458282		Transcribed sequence with strong similarity to protein ref:NP_065136.1 (H.sapiens) protocadherin 9 precursor; cadherin superfamily protein VR4-11	-2.62	2.23
Hs.98314		cDNA DKFZp586L0120 (from clone DKFZp586L0120)	-1.86	1.14
Hs.468490		hypothetical protein FLJ20489	-1.25	1.58

*For PC-3, the ratio is the maximum value of the data points from all the time- and concentration-series of selenium treatment. For PCa, it is the average tumor to normal ratio.

Table V. *Selenium reverses the expression of androgen-regulated genes.*

UniGene ID	Symbol	Gene description	Maximum Fold (log_2)#	
			AR	Se
Cell proliferation				
Hs.8230	ADAMTS1	a disintegrin-like and metalloprotease with thrombospondin type 1 motif, 1	2.00	-1.66
Hs.13291	CCNG2	cyclin G2	-2.82	1.46
Hs.405958	CDC6	CDC6 cell division cycle 6 homolog (S. cerevisiae)	1.28	-1.99
Hs.374378	CKS1B	CDC28 protein kinase regulatory subunit 1B	1.23	-1.84
Hs.119324	KIF22	kinesin family member 22	1.54	-1.08
Signal transduction				
Hs.197922	CaMKIINalpha	calcium/calmodulin-dependent protein kinase II	-3.43	1.41
Hs.78888	DBI	diazepam binding inhibitor	2.00	-1.69
Hs.433488	GUCY1A3*	guanylate cyclase 1, soluble, alpha 3	1.72	-1.53
Hs.81328	NFKBIA	nuclear factor of kappa light polypeptide gene enhancer in B-cells inhibitor, alpha	1.68	-1.78
Hs.154151	PTPRM	protein tyrosine phosphatase, receptor type, M	1.33	-1.74
Hs.432842	RALGPS1A	Ral guanine nucleotide exchange factor RalGPS1A	-1.28	1.21
Transcriptional regulation				
Hs.55999	NKX3-1	NK3 transcription factor related, locus 1 (Drosophila)	3.90	-1.47
Hs.408222	PBX1*	pre-B-cell leukemia transcription factor 1	-1.98	1.29
Transporter				
Hs.307915	ABCC4*	ATP-binding cassette, sub-family C (CFTR/MRP), member 4	2.96	-1.08
Hs.20952	ATP2B1	ATPase, Ca++ transporting, plasma membrane 1	-1.76	2.53
Metabolism				
Hs.75616	DHCR24*	24-dehydrocholesterol reductase	2.58	-1.07
Hs.35198	ENPP5	ectonucleotide pyrophosphatase/phosphodiesterase 5 (putative function)	-1.78	1.01
Hs.268012	FACL3*	fatty-acid-Coenzyme A ligase, long-chain 3	3.98	-1.14
Hs.167531	MCCC2	methylcrotonoyl-Coenzyme A carboxylase 2 (beta)	1.98	-1.27
Hs.237323	PGM3	phosphoglucomutase 3	2.07	-1.16
Hs.119597	SCD	stearoyl-CoA desaturase (delta-9-desaturase)	2.56	-2.29
Other functions				
Hs.6790	DNAJB9	DnaJ (Hsp40) homolog, subfamily B, member 9	2.00	-2.05
Hs.173381	DPYSL2*	dihydropyrimidinase-like 2	-1.75	1.14
Hs.181350	KLK2*	kallikrein 2, prostatic	3.17	-2.27
Hs.171995	KLK3*	kallikrein 3, (prostate specific antigen)	3.35	-2.45
Hs.423095	NUCB2	nucleobindin 2	-3.18	1.36
Hs.171952	OCLN	occludin	-2.01	1.34
Hs.188361	RPS6KA3	ribosomal protein S6 kinase, 90kDa, polypeptide 3	1.44	-1.21
Hs.152207	SSBP2	single-stranded DNA binding protein 2	-1.59	1.72
Unknown				
Hs.180197		LOC375504 (LOC375504), mRNA	-1.42	1.63
Hs.22247		CDNA FLJ42250 fis, clone TKIDN2007828	2.40	-1.04
Hs.29189	ATP11A	ATPase, Class VI, type 11A	-2.75	1.27
Hs.512643	AZGP1	alpha-2-glycoprotein 1, zinc	2.49	-1.86
Hs.7557	FKBP5	FK506 binding protein 5	4.67	-1.20
Hs.90797	LOC129642	hypothetical protein BC016005	3.90	-1.40
Hs.298646	PRO2000	PRO2000 protein	3.28	-1.76
Hs.203557	ST7	suppression of tumorigenicity 7	-2.07	1.14

#the maximum value of the data points from all the time- and concentration-series of MSA or R1881 treatment.
*Genes implicated in prostate cancinogenesis.

there are five cell cycle regulatory genes (ATF5, AHR, CDKN1C, EXT1, and CHC1) which are modulated in opposite directions in prostate cancer and by selenium (Table II). More interestingly, selenium alters the expression of these genes in a manner that is consistent with growth inhibition.

In androgen responsive prostate cancer, AR signaling is such a dominant pathway that shutting it down is likely to be sufficient for growth inhibition. Our previous publication showed that selenium markedly downregulates AR signaling in LNCaP cells (5). Furthermore, we were able to confirm that overexpression of AR diminishes the sensitivity to

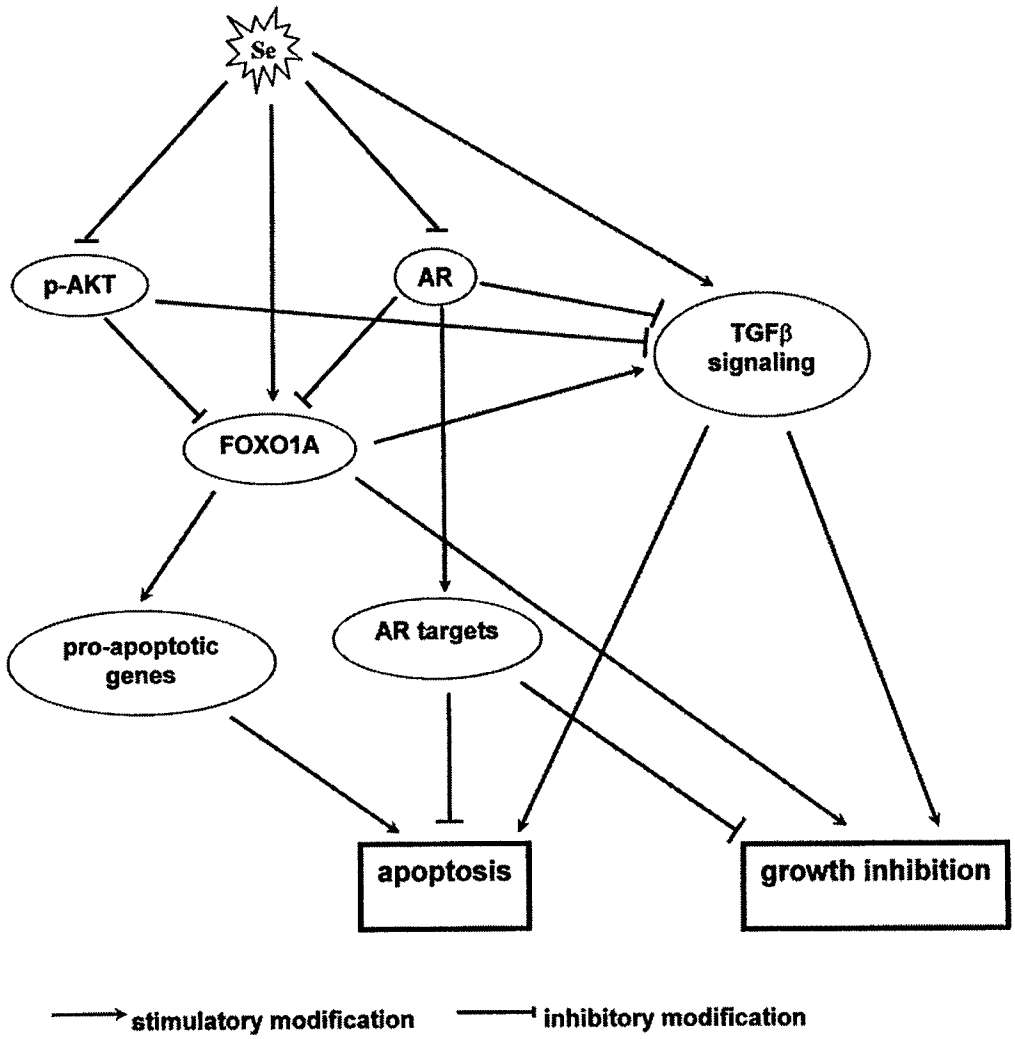

Figure 2. *Proposed model of apoptosis induction and growth inhibition by selenium through the interplay of AKT, AR, and TGFβ signaling pathways.*

selenium (unpublished data), suggesting that disruption of AR signaling by selenium is biologically relevant. Additionally, selenium is known to modulate a diverse number of cell cycle and apoptosis regulatory molecules, as well as survival signaling molecules, in different cell types regardless of the presence or absence of AR. Different cell types may present both common and unique targets to selenium intervention. Thus, it is apparent that selenium has many targets and there is no one key mechanism to account for the anticancer effect of selenium. The multitude of genes in Table II lends support to common mechanisms for the anticancer activity of selenium in both the androgen-responsive LNCaP cells and the androgen-unresponsive PC-3 cells. However, despite the overall similarity of their cellular responses to selenium, subtle differences exist between the two cell types. For example, selenium slows down cell cycle progression at multiple transition points in PC3 (5), whereas mostly through G1 arrest in LNCaP (unpublished data). Genes distinctly targeted by selenium in these cells, as presented in Tables III and IV, could be attributable to the above disparities. They might also reflect the difference in genetic background such as response to androgen. Indeed, a noticeable distinction between Table III and Table IV is the presence of androgen-regulated genes in Table III.

Our analysis has identified 92 genes that are regulated by both selenium and androgen. However, only a modest proportion (38 out of 92) of these genes are modulated in reciprocal directions by selenium and androgen. A possible explanation for this is that genes have multiple regulatory elements, both positive and negative, in their promoter regions. Selenium is known to alter the expression of many transcription factors, co-activators and co-repressors (5). AR regulates the expression of its targets through both

direct and indirect mechanisms. In other words, many other transcription factors and co-regulators are likely to be involved by virtue of the rippling effect initiated through AR signaling. Thus it is to be expected that selenium could counteract the expression of some, but not all, androgen-regulated genes. The litmus test in the future is to study which AR-regulated genes sensitive to selenium reversal are important for modulation of prostate cancer risk.

The induction of forkhead O1A (FOXO1A) by selenium in both LNCaP and PC-3 cells is of special interest to us. FOXO1A is a member of the FOXO family of transcription factors that induce the expression of pro-apoptotic genes including Fas ligand (38-40), bcl-2 family proteins (19,40,41), and TRAIL (20). Furthermore, FOXO1A is involved in cell cycle arrest (21). FOXO1A is phosphorylated and suppressed by AKT (42,43), which is an important survival molecule for prostate cancer (44). Androgen receptor (AR) also interacts with FOXO1A and inhibits its activation of Fas ligand expression (45). Selenium conveniently down-regulates both AKT and AR signaling (4,46). As shown in Figure 2, the stimulatory effect of selenium on FOXO1A signaling could be due to a direct induction of FOXO1A transcription coupled to an indirect activation of FOXO1A by alleviating the inhibitory modulation through AR and/or AKT.

Three key components of the transforming growth factor β (TGFβ) signaling pathway are consistently repressed in a large set of primary prostate tumors. These genes are TGFβ2, TGFβ receptor type II, and TGFβ receptor type III. Type I and II receptors have serine/threonine protein kinase domains and are directly involved in TGFβ signaling (47). Type III receptor does not have an intrinsic signaling domain; however, it facilitates the binding of all TGFβs, and especially TGFβ2, to the type II receptor (47). TGFβ is a pleiotropic cytokine, but is mainly a growth inhibitor of epithelial cancer particularly at the early stage of development (48). It has been shown that the type I and II receptors are down-regulated in prostate cancer (49,50) and that loss of expression of the receptors is associated with poor prognosis (51). Therefore, from a prevention standpoint, stimulating TGFβ signaling is likely to produce a desirable outcome. In this study, we found that the expression of TGFβ2, TGFβ type II and III receptors is concertedly up-regulated by selenium. It is also worth mentioning that the expression of TGFβ2 is known to be induced by a forkhead transcription factor closely related to FOXO1A (52) and that both AR and AKT repress TGFb signaling (53). Thus the effect of selenium could be amplified by the crosstalk of TGFβ, AKT, and AR signals as illustrated in Figure 2. Our future research effort will be directed towards elucidating the contribution of these pathways in selenium chemoprevention of prostate cancer.

Acknowledgements

This work was supported by a Department of Defense Postdoctoral Fellowship Award and an AACR-Cancer Research Foundation of America Fellowship in Prevention Research Award, grant 62-2141 from the Roswell Park Alliance Foundation, grant CA91990 from the National Cancer Institute, and also in part by Cancer Center Support Grant P30 CA16056 awarded to RPCI from the National Cancer Institute. H. Zhao is supported by a Postdoctoral Traineeship Award from the United States Army MRMC Prostate Cancer Research Program (Award Number W81XWH-04-1-0080).

References

1 Clark LC, Combs GF Jr, Turnbull BW, Slate EH, Chalker DK, Chow J, Davis LS, Glover RA, Graham GF, Gross EG, Krongrad A, Lesher JL Jr, Park HK, Sanders BB Jr, Smith CL and Taylor JR: Effects of selenium supplementation for cancer prevention in patients with carcinoma of the skin. A randomized controlled trial. Nutritional Prevention of Cancer Study Group. JAMA *276*: 1957-1963, 1996.

2 Clark LC, Dalkin B, Krongrad A, Combs GF Jr, Turnbull BW, Slate EH, Witherington R, Herlong JH, Janosko E, Carpenter D, Borosso C, Falk S and Rounder J: Decreased incidence of prostate cancer with selenium supplementation: results of a double-blind cancer prevention trial. Br J Urol *81*: 730-734, 1998.

3 Duffield-Lillico AJ, Dalkin BL, Reid ME, Turnbull BW, Slate EH, Jacobs ET, Marshall JR and Clark LC: Selenium supplementation, baseline plasma selenium status and incidence of prostate cancer: an analysis of the complete treatment period of the Nutritional Prevention of Cancer Trial. BJU Int *91*: 608-612, 2003.

4 Dong Y, Lee SO, Zhang H, Marshall J, Gao AC and Ip C: Prostate specific antigen expression is down-regulated by selenium through disruption of androgen receptor signaling. Cancer Res *64*: 19-22, 2004.

5 Dong Y, Zhang H, Hawthorn L, Ganther HE and Ip C: Delineation of the Molecular Basis for Selenium-induced Growth Arrest in Human Prostate Cancer Cells by Oligonucleotide Array. Cancer Res *63*: 52-59, 2003.

6 Zhao H, Whitfield ML, Xu T, Botstein D and Brooks JD: Diverse effects of methylseleninic acid on the transcriptional program of human prostate cancer cells. Mol Biol Cell *15*: 506-519, 2004.

7 Singh D, Febbo PG, Ross K, Jackson DG, Manola J, Ladd C, Tamayo P, Renshaw AA, D'Amico AV, Richie JP, Lander ES, Loda M, Kantoff PW, Golub TR and Sellers WR: Gene expression correlates of clinical prostate cancer behavior. Cancer Cell *1*: 203-209, 2002.

8 Welsh JB, Sapinoso LM, Su AI, Kern SG, Wang-Rodriguez J, Moskaluk CA, Frierson HF Jr and Hampton GM: Analysis of gene expression identifies candidate markers and pharmacological targets in prostate cancer. Cancer Res *61*: 5974-5978, 2001.

9 Lapointe J, Li C, Higgins JP, van de RM, Bair E, Montgomery K, Ferrari M, Egevad L, Rayford W, Bergerheim U, Ekman P, DeMarzo AM, Tibshirani R, Botstein D, Brown PO, Brooks JD and Pollack JR: Gene expression profiling identifies clinically relevant subtypes of prostate cancer. Proc Natl Acad Sci USA *101*: 811-816, 2004.

10 Jenster G: The role of the androgen receptor in the development and progression of prostate cancer. Semin Oncol *26*: 407-421, 1999.
11 DePrimo SE, Diehn M, Nelson JB, Reiter RE, Matese J, Fero M, Tibshirani R, Brown PO and Brooks JD: Transcriptional programs activated by exposure of human prostate cancer cells to androgen. Genome Biol *3*: RESEARCH0032, 2002.
12 Nelson PS, Clegg N, Arnold H, Ferguson C, Bonham M, White J, Hood L and Lin B: The program of androgen-responsive genes in neoplastic prostate epithelium. Proc Natl Acad Sci USA *99*: 11890-11895, 2002.
13 Kaminski N, Allard JD, Pittet JF, Zuo F, Griffiths MJ, Morris D, Huang X, Sheppard D and Heller RA: Global analysis of gene expression in pulmonary fibrosis reveals distinct programs regulating lung inflammation and fibrosis. Proc Natl Acad Sci USA *97*: 1778-1783, 2000.
14 Wang Y, Rea T, Bian J, Gray S and Sun Y: Identification of the genes responsive to etoposide-induced apoptosis: application of DNA chip technology. FEBS Lett *445*: 269-273, 1999.
15 Puga A, Xia Y and Elferink C: Role of the aryl hydrocarbon receptor in cell cycle regulation. Chem Biol Interact *141*: 117-130, 2002.
16 Ohtsubo M, Kai R, Furuno N, Sekiguchi T, Sekiguchi M, Hayashida H, Kuma K, Miyata T, Fukushige S, Murotsu T and: Isolation and characterization of the active cDNA of the human cell cycle gene (RCC1) involved in the regulation of onset of chromosome condensation. Genes Dev *1*: 585-593, 1987.
17 Matsuoka S, Edwards MC, Bai C, Parker S, Zhang P, Baldini A, Harper JW, and Elledge SJ: p57KIP2, a structurally distinct member of the p21CIP1 Cdk inhibitor family, is a candidate tumor suppressor gene. Genes Dev *9*: 650-662, 1995.
18 Persengiev SP, Devireddy LR and Green MR: Inhibition of apoptosis by ATFx: a novel role for a member of the ATF/CREB family of mammalian bZIP transcription factors. Genes Dev *16*: 1806-1814, 2002.
19 Gilley J, Coffer PJ and Ham J: FOXO transcription factors directly activate bim gene expression and promote apoptosis in sympathetic neurons. J Cell Biol *162*: 613-622, 2003.
20 Modur V, Nagarajan R, Evers BM and Milbrandt J: FOXO proteins regulate tumor necrosis factor-related apoptosis inducing ligand expression. Implications for PTEN mutation in prostate cancer. J Biol Chem *277*: 47928-47937, 2002.
21 Nakamura N, Ramaswamy S, Vazquez F, Signoretti S, Loda M, and Sellers WR: Forkhead transcription factors are critical effectors of cell death and cell cycle arrest downstream of PTEN. Mol Cell Biol *20*: 8969-8982, 2000.
22 Cher ML, Biliran HR Jr, Bhagat S, Meng Y, Che M, Lockett J, Abrams J, Fridman R, Zachareas M and Sheng S: Maspin expression inhibits osteolysis, tumor growth, and angiogenesis in a model of prostate cancer bone metastasis. Proc Natl Acad Sci USA *100*: 7847-7852, 2003.
23 Zou Z, Anisowicz A, Hendrix MJ, Thor A, Neveu M, Sheng S, Rafidi K, Seftor E and Sager R: Maspin, a serpin with tumor-suppressing activity in human mammary epithelial cells. Science *263*: 526-529, 1994.
24 Bass R, Fernandez AM and Ellis V: Maspin inhibits cell migration in the absence of protease inhibitory activity. J Biol Chem *277*: 46845-46848, 2002.
25 Chen Z, Fan Z, McNeal JE, Nolley R, Caldwell MC, Mahadevappa M, Zhang Z, Warrington JA and Stamey TA: Hepsin and maspin are inversely expressed in laser capture microdissectioned prostate cancer. J Urol *169*: 1316-1319, 2003.
26 Lee HK, Driscoll D, Asch H, Asch B and Zhang PJ: Downregulated gelsolin expression in hyperplastic and neoplastic lesions of the prostate. Prostate *40*: 14-19, 1999.
27 Asch HL, Head K, Dong Y, Natoli F, Winston JS, Connolly JL and Asch BB: Widespread loss of gelsolin in breast cancers of humans, mice, and rats. Cancer Res *56*: 4841-4845, 1996.
28 Dosaka-Akita H, Hommura F, Fujita H, Kinoshita I, Nishi M, Morikawa T, Katoh H, Kawakami Y and Kuzumaki N: Frequent loss of gelsolin expression in non-small cell lung cancers of heavy smokers. Cancer Res *58*: 322-327, 1998.
29 Tanaka M, Mullauer L, Ogiso Y, Fujita H, Moriya S, Furuuchi K, Harabayashi T, Shinohara N, Koyanagi T and Kuzumaki N: Gelsolin: a candidate for suppressor of human bladder cancer. Cancer Res *55*: 3228-3232, 1995.
30 Trompouki E, Hatzivassiliou E, Tsichritzis T, Farmer H, Ashworth A and Mosialos G: CYLD is a deubiquitinating enzyme that negatively regulates NF-kappaB activation by TNFR family members. Nature *424*: 793-796, 2003.
31 Castro P, Liang H, Liang JC and Nagarajan L: A novel, evolutionarily conserved gene family with putative sequence-specific single-stranded DNA-binding activity. Genomics *80*: 78-85, 2002.
32 Semba K, Nishizawa M, Miyajima N, Yoshida MC, Sukegawa J, Yamanashi Y, Sasaki M, Yamamoto T and Toyoshima K: yes-related protooncogene, syn, belongs to the protein-tyrosine kinase family. Proc Natl Acad Sci USA *83*: 5459-5463, 1986.
33 Chen D, Guo J, Miki T, Tachibana M and Gahl WA: Molecular cloning of two novel rab genes from human melanocytes. Gene *174*: 129-134, 1996.
34 Williams ED and Brooks JD: New molecular approaches for identifying novel targets, mechanisms and biomarkers for prostate cancer chemopreventive agents. Urology *57*: 100-102, 2001.
35 Rhodes DR, Barrette TR, Rubin MA, Ghosh D and Chinnaiyan AM: Meta-analysis of microarrays: interstudy validation of gene expression profiles reveals pathway dysregulation in prostate cancer. Cancer Res *62*: 4427-4433, 2002.
36 Luo J, Dunn T, Ewing C, Sauvageot J, Chen Y, Trent J and Isaacs W: Gene expression signature of benign prostatic hyperplasia revealed by cDNA microarray analysis. Prostate *51*: 189-200, 2002.
37 Prakash K, Pirozzi G, Elashoff M, Munger W, Waga I, Dhir R, Kakehi Y and Getzenberg RH: Symptomatic and asymptomatic benign prostatic hyperplasia: molecular differentiation by using microarrays. Proc Natl Acad Sci USA *99*: 7598-7603, 2002.
38 Kavurma MM and Khachigian LM: Signaling and transcriptional control of Fas ligand gene expression. Cell Death Differ *10*: 36-44, 2003.
39 Suhara T, Kim HS, Kirshenbaum LA and Walsh K: Suppression of Akt signaling induces Fas ligand expression: involvement of caspase and Jun kinase activation in Akt-mediated Fas ligand regulation. Mol Cell Biol *22*: 680-691, 2002.
40 Dijkers PF, Medema RH, Lammers JW, Koenderman L and Coffer PJ: Expression of the pro-apoptotic Bcl-2 family member Bim is regulated by the forkhead transcription factor FKHR-L1. Curr Biol *10*: 1201-1204, 2000.
41 Tang TT, Dowbenko D, Jackson A, Toney L, Lewin DA, Dent AL and Lasky LA: The forkhead transcription factor AFX activates apoptosis by induction of the BCL-6 transcriptional repressor. J Biol Chem *277*: 14255-14265, 2002.

42 Tang ED, Nunez G, Barr FG and Guan KL: Negative regulation of the forkhead transcription factor FKHR by Akt. J Biol Chem *274*: 16741-16746, 1999.
43 Guo S, Rena G, Cichy S, He X, Cohen P and Unterman T: Phosphorylation of serine 256 by protein kinase B disrupts transactivation by FKHR and mediates effects of insulin on insulin-like growth factor-binding protein-1 promoter activity through a conserved insulin response sequence. J Biol Chem *274*: 17184-17192, 1999.
44 Lin J, Adam RM, Santiestevan E and Freeman MR: The phosphatidylinositol 3'-kinase pathway is a dominant growth factor-activated cell survival pathway in LNCaP human prostate carcinoma cells. Cancer Res *59*: 2891-2897, 1999.
45 Li P, Lee H, Guo S, Unterman TG, Jenster G and Bai W: AKT-independent protection of prostate cancer cells from apoptosis mediated through complex formation between the androgen receptor and FKHR. Mol Cell Biol *23*: 104-118, 2003.
46 Jiang C, Wang Z, Ganther H and Lu J: Distinct effects of methylseleninic acid versus selenite on apoptosis, cell cycle, and protein kinase pathways in DU145 human prostate cancer cells. Mol Cancer Ther *1*: 1059-1066, 2002.
47 Massague J: TGF-beta signal transduction. Annu Rev Biochem *67*: 753-791, 1998.
48 Moses HL, Yang EY and Pietenpol JA: Regulation of epithelial proliferation by TGF-beta. Ciba Found Symp *157*: 66-74, 1991.
49 Eastham JA, Truong LD, Rogers E, Kattan M, Flanders KC, Scardino PT and Thompson TC: Transforming growth factor-beta 1: comparative immunohistochemical localization in human primary and metastatic prostate cancer. Lab Invest *73*: 628-635, 1995.
50 Williams RH, Stapleton AM, Yang G, Truong LD, Rogers E, Timme TL, Wheeler TM, Scardino PT and Thompson TC: Reduced levels of transforming growth factor beta receptor type II in human prostate cancer: an immunohistochemical study. Clin Cancer Res *2*: 635-640, 1996.
51 Kim IY, Ahn HJ, Lang S, Oefelein MG, Oyasu R, Kozlowski JM and Lee C: Loss of expression of transforming growth factor-beta receptors is associated with poor prognosis in prostate cancer patients. Clin Cancer Res *4*: 1625-1630, 1998.
52 Samatar AA, Wang L, Mirza A, Koseoglu S, Liu S and Kumar CC: Transforming growth factor-beta 2 is a transcriptional target for Akt/protein kinase B *via* forkhead transcription factor. J Biol Chem *277*: 28118-28126, 2002.
53 Chipuk JE, Cornelius SC, Pultz NJ, Jorgensen JS, Bonham MJ, Kim SJ and Danielpour D: The androgen receptor represses transforming growth factor-beta signaling through interaction with Smad3. J Biol Chem *277*: 1240-1248, 2002.

Received February 13, 2005
Accepted February 25, 2005